THESIS APPROVAL

GRADUATE SCHOOL, KASETSART UNIVERSITY

Master of Science (Chemistry)

DEGREE

Chemistry	Chemistry
FIELD	**DEPARTMENT**

TITLE: Orthophosphate Adsorption on Mordenite and Its Calcination Effect

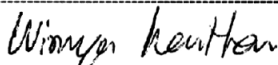NAME: Miss Noppakao Ex-un

THIS THESIS HAS BEEN ACCEPTED BY

_____ THESIS ADVISOR
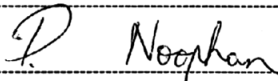
(Miss Pinsuda Viravathana, Ph.D.   )

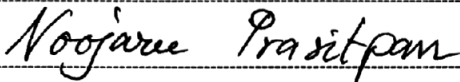_____ COMMITTEE MEMBER

(Associate Professor Cholticha Noomhorm, Ph.D.   )

_____ COMMITTEE MEMBER

(Miss Wirunya Keawwattana, Ph.D.   )

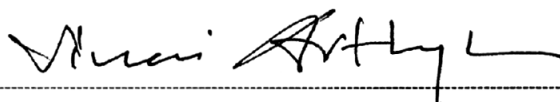_____ COMMITTEE MEMBER

(Assistant Professor Pongsak Noophan, Ph.D.   )

_____ DEPARTMENT HEAD

(Assistant Professor Noojaree Prasitpan, Ph.D.   )

APPROVED BY THE GRADUATE SCHOOL ON   02 / 11 / 06

_____ DEAN

(Associate Professor Vinai Artkongharn, M.A.   )

THESIS

ORTHOPHOSPHATE ADSORPTION ON MORDENITE AND ITS CALCINATION EFFECT

NOPPAKAO EX-UN

A Thesis Submitted in Partial Fulfillment of

the Requirements for the Degree of

Master of Science (Chemistry)
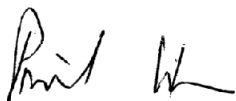
Graduate School, Kasetsart University

2006

Mordenite (MOR), one type of natural zeolite, was used as adsorbent for
orthophosphate removal in solutions. The aims of this study are to investigate the
influence of calcination temperature, time, and initial orthophosphate concentration
on the adsorption. For characterization, Brunauer-Emmett-Teller (BET), scanning
electron microscope (SEM), energy dispersive X-ray spectrometer (EDS), X-ray
diffractometer (XRD), and Fourier transform infrared spectrometer (FTIR) were used
to investigate surface properties, composition, and structure of MOR. The results
showed that the maximum orthophosphate adsorption happened after MOR was
calcined at 750°C. Adsorption coverage over the MOR surface was studied using two
well-known isotherm models: Langmuir's and Freundlich's. The Langmuir
adsorption isotherm was used to calculate the maximum phosphorus (P) adsorption
capability of MOR. The result showed the highest P adsorption capability of 769.23
mg-P/Kg (R^2=0.8532). Atomic absorption spectrometer indicated the quantity of
Ca^{2+} and Fe^{2+} dissolved from MOR in water, basic, and acidic solution. Zeta sizer
was used to measure the zeta potential on MOR surface and study the adsorption
behavior. The information on zeta potential showed that the calcined MOR at 750°C
had the increased amount of Al at the surface and had the high capability on
orthophosphate adsorption which was agreed to the adsorption experiment.

Noppakao Ex-un		30 / 10 / 06
Student's signature	Thesis Advisor's signature	

ACKNOWLEDGEMENTS

TABLE OF CONTENTS

Page

LIST OF TABLES

LIST OF TABLES (Cont'd)

LIST OF TABLES (Cont'd)

LIST OF FIGURES

LIST OF FIGURES (Cont'd)

LIST OF FIGURES (Cont'd)

LIST OF ABBREVIATIONS

AAS = Atomic Absorption Spectrophotometer

BJH   = Barrett-Joyner-Halenda

BET   = Brunauer-Emmett-Teller

EDS   = energy dispersive X-ray spectroscopy

FTIR = Fourier transform infrared spectrometer

MOR = mordenite

mg-P = milligram phosphorus

SEM = scanning elecrtron microscope

XRD = X-ray diffraction

g P   = gram phosphorus

mg-P/L = milligram phosphorus per liter

ORTHOPHOSPHATE ADSORPTION ON MORDENITE AND ITS CALCINATION EFFECT

INTRODUCTION

Nowadays, human beings use water for several activities such as washing, taking a bath, and in industry. Certainly, wastewater from various sources including domestic, agricultural, and industrial uses has different kinds and quantities of contaminants, for example, domestic, and agricultural wastewaters have nitrogen and phosphorus compounds as contaminants (Boari and Liberty, 1975). The textiles, printing, dyeing, food, and paper-making industries have dyes, such as methyl violet, nutrients (nitrogen and phosphate) as contaminants (Doğan and Alkan, 2003). Many industries, like tanneries, metal plating facilities and mining operations have also heavy metal contaminants, especially Cu^{2+}, Fe^{3+} and Cr^{3+} (Inglezakis $et\ al.$, 2003). Therefore, the contaminants' removal from different aqueous solution is many ways, for instance, Cu^{2+}, Fe^{3+} and Cr^{3+} removal through ion exchange on natural clinoptilolite (Inglezakis $et\ al.$, 2003), methylene blue removal by adsorption onto perlite (Doğan $et\ al.$, 2004), and nitrogen and phosphorus removal by biological treatment in anaerobic/anoxic and aerobic sequencing batch reactor with separated biofilm nitrification, denitrification, and bio-phosphorus removal (Bortone $et\ al.$, 1994). The human feces in domestic wastewater and from the detergents used in households produce phosphorus compounds. The population correction factor is 3.5 g P per person per day, with 30 to 50% resulting from detergents (Fresenius $et\ al.$, 1989). In addition, phosphorus is introduced into the sewage plant through industrial and agricultural wastewater and uncontrolled inflowing rainwater.

The phosphorus compounds have an important effect on the dynamics of metabolism. It is one of the most important elements and is the main factor responsible for eutrophication (Fresenius *et al.*, 1989), which leads to short- and long-term environmental and aesthetic problems in lakes, coastal areas, and other confined water bodies. For this reason, phosphorus must be removed from wastewater before it is discharged into the environment or retained as far as this is possible under engineering and economic conditions. In general, the total amount of phosphorus present in domestic wastewater is typically of the order of 10 to 25 mg-P/L (Henri, 1996). Phosphorus compounds in wastewater and in natural waters are mostly in the form of three types of phosphate. These forms are commonly classified into orthophosphates, condensed phosphates, and organically bound phosphates (Andrew, 1995). Phosphorus is essential to the growth of organisms and can be the nutrient of aquatic plants such as java weed and lemnaceae that limit the productivity of a body of water. Consequently, phosphorus must be removal from several wastewaters in order to control the amount of it as low as minimum in the range of 0.10-2.0 mg-P/L depending on wastewater treatment plant location and potential impact on receiving water (Burton and Stensel, 2003). Consequently, there has been an interest among the academic community in environmental issues and research on ways to treat phosphorus problems. Considerable research and development efforts are devoted to wastewater treatment, to find new methods, and for the most efficient methods. There are several routes for phosphorus treatment; biological, chemical, and physicochemical treatments.

Biological treatment for phosphorus removal is inexpensive cost. This process depends on the role of microorganisms. This method can transform and remove specific trace organic constituents, compounds and nutrients such as nitrogen and phosphorus (Burton and Stensel, 2003). The phosphate

concentration in the wastewater is reduced, mainly by its introduction into biological cell mass, by adsorption to activated sludge, and by biogenous precipitation phenomena (Fresenius *et al.*, 1989). However, phosphorus removal by biological treatment is difficult to operate. In chemical treatment process for phosphorus removal is very effective but it is quit expensive. The phosphorus removal from wastewater involves the incorporation of phosphate into suspended solids (TSS) and the subsequent removal of those solids. The reagents are used to precipitate phosphorus such as calcium, aluminum, and iron (Burton and Stensel, 2003). Physicochemical treatment is a process to co-eliminate contaminants from wastewater by physical and chemical treatment. Methods are used to eliminate contaminants such as ion exchange, ultrafiltration, reverse osmosis, electrodialysis, and adsorption. However, precipitation and adsorption are a major process to remove phosphorus. The researchers used different materials to ion exchanger for wastewater treatment. For instance, polyacrylonitrile fiber has been used to remove fluoride, arsenate, and phosphate ions (Liu *et al.*, 2002), clinoptilolite in its Na form and Kastal A 510 in its Cl form to remove eutrophic species such as chloride, sulphate, bicarbonate, ammonium, and phosphate (Liberti and Passino, 1981).

Adsorption has become an important method for phosphorus removal. Even though the adsorption process has not been used extensively in wastewater treatment, demands for a better quality of treated wastewater effluent, have led to an intensive examination and use of the process of adsorption. There are many materials used to adsorb, for example, activated carbon, silica powders and gels, activated alumina, titanium oxide, magnesium oxide, clay, and natural zeolite. Materials such as soils, slags, and zeolite have been used as adsorbent for eliminating phosphorus (Sakadevan and Bavor, 1998).

The most industrially important natural zeolites are mordenite, clinoptilolite, chabazite, and erionite (Dyer, 1988). In this work, mordenite was used to study adsorption due to its low cost and available material. Because many zeolites have evident channels and cavities within their structure, molecular dimensions, their size, and configuration are intrinsic properties of the particular crystalline framework. Moreover, the local electrostatic fields, which emanate from the exchangeable cations, are to a large extent responsible for the strong affinity for water and other polar molecules. Natural zeolites are indirect results from volcanic activity. They are formed by hydrothermal transformation of basalt, volcanic ash, and pumice which can be found e.g. in basalt cavities and in large sedimentary deposits. For this reason, phosphorus removal by natural zeolite adsorption comes to one's interest.

In order to improve the ability of materials to adsorb other ions, thermal treatment is one of the major methods to dislodge aluminum from framework to non-framework positions in zeolite. From the relationship between the unit cell shrinkage and the micropore volume decrease, it is suggested that the non-framework position goes to the pores. Upon increasing the calcination temperature, the number of non-framework position species increases while the total number of aluminum atoms stays the same (Hong, 1995). Upon calcination, structures of mordenite would be altered leading to the change in its adsorption capability. In this study, orthophosphate adsorption in mordenite frameworks after calcinations was determined by UV/visible spectrophotometry, and their structures as well as the adsorption behavior were investigated.

The purposes of this study were:

1. To study the effect of calcination temperatures of natural zeolite on the orthophosphate adsorption.

2. To study the effects of orthophosphate concentrations and shaking periods on the natural zeolite adsorption.

3. To investigate the behavior of phosphorus adsorption on natural zeolite after calcination at various temperatures.

Scope of Research:

1. To focus on the temperature of calcination from 0°C to 900°C.

2. To study the orthophosphate concentration of 5, 10, 20, and 30 mg-P/L and shaking time of 20, 40, 60, 120, 180, and 240 minutes.

3. Materials used to study the orthophosphate adsorption were natural adsorbents including natural zeolite, diatomite, perlite, ball clay, and kaolin.

LITERATURE REVIEW

Phosphorus from wastewater is one pollutant that has an effect on the environment and humans. Phosphorus is a major source of eutrophication - algal bloom- (Henri, 1996). Therefore, scientists attend to eliminate phosphorus from water source in order to prevent eutrophication water pollution.

Definition of phosphorus

Phosphorus is the 15th element in the periodic table. It has five valence electrons: three solitary and one doublet. It forms three covalent bonds involving the solitary electrons and one can predict that this atom should be able to form a semipolar bond by doublet exchange. This possibility is perfectly illustrated by the phosphorus anhydride molecule (P_2O_5) (Henri, 1996).

The P_2O_5 molecule reacts with water to orthophosphate acid form:

$$P_2O_5 \ + \ 3H_2O \longrightarrow 2H_3PO_4$$
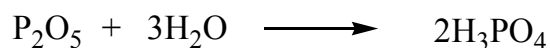
This triacid can undergo successive ionization to yield the ions:

$$H_3PO_4 \rightleftharpoons H_2PO_4^- \ + \ H^+ \qquad \text{with } pK_1 = 2.16$$
$$H_2PO_4^- \rightleftharpoons HPO_4^{2-} \ + \ H^+ \qquad \text{with } pK_2 = 7.16$$
$$HPO_4^{2-} \rightleftharpoons PO_4^{3-} + \ H^+ \qquad \text{with } pK_3 = 12.40$$
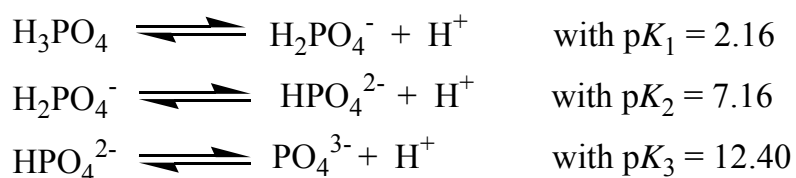
The pH-dependent partitions of total phosphate among these four forms are as shown in Figure1.
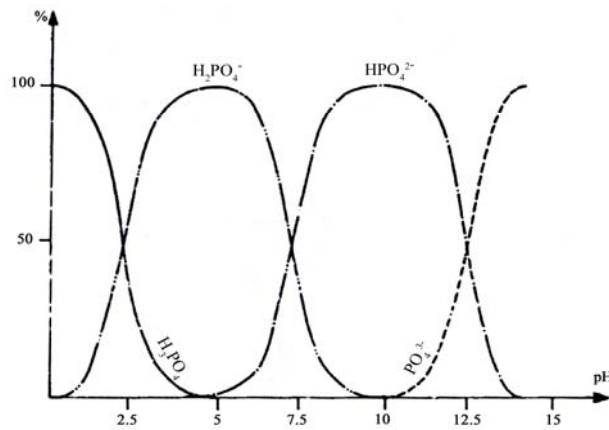
Figure 1 pH-dependent variation of phosphorus speciation.
Source: Henri (1996)

Role and importance of phosphorus in pollution

Phosphorus is responsible for nearly all of the pollutant compounds presented in domestic or urban wastewaters. Approximately 50% to 70% of wastewater phosphate compounds are in orthophosphate form, the balance being polyphosphates and organic phosphorus compounds (Henri, 1996). Because polyphosphates and organic phosphorus compounds are hydrolyzed as they pass through a biological treatment plant, so the phosphorus present in the effluent is 90% orthophosphate form (Henri, 1996). The various sources of these compounds in municipal wastewaters are shown in Table1.

Table 1 The sources of phosphorus compounds in municipal wastewaters

sources	quantity (g/person-equivalent)
Metabolic contributions	1.5
Food preparation and cooking	0.3
Detergents	2.1 to 2.3

Source: Henri (1996)

Phosphorus removal

1. Biological phosphorus removal

Microorganisms are used to remove phosphorus in wastewater. Biological processes are configured to encourage the growth of bacteria with the ability to take up and store large amounts of inorganic phosphorus. Due to biomass having a specific gravity slightly greater than water, the biomass can be removed from wastewater by gravity settling.

Biological treatment is the traditional method of phosphorus removal. Biological phosphorus removal in an activated sludge system is caused by bacteria (Subramanial and Arnot, 2001), which are able to store phosphate intracellularly as polyphosphate. The bacterial cells consume polyphosphate by changing it into the form of orthophosphate. There utilize polyphosphate as an energy source and the excreted orthophosphate leaves the system or can be stripped from the biomass. The biomass is retained inside the reactor behind the anaerobic membranes and the resulting high sludge ages losing the potential benefit of a high efficiency of phosphorus released as solids can cause fouling, and reduction in membrane flux.

In conventional sludge activation process (Fresenius *et al*., 1989), the mechanical stage of conventional mechanical-biological systems can reduce phosphorus concentration in fresh sludge from about 15 to 20 mg-P/L to about 10 to 15 mg-P/L and in the joining biological stage i.e. activation or biological filter system, to about 5 to 10 mg-P/L.

There are combination uses of microorganisms and adsorbent to increase the capability of phosphorus removal. Hrenović *et al*. (2003) investigated the influence and performance of the addition of support material on the orthophosphate uptake in a pure culture of *A. calcoaceticus*, and addition of natural zeolite or clay in the aerobic phase resulted in a significantly higher final efficiency of phosphate removal. The amount of phosphate removed depended on particle size and type of material used.

To eliminate phosphorus by algae, the process is to combine the oxidation trench containing an algal activated sludge mixture and a subsequent precipitation stage with the addition of a precipitation reagent such as sodium hydroxide and calcium hydroxide. In this process, the phosphate concentration can be reduced to about 0.6 to 0.9 mg-P/L.

As a result of biological treatment of phosphate, phosphate concentration is reduced mainly by its storage into biological cell mass. It makes phosphate elimination depend on intricate conditions such as pH, temperature, and oxygen dissolved in water, which are optimum conditions for bacterial growth.

Even though phosphorus removal by biological treatment reduces chemical costs and lessens sludge production as compared to chemical

precipitation, it has a longer time for treatment of wastewater than chemical precipitation. Moreover, the phosphorus removal by biological treatment is difficult and complicated operation.

2. Chemical phosphorus removal

Phosphorus is removed from wastewater using chemical reagents, for example, aluminum, calcium, and iron salts, to precipitate phosphorus. The phosphate precipitates are insoluble and flocculates aid removal of suspended matter.

Chemical treatment is the chemical precipitation of phosphorus by the addition of the salts of multivalent metal ions that form precipitates of sparingly soluble phosphate.

In ion exchange, Jorgensen (1973) used a new wastewater treatment system examined on a pilot plant scale. Approximately 400 g of calcium hydroxide, 100 g of bentonite and 1 g polyflocculant were used in ion exchange process per m^3. This was followed by an ion exchange process on a weak base anion exchanger removing phosphate and nitrate.

In the coagulation process, experiments were conducted by Simmonds (1973) to determine the efficiency of phosphate removal. Aluminium sulphate was used in coagulation tests. The coagulation experiments were conducted to determine the efficiency of phosphate removal. The study was performed on different samples of sewage with different initial concentrations of phosphate. The results indicated that, after the initial coagulation requirement of the sewage had been satisfied, these were a requirement for precipitation of

aluminium phosphate. Boisvert *et al.* (1997) used aluminium sulphate (alum) and poly-aluminium-silicate-sulphate (PASS) for coagulation of phosphate. The results indicated that phosphate ion binding by alum and PASS where the interaction involved H^+ or OH^- transfer depended on the pH range 5-7. In some conditions, low pH, size of PO_4 ions and the resistance to shear stress, PASS was found better than alum for coagulation. Akay *et al.* (1998) used red mud as a coagulant in crossflow microfiltration. The results shown that the colloidal red mud particles could coagulate phosphate ions. Seida and Nakano (2002) studied phosphate removal using layered double hydroxides containing iron. Iron-based layered double hydroxides were synthesized, consisting of Mg^{2+}, Ca^{2+}, Fe^{3+} ions. When cations and/or hydroxides were released, it worked effectively as a coagulant for the phosphate removal. Özacar and Şengil (2003) used polyelectrolytes, tannin (natural polyelectrolyte) and AN913 (synthetic anionic polyelectrolyte), and clay in coagulation/flocculation processes for water treatment. The results found that alum was the most effective coagulant at all phosphate concentrations. Adding clay, tannin and AN913 significantly increased phosphorus removal efficiency and addition of coagulants significantly decreased the required alum dose.

3. Physicochemical phosphorus removal

Physicochemical removal is a process to co-eliminate phosphorus removal from wastewater by physical and chemical treatment. Methods are used to eliminate contaminants such as adsorption, ion exchange, ultrafiltration, reverse osmosis, and electrodialysis.

There are many ion exchangers that are used for phosphate removal. Gregory and Dhond (1972) studied anion exchange equilibria involving phosphate, sulphate, and chloride. They investigated different anion exchange resins in order to determine their applicability in the removal of phosphate from wastewater. All synthetic ion exchange resins consisted of a polymeric matrix with chemically bound ionic groups throughout the resin structure. There found the ability of phosphate adsorption on their surface related to the type of functional group. Moreover, Liberti *et al.* (1979, 1981, and 1986) used Kestel as a strong base anion resin to removed phosphate. The results found an average phosphate removal of more than 95%. In 1998, Zhao and Sengupta used a new class of sorbent, referred to as polymeric ligand exchanger (PLE), to remove phosphate from contaminated wastewater. Their works showed strong evidence that the PLE was very selective toward phosphate, chemically stable, and also amenable to efficient regeneration.

Wastewater is the one pollution which has effect on the environment and a human. Wastewater from domestic or urban has elements- phosphorus, carbon, and nitrogen- which they are responsible for nearly the entire pollutant compound (Henri, 1996). Domestic wastewater is produced by plant workers, shower facilities, and cafeterias. The statistic of human using the tap water to consume in Bangkok and other provinces are about 440 and 150 liters per person per day respectively (Udomsinrod, 1996). Therefore, in the city will be has effluence and the tendency of wastewater pollution higher than in the country.

The physical characteristics of domestic wastewater have the odor of freshly turned earth. Fresh sewage is gray color but septic sewage is black color. Septic sewage is considerably more offensive to the olfactory nerves. It

is rotten egg odor of hydrogen sulfide and the mercaptans. In general, the temperature of the wastewater will be higher than the water supply normally by 10 - 20°C. This is because of the addition of warm water from households and heating within the plumbing system of the structure.

Due to the number of chemical compounds found in wastewater are almost limitless, so chemical characteristics normally restricting its consideration to a few general classes of compounds three typical compositions of untreated domestic wastewater were summarized in Table 2. The pH of these wastewaters will be in the range of 6.5 to 8.5. Industrial wastewater composition may be significantly different from domestic wastewater.

Table 2 Typical composition of untreated domestic wastewater

Constituent	Weak	Medium	Strong
	(all mg/L except settle able solids)		
Alkalinity	50	100	200
BOD_5	100	200	300
Chloride	30	50	100
COD	250	500	1,000
Suspended solids (SS)	100	200	350
Settle able solids, ml/L	5	10	20
Total dissolved solids (TDS)	200	500	1,000
Total Kjedahl nitrogen (TKN)	20	40	80
Total organic carbon (TOC)	75	150	300
Total phosphorus (as P)	5	10	20

Source: Machenzie and David (1991)

Domestic effluents generally contain elevated phosphorus concentration, largely as orthophosphate, which is then discharged to surface waters. The problems created when phosphorus is discharged to surface water well known and largely involve accelerated eutrophication such as lake, ponds, and reservoirs. Recently, the scientists have demonstrates an adsorption to pollution treatments (such as Liu Ruixai *et al.,* 2002). Therefore, adsorption is an interesting method to study.

Definition of surface and interfaces

The term *surface* is the outer boundary of an artifact or material layer. It is an area in which the properties vary from those of one phase to those of the connecting phase. This transition occurs over distances of molecular dimensions at least. *Interface* is the point of interconnection between two distinct but adjacent communications systems having different function.

General definition

Some of the principal terms and properties associated with adsorption and porous solids were defined in Table 3 and Table 4, respectively.

Table 3 Definitions: adsorption

Term	Definition
Adsorption	Enrichment of one or more components in an interfacial layer
Adsorbate	Substance in the adsorbed state
Adsorbent	Solid material on which adsorption occurs

Table 3 Definitions: adsorption (Cont'd)

Term	Definition
Chemisorption	Adsorption involving chemical bonding
Physisorption	Adsorption without chemical bonding
Surface coverage	Ratio of amount of adsorbed substance to monolayer capacity
Monolayer capacity	Ether chemisorbed amount required to occupy all surface sites or physisorbed amount required to cover surface

Source: Rouguerol *et al.* (1999)

Table 4 Definitions: porous solids

Term	Definition
Porous solid	Solid with cavities or channels
Open pore	Cavity or channel with access to the surface
Closed pore	Cavity not connected to the surface
Pore volume	Volume of pores determined by stated method
Pore size	Pore width (diameter of cylindrical pore or distance between opposite walls of slit)
Porosity	Ratio of total pore volume to apparent volume of particle
Surface area	Extent of total surface area as determined by given method under stated conditions
External surface area	Area of surface outside pore
Internal surface area	Area of pore walls

Source: Rouguerol *et al.* (1999)

From Table 3, the term *adsorption* is the enrichment of one or more of the components in the region of surface or interface between two phases. In any solid or liquid, atoms at the surface are subject to unbalanced forces of attraction normal to the surface plane. These forces are merely extensions of the forces acting within the body of material and are ultimately responsible for the phenomenon of adsorption.

Investigation into adsorption should provide information concerning the amount of a substance which can be adsorbed on a surface, the influence of pressure and temperature on this amount, and the strength of the adsorption bond. Investigation should also reveal the changes which the adsorbing surface and the adsorbed particles undergo as a result of adsorption, and desorption should be given of the condition of the orbital which take part in the adsorption bond.

Researchers have used different materials as adsorbent for eliminating phosphorus. Liu Ruixai *et al.* (2002) studied the adsorption properties, including adsorption rate, adsorption isotherm, and effect of solution conditions on adsorption, of phosphate, fluoride, and arsenate onto a newly developed ion exchange fiber, that was polyacrylonitrile fiber. They found that the adsorption properties of the ion exchange fiber for three anions depended on the pH value and anion concentration. The adsorption percentage of phosphate was more than 99% in the pH range of 3.0 to 5.5 (Liu Ruixai *et al.*, 2002). This study used the Freundlich model to describe the adsorption equilibrium data. The adsorption of phosphate on the ion exchange fiber was a rapid process. Adams *et al.* (1987) studied the adsorption of phosphate by soils. The soil used in that experiment was treated by extraction with oxalate, citrate and dithionite, and sodium hydroxide. Barrow (1984) studied the effect

of pH on phosphate adsorption by soils. The effect of pH on phosphate adsorption differed between soils. For unfertilized soils, increase in pH up to about 5.5 decreased adsorption. For fertilized soils, measured adsorption increased with pH. Clark *et al.* (1997) used sand, activated carbon, peat-moss, zeolite, compost, cotton milling waste product and a chemically-modified agrofiber for filtration of pollutants. Phosphate adsorption was also measured in all the media. It was found that the compost filter leached phosphate throughout the testing period. Eighty percent of the sorption capacity of phosphate had been used when the cumulative loadings to the columns were greater than 0.2 mg-PO_4^{3-}/g zeolite, 0.5 mg-PO_4/g peat, 1.5 mg-PO_4^{3-}/g carbon, and 3 mg-PO_4^{3-}/g agrofiber. Sakadevan and Bavor, (1998) studied the phosphate adsorption characteristics of soil, slags and a clinoptilolite material (zeolite) to be used as substrates in constructed wetland systems and examined the potential to improve their adsorption characteristics. The experiment used Freundlich and Langmuir adsorption isotherms to describe the adsorption behaviors.

The principles of adsorption

In the fundamentals of adsorption, it is useful to distinguish between physical adsorption (physisorption) and chemical adsorption (chemisorption).

1. Physisorption

Physisorption involves the balancing of a weak attractive force, for example, of van der waals, between the surface and the adsorbate, with the repulsive force associated with close contact. The process is always exothermic and the energy given out on adsorption, the heat of adsorption,

ΔH_{ads}, is low, typically in the region -10 to -40 kJ mol^{-1} (McCash, 2001). Physisorption is non-specific and any atom or molecule can adsorb on any surface under appropriate experimental conditions; large amounts of physisorption are favored when the surface is at low temperature.

2. Chemisorption

Chemisorption is characterized mainly by a strong chemical bond forming between the surface and the adsorbate. Because chemisorption involves chemical bonding, also, it involves the exchange of electrons between the adsorbing molecule and surface. The heats of adsorption for chemisorption are generally larger than for physisorption. ΔH_{ads} tends to be in the range -40 to -1000 kJ mol^{-1} (McCash, 2001) and it is found that chemisorbed layers with large heats of adsorption tend to be very stable at high temperature. The bond formed may be ionic, covalent, or a mixture of the two.

<u>The comparison of chemisorption and physisorption</u>

A summary to compare the chemisorption and physisorption processes in order to help to distinguish between them follows in Table 5.

Table 5 Comparison of chemisorption and physisorption processes.

	Chemisorption	Physisorption
ΔH_{ads}	-40 to -1000 kJ mol^{-1}	-10 to -40 kJ mol^{-1}
kinetic of activation	can be activated	non-activated
number of layer	monolayer	multilayer
chemical reaction	can cause reactivity change in the adsorbate	little change
specificty	normally dependent on specific adsorbate surface interaction	non-specific, needs low temperature to get substantial amounts

Source: McCash (2001)

Energetic of adsorption

The thermodynamics of adsorption only enables one to obtain the magnitude of the bond strength in adsorption; one cannot also discover the nature of the forces involved in bonding. A number of quite different types of forces are responsible for the bonding which keeps the adsorbate and adsorbent together. The forces may be identified as:

1. Dispersion forces

Dispersion forces arise from fluctuations in the electron density clouds of two atoms. The time average of the charge distribution in these atoms may be symmetrical, yet the charge fluctuations are sufficient to induce resonance and cause an attraction. The resultant force has a relatively long range. Thus, they often account for the major part of the adsorbate-adsorbent

potential. These forces exist in all types of matter and always act as an attractive force between adjacent atoms and molecules no matter how dissimilar.

2. The overlap or repulsive forces

When an adsorbate molecule comes very near to a solid surface molecule to allow interpenetration of the electron clouds, a repulsive interaction will arise and their electron orbitals or eigen functions overlap.

3. Dipole interaction

These forces arise in addition to the above forces whenever a non polar adsorbate is adsorbed on a polar adsorbent, or whenever a polar adsorbate is adsorbed on a non-polar or a polar adsorbent. In the latter instance, the action of the polar partner is also to induce an electric moment in the non-polar molecule.

4. Valency forces

Valency forces are similar to the repulsive forces in that they arise at sufficiently close distances. They arise owing to the electron orbitals overlapping in a suitable way and they are responsible for chemisorption.

5. Interaction forces

These are the forces between the atoms or molecules of the bound adsorbate themselves. These forces must be considered in both physisorption

and chemisorption when the coverage of adsorbate on the adsorbent attains the stage at which the distance separating adsorbate molecules is small.

Adsorption equilibria

Adsorption from aqueous solution involves concentration of the solute on the solid surface. The term adsorption equilibrium is an equilibrium state in which equal amounts of solute eventually are being adsorbed and desorbed simultaneously; in other words, the rate of adsorption equals desorption. Therefore, at equilibrium, no change can be observed in the concentration of the solute on the solid surface or in the bulk solution.

Adsorption isotherm

Adsorption isotherm is the presentation of the amount of solute adsorbed per unit of adsorbent as a function of the equilibrium concentration in bulk solution at constant temperature. Measurements of isotherms can be made using either gravimetric or volumetric techniques. The shape of the adsorption gives qualitative information about the adsorption process and the extent of the surface coverage by the adsorbate. The five main shapes of adsorption isotherm are shown in Figure 2.
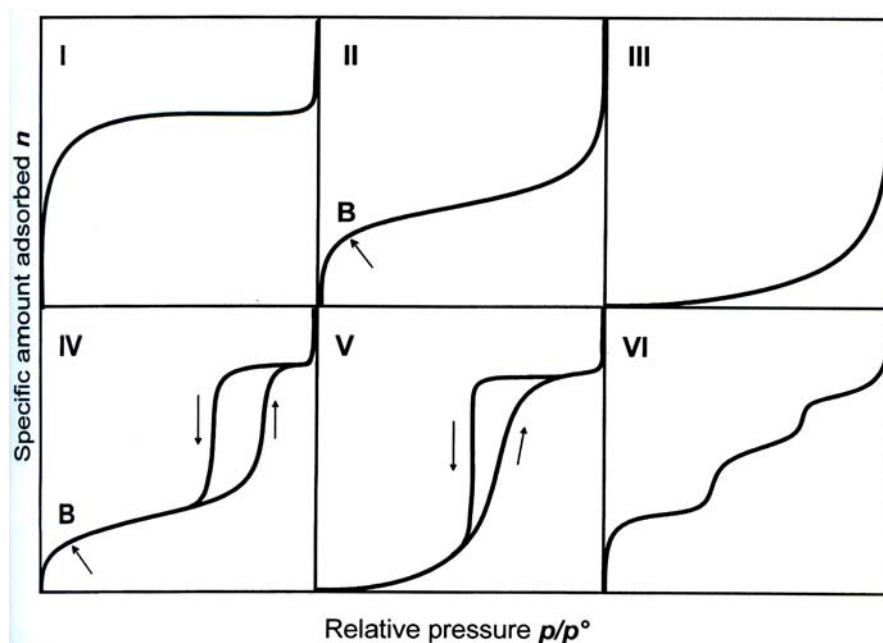
Figure 2 The five main shapes of adsorption isotherm, given as plats of
coverage against equilibrium pressure.

Source: Elain M. McCash, 2001

The type I is associated with systems where adsorption does not proceed
beyond the monomolecular layer. This isotherm describes ideal chemisorption,
where molecules chemisorb unit the surface becomes saturated with adsorbate,
whereupon adsorption ceases. The type II is a further increase in the amount
adsorbed and many layers are ultimately adsorbed. This type is usually
associated with physisorption. The other three types: the type III is associated
with multilayer formation from the onset, and types IV and V are associated
with formation of monolayer where there are variations of heat of adsorption
with θ.

The Langmuir adsorption isotherm

This is the most commonly used model for an adsorption isotherm and describes ideal chemisorption systems. The assumptions made in this model, which is also called *the ideal localized monolayer*, is that:

1. Adsorption occurs on specific sites and all adsorption sites are identical.
2. Each site can accommodate only one molecule i.e. monolayer.
3. The energy for the adsorption is independent of how many of the surrounding sites are occupied and it is the same at all sites.
4. The adsorbed molecule cannot migrate across the surface or interact with adjacent molecules.

The Langmuir equation was originally derived from kinetic consideration.

$$\text{Rate of adsorption} \ = \ k_a P(1-\theta) \qquad\qquad\qquad (\text{eq.1})$$
$$\text{Rate of desorption} \ = \ k_d \theta \qquad\qquad\qquad (\text{eq.2})$$

Where $\quad \theta$ = fraction of the site already filled
$\qquad (1-\theta)$ = fraction of the site to be vacant
$\qquad\quad k_a$ = rate of adsorption
$\qquad\quad k_d$ = rate of desorption from a fully covered surface
$\qquad\quad P$ = pressure

At equilibrium the amount of molecules in the adsorbed state is constant; thus:

$$k_a P(1-\theta) = k_d \theta \qquad\qquad\qquad (\text{eq.3})$$

and

$$\frac{\theta}{(1-\theta)} = \frac{k_a}{k_d} p \qquad \text{(eq.4)}$$

Taking $k_a/k_d = b$, which is the adsorption equilibrium constant. Therefore, Equation 4 becomes:

$$bP = \frac{\theta}{1-\theta} \qquad \text{(eq.5)}$$

or

$$\theta = \frac{bP}{1+bP} \qquad \text{(eq.6)}$$

This is known as the Langmuir adsorption isotherm. For adsorption from solution by solid adsorbents, the Langmuir adsorption isotherm is expressed as:

$$X = \frac{X_m bC_e}{1+bC_e} \qquad \text{(eq.7)}$$

Where $X = x/m$, which is the amount adsorbed per unit weight of adsorbent (the same as Freundlich equation)

X_m = amount of solute adsorbed per unit weight of adsorbent Required for monolayer coverage of the surface i.e. monolayer capacity

C_e = equilibrium concentration of the solute

b = constant related to the heat of adsorption

For linearization of the data, Equation 7 can be written in the form

$$\frac{C_e}{X} = \frac{1}{bX_m} + \frac{C_e}{X_m} \qquad \text{(eq.8)}$$

Dividing Equation 8 by C_e:

$$\frac{1}{X} = \frac{1}{X_m} + \left(\frac{1}{C_e}\right)\left(\frac{1}{bX_m}\right) \qquad \text{(eq.9)}$$

Plotting $1/X$ against $1/C_e$ is straight-lined

$$\text{slope} = \frac{1}{bX_m}$$

$$\text{intercept} = \frac{1}{X_m}$$

The Langmuir isotherm can be determined the monolayer capacity (X_m), where X_m defines the total capacity of the adsorbent for a specific adsorbate.

The Freundlich adsorption isotherm

This form of isotherm was developed to take into account the observation of a coverage dependence of the heat of adsorption. For the Freundlich adsorption equation is perhaps the most widely used mathematical description of adsorption in aqueous systems. The assumptions made in the Freundlich isotherm are:

1. The heat of adsorption declines logarithmically with coverage so $\Delta H = -\Delta H_m \ln \theta$ (ΔH_m, the heat of adsorption for the monolayer, is a constant for a given system).

2. θ has values which do not approach 0 or 1, that is, it applies for intermediate coverage only, usually in the range 0.2-0.8.

3. This isotherm can be applied to both chemisorption and physisorption systems.

Empirically, the Freundlich equation is expressed as:

$$\frac{x}{m} = KC_e^{\frac{1}{n}} \qquad (eq.10)$$

Where x = amount of solute adsorbed

m = weight of adsorbent

C_e = solute equilibrium concentration

K and $1/n$ = constants characteristic of the system

For linearization of the data, it is written in logarithmic form

$$\log\frac{x}{m} = \log K + \frac{1}{n}\log C_e \qquad (eq.11)$$

Substituting $C_o - C_e$ in Equation 11 for x

$$\log\left(\frac{C_o - C_e}{m}\right) = \log K + \frac{1}{n}\log C_e \qquad (eq.12)$$

Where C_o = initial concentration

Plotting $\log(C_o - C_e)/m$ versus $\log C_e$ should give a straight line.

$$\text{slope} = \frac{1}{n}$$

$$\text{intercept} = \frac{1}{K}$$

The Brunauer-Emmett-Teller (BET) adsorption isotherm

The Langmuir isotherm is limited to the adsorption of one monolayer of adsorbate. The formation of multilayers is modeled by BET isotherm and this essentially uses the basis of the Langmuir model and extends it to encompass physisorbed multilayer. The assumptions made are that:

1. Each layer of adsorbate is treated as a Langmuir monolayer and each layer must be complete before the next layer starts to form.
2. The heat of adsorption for the first layer is characteristic of the adsorbate/adsorbent system.
3. The heat of adsorption for subsequent layers is equal to the heat of condensation.

The resulting equation for BET equilibrium isotherm is

$$V = \frac{V_m BP}{(P_o - P)[1 + (B-1)P/P_o]} \qquad \text{(eq.13)}$$

Where V = volume of gas adsorbed at pressure

V_m = volume adsorbed at infinite pressure

P_o = saturation vapor pressure of the saturated liquid sorbate

B = constant

by

$$B = \frac{a_1 b_2}{a_2 b_1} e^{(E_1 - E_L)/RT}$$ (eq.14)

which can be simplified to

$$B = e^{(E_1 - E_L)/RT}$$ (eq.15)

Where a_1 and a_2 = rate of condensation on the first and second layers

b_1 and b_2 = rate of evaporation from first and second layers

E_1 = heat of adsorption at first layer

E_L = heat of liquefactions of the bulk phase

the term $E_1 - E_L$ is the net heat of adsorption.

For the adsorption from solution, the application of the BET equation takes the form

$$X = \frac{X_m B C}{(C_s - C_e)[1 + (B-1)C_e / C_s]}$$ (eq.16)

Where C_s = solubility of the solute in water at a specified temperature.
Transforming Equation 16 to

$$\frac{C_e}{X(C_s - C_e)} = \frac{1}{X_m B} + \frac{(B-1)}{X_m B} \frac{C_e}{C_s}$$ (eq.17)

plotting $\dfrac{C_e}{X(C_s - C_e)}$ versus $\dfrac{C_e}{C_s}$ should give a straight line

$$\text{slope} = \frac{(B-1)}{X_m B}$$

$$\text{intercept} = \frac{1}{X_m B}$$

Adsorption on surfaces can take place via three mechanisms illustrated in Figure 3:

1. The inner-sphere surface complex involves the cavity.
2. The outer-sphere surface complex includes the cation salvation shell.
3. The diffuse-ion swarm involves ions that are fully dissociated from surface functional groups and freeing to nearby in solution.
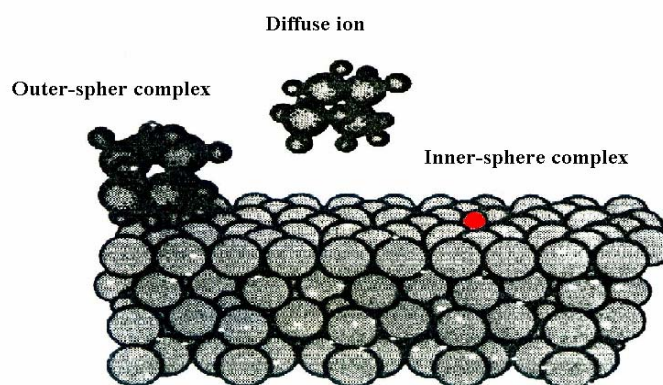
Figure 3 The three mechanism of ions adsorption on siloxane surface

Source: Sposito (1989)

(a)   (b)
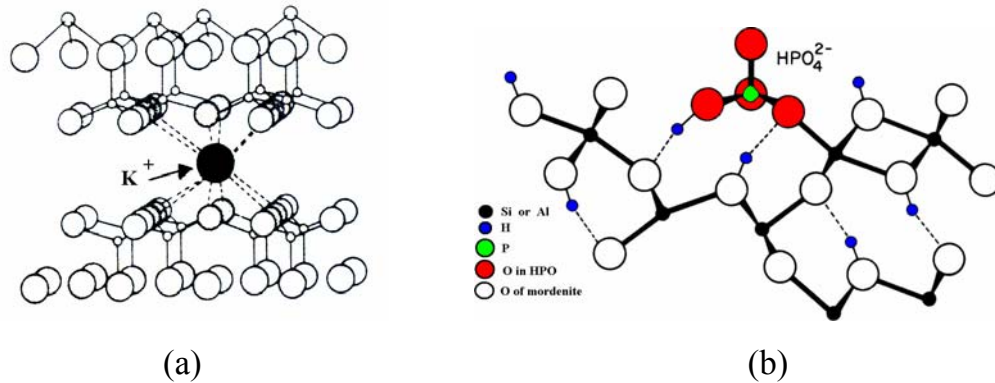
Figure 4 (a) inner-sphere surface complex of K^{2+} on mordenite

(b) inner-sphere surface complex of HPO_4^{2-} on mordenite

Source: Sposito (1989)

Surface charge

Zeolite surfaces develop electrical charge in two principal ways: either from isomorphic replacement among ions of different valence in zeolite, or from the reactions of surface functional groups with ions in solution (Sposito, 1989).

The net total particle charge, σ_P, is parameter depending on chemical conditions. It can represent by equation:

$$\sigma_P = \sigma_0 + \sigma_H + \sigma_{IS} + \sigma_{OS} \qquad (eq.18)$$

Where σ_0 = permanent structural charge

σ_H = net proton charge

σ_{IS} = inner-sphere complex charge

σ_{OS} = outer-sphere complex charge

which

$$\sigma_H = q_H + q_{OH}$$

Where q_H and q_{OH} = mole of ion H^+ and OH^-

When the surface charge is non zero, σ_P must be balanced with the diffuse-ion swarm. This ions move about freely near enough to zeolite surface to create the effective surface charge, σ_D. The statement of the balance of surface charge represent by equation:

$$\sigma_P + \sigma_D = 0 \qquad\qquad (eq.19)$$

From this equation, points of zero charge are pH values at which one or more of surface charge components vanishes. Table 6 showed the most important points of zero charge.

Table 6 Some points of zero charge

Name	Symbol	Defining condition
Point of zero charge	PZC	$\sigma_P = 0$
Point of zero net proton charge	PZNPC	$\sigma_H = 0$
Point of zero net charge	PZNC	$\sigma_{IS} + \sigma_{OS} + \sigma_D = 0$

Source: Sposito (1989)

From Table 6, PZNC equals zero when the moles of adsorbed cation charge equals the moles of adsorbed anion charge, if cations and anions in surface complexes balance in charge, there will be no need for a diffuse ion swarm contribution ($\sigma_D = 0$), from equation 19, it made also $\sigma_P = 0$, thus PZNC equal PZC.

Iso-electric point (IEP) is parameter for characterizing surface properties of colloids. It is the pH at the net charge on the slip surface of the electric double layer is zero and so the potential equals zero. The relationship between the overall PZC of a mixture and the individual IEP of each component are eq.20.

$$PZC = \sum_i f_i IEP_i \qquad \text{(eq.20)}$$

Where f_i = the fraction of i component

IEP$_i$ = the IEP of component i

<u>Type of adsorption on the surface</u>

Soil on earth may be classified into two basic categories: permanent charge soil and variable charge soil (Yu, 1997). The permanent charge soil is surface charges of layer silicate minerals. The variable charge soil is surface charges of free oxide, iron, aluminum, manganese oxide and humus. It is difficult to have a clear-cut definition between the two categories of soils.

The charges on surface can be positive or negative charges, thus the counter ions adsorbed on surface contain could be cation and anion. There are four types of adsorption force (Yu, 1997).

1. Electrostatic adsorption of cations

Electrostatic adsorption of cations is the adsorption of cations by particle which the interaction force between cations and the surface of particle

during adsorption is electrostatic in nature. The heterogeneity in distribution of ions in soil colloidal systems is interpreted mainly in terms of electrostatic interactions occurring at the interface between soil colloidal particles and the liquid phase. When cations are electrostatically adsorbed by negatively charge soil, it can be expected that the affinity of soil colloid surface for cations of different valencies should generally be of the order $M^+ < M^{2+} < M^{3+}$.

2. Electrostatic adsorption of anions

Electrostatic adsorption of anions is the adsorption subject to attractive force of positive charges and repulsive force of negative charge carried by particle, and they stay in the outer layer of the electric double layer through dynamic balance between electrostatic attraction and thermal motion. Some anion species both electrostatic force and specific force may be involved during their interactions with variable charge soils.

3. Specific adsorption of cations

Specific adsorption of cations is the adsorption of cations by particle with specific forces between the surface of particle and cations. This adsorption is related to both the nature of cations and the surface properties. Most of cation species can be adsorbed specifically to the surface of soil. Examples belong to heavy metals, such as copper, zinc, and cobalt, belong to heavy metals. Alkali metal and alkaline earth metal ions can also be adsorbed specifically to some extent by soil under certain conditions. Nevertheless, specific adsorption is less importance when compared to electrostatic adsorption and the mechanism involved may be different from that for heavy metals. The reason of the difference in properties between the transition metal

ions and alkali metal and alkaline earth metal ions with respect to adsorption lies primarily in the difference in their atomic structure. The transition metal ions are characterized by a large amount of electric charge in the atomic nucleus, small ionic size, and strong polarizability. By contrast, alkali metal and alkaline earth metal ions are characterized by a smaller amount of electric charge in the atomic nucleus, larger ionic size, and weak polarizability.

4. Coordination adsorption of anions

Coordination adsorption of anions is the specific adsorption of anions by particle. For anions, the mechanism of specific adsorption is ligand exchange between these ions and some groups that have already been coordinating linked on the surface of particles. For variable charge soil, phosphate is the strongest specifically adsorbed anion species. The valence status of phosphate ions is trend to change with the change in environmental conditions. Therefore, the phenomenon of phosphate adsorption is rather complex and it is often difficult to make definitive interpretations of experimental results. Al-OH, Fe-OH, Al-OH$_2$, and Fe-OH$_2$ groups on the surface of soil particles are the important sites for coordination adsorption of anions. Consequently, when a soil contains large amounts of aluminum and iron oxides, the phenomenon of coordination adsorption of anions will be more pronounced.

Zeta potential

Zeta potential (ζ) can be defined as the potential at the surface of shear. It is probably fairly close to the stern potential in magnitude, and definitely less than the potential at the surface (Hiemenz and Rajagopalan, 1997). The

relative values of these different potentials are shown in Figure 5. Distances within the double layer are considered large or small, depending on their magnitude relative κ^{-1}. Thus in dilute electrolyte solutions, in which κ^{-1} is large, the surface of shear- which is close to the particle surface even in absolute units- may be safely regarded as coinciding with the surface in units relative to the double layer thickness.

Stern is to divide the aqueous part of the double layer by the hypothetical boundary known as the *stern surface* or stern plane (Hiemenz and Rajagopalan, 1997). The stern surface is situated a distance (δ) from the actual surface. The stern surface is drawn through the ions that are assumed to be adsorbed on the charge wall.
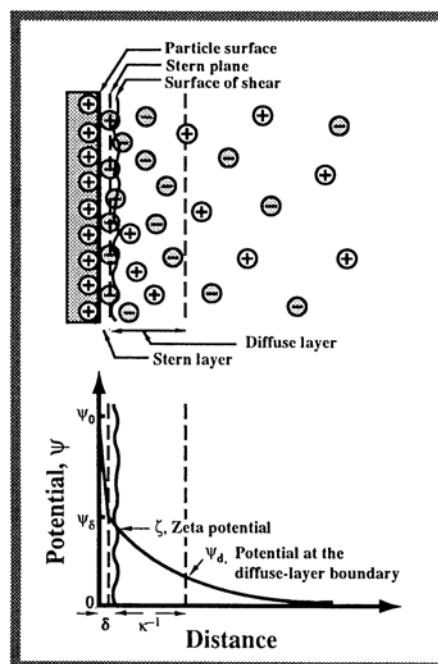
Figure 5 The variation of potential with distance from a charged wall in the presence of a Stern layer

Source: Hiemenz and Rajagopalan (1997)

Effect of temperature on amount adsorbed

The effect of temperature on the amount of material chemisorbed at equilibrium varies in a complex way with different systems. For gas system, the amount is usually correlated with the relative pressure. At lower temperature, the amount observed to be chemisorbed is frequently less than this because the rate of adsorption is so low that saturation is not reached.

Effect of time on amount adsorbed

In general, when the time of adsorption increasing amount of adsorbed is also increasing until the adsorption achieve equilibrium. At equilibrium, the rate of adsorption equal the rate of desorption lead into the maximum of adsorbed on adsorbent. The time after equilibrium, amount of adsorbed is decreasing because the rate of desorption more than the rate of adsorption.

Zeolites are the most materials use in industry. There was used to pollutants removal, catalyst including the reactants for various reactions.

Definition of Zeolite

Zeolites are mainly compounds of crystalline, naturally-occurring aluminosilicate minerals. They have a three-dimensional framework structure bearing $[SiO_4]^{4-}$ and $[AlO_4]^{5-}$ coordination polyhedra linked by all their corners. Their frameworks generally are very open and contain channels and cavities in which are located water molecules and cations. Water molecules are readily lost and regained when the zeolites are heated and cations often have a high degree of mobility giving rise to easy ion exchange. In their channels and

cavities they are able to selectively take up some molecules into porous structure.

There are 39 kinds of natural zeolites and about 100 kinds of synthesized zeolites (Dyer, 1998). Natural zeolites are formed by hydrothermal transformation of basalt, volcanic ash, and pumice which can be found e.g. in basalt cavities and in large sedimentary deposits. The most important industrial natural zeolites are clinoptilolite, mordenite, chabazite, and erionite. Synthesized zeolites are synthesis of crystalline from an inhomogeneous gel, created from a silica sources and an alumina sources, combined with water under high pH conditions generated by hydroxyl ion concentrations. Control of the SiO_2:Al_2O_3 ratio in this gel qualifies the final framework composition of the product taken into the zeolite composition

Structure of zeolites

Zeolites have framework structures constructed by joining $[SiO_4]^{4-}$ and $[AlO_4]^{5-}$ coordination polyhedra. These tetrahedra are assembled together so that the oxygen at each corner is shared with an identical tetrahedron, Si or Al, as shown in Figure 6.

Figure 6 The tetrahedra linked together to create a three-dimensional structure
Source: Dyer (1988)

Composition of zeolite consist of Si, Al, and O positions in space relative to each other and excluding cations and water molecules sited within cavities and channels of framework.

Zeolites are a porous solid and as promoters in liquid-phase organic reactions provide some advantages:

1. Easy to separate products from solids by means of a sample procedure of filtration.

2. Adsorption or inclusion of reagent molecules into the small pores of solids with nanometer dimensions organizes the molecules in close proximity to lower the activation entropy of reaction.

3. The coexisting acid and base sites on solid surfaces accelerate organic reactions.

4. Pore structures of the solid discriminate between reactant molecules with respect to molecular dimensions.

Natural zeolite

In nature, the zeolites are often formed where volcanic rock of specific chemical composition is immersed in water so as to leach away some of the components. The composition and pore size depend upon what kinds of rock minerals are involved.

Mordenite is a kind of natural zeolite. Their structure type is MOR and based upon the 5-1 units in SBU's. The 5-1 units are linked into a series of chains joined together to form major channels, one restricted by 12 oxygen windows and one by 8 oxygen windows.
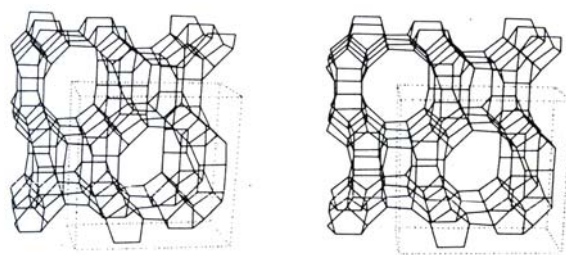
Figure 7 The structure of mordenite

Source: Dyer (1988)

Mordenite is found widespread in industrial applications as highly selective adsorbents, ion exchangers and, most importantly, catalysts of exceptionally high activity and selectivity in a wide range of reactions. Hayakawa *et al.* (1996) studied adsorption of cationic surfactants on mordenites. This study found adsorption isotherms of dodecyltrimethy-lammonium bromide (DTAB) and decyltrimethylammonium bromide (DeTAB) on mordenites were dependent on Si/Al ratios. DTAB showed a stronger adsorption than DeTAB did and both surfactants interacted more strongly with mordenites of higher Si/Al ratio. The data was ascribed to the increasing hydrophobic interaction between surfactant and mordenite with increasing Si/Al ratio. Deka and Vetrivel (1998) studied the adsorption and diffusion behavior of large molecules inside the micropores of zeolites such as faujasite, zeolite L, mazzite, and mordenite. They used the efficiency of force field energy minimization technique to investigate them. The results indicated that mordenite is a good catalyst for selective synthesis of *p*-isobutylethyl-benzene. The adsorptions of the molecules in general are energetically favorable when the alkyl groups have maximum interaction with the surface of the zeolite pores. Poborcbiia *et al.* (1998) used Raman and X-ray absorption spectroscopy to study influence of ion exchange and method of selenium incorporation into mordenite channels on the structure of incorporated

selenium species. The results showed that Se chains prepared by Se vapor adsorption are more regular than Se chains prepared by pressure injection of liquid Se. Selenium incorporated into II-form of mordenite was found to be located not only in the original mordenite channels, but also in meso-channels organized due to partial destruction of the interchannel walls. Ahmad *et al.* (1998) used FTIR spectroscopy to study acetophenone adsorption on mordenite and acid-leached mordenite. Moreover, the experiment studied the effects of dealumination characterized by pyridine adsorption and ^{29}Si and ^{27}Al magic angle spinning nuclear magnetic resonance spectroscopy (MAS-NMR). The results showed acetophenone adsorption on mordenite with weak physisorption that was accompanied by three other modes of adsorption involving hydrogen bonding to internal and external silanol groups, hydrogen bonding to Brønsted acidic Si(OH)Al groups, and ligation to Lewis acidic Al^{3+} ions. Dealumination of mordenite by acid leaching converted a proportion of the Si(1Al) species to Si(OAl), reduced the concentrations of framework and extraframework Al and of Si(OH)Al groups, greatly reduced the population of Lewis acidic sites, and generated additional silanol groups. Moreau *et al.* (2002) studied the influence of Na exchange on the acidic and catalytic properties of an HMOR zeolite. The experiment used IR spectroscopy to characterize the hydroxyl groups of a series of NaHMOR samples resulting from sodium exchange of an HMOR sample. From the experiment, they found Na exchange occurs preferentially with the OH groups of the side pockets and the first Na cations exchange causes a significant decrease in the activity of mordenite and decrease in the turnover frequency of the protonic sites. In addition, when the selectivities are compared at the same temperature, sodium exchange of mordenite causes an increase in the isomerization selectivity. Metaxas *et al.* (2003) used mordenite and other adsorbents to remove thorium. The results showed that mordenite (NaMOR) utilized 38.6% of the theoretical

ion-exchange capacity based on Al content. Wernert *et al.* (2005) studied methods of elimination of uremic toxins such as urea, uric acid, creatinine, p-cresol and indoxyl sulfate from solutions by adsorption onto zeolites. They studied the physical and chemical properties of microporous materials varied following pore size, acidity, hydrophobicity, grain size, charge compensating cations, and stabilization by high pressure hydrothermal treatment. The results showed for initial concentrations close to that of persons having renal failure, it is possible to eliminate 75% creatinine by adsorption onto an acidic mordenite. In wastewater treatment, natural zeolite(clinoptilolite and mordenite) supplied from Dogantepe (Amasya) region in Turkey was used to remove ammonium ion from municipal wastewater (Sarioglu, 2005). The highest adsorption capacity obtained with acid-washed sample was determined to be 1.32 mg NH_4^+-N/g and the cation exchange capacity of Dogantepe zeolite was found to be 164.62 meq. per 100 g. However, the efficiency of the natural or acid washed zeolite can be further increased through conditioning with Na.

Researchers have studied the structure of mordenite. Korkuna *et al.* (2005) characterized mordenite using adsorption, AFM, FTIR, and TG–DTA methods. The initial natural mordenite have small specific surface area which increases significantly after their modification. The results of TG data show the presence of several types of water, and larger amounts of water desorbed from H-forms of mordenite up to 120ºC that can be caused by stronger changes in the mordenite structure. Covarrubias *et al.* (2005) synthesized zeolites with high Cr(III) exchange capacity (CrEC) using kaolin and natural mordenite as starting materials, and evaluated the effect related to the reaction time on the crystallization/transformation process and on product CrEC. The XRD, FTIR, SEM, N2-adsorption and TG/DTG were used to characterize the synthetic material. Synthesized zeolite products presented higher Cr(III) exchange

capacity than commercial zeolites. These results suggest that the use of these synthesized materials in Cr(III) removal from industrial wastewater could be promising.

Moreover, other natural zeolites, clinoptilolite, perlite, and diatomite were also used as adsorbent ion exchangers to eliminate contaminant ions from wastewater. Doula *et al.* (2002) used clinoptilolite to adsorb copper ion. Copper adsorption was found to increase with increased pH and with decreased electrolyte concentration. Besides, they also examined effects of [HC] differentiation on Cu adsorption and on Al/Si dissolution by FTIR. From the study of FTIR, it was proposed that the Cu species caused the destruction of H-bonded structures, whereas K adsorbed species were located at exchangeable sites after an ion-exchange process between K and Ca, Mg, and Na from the zeolite's surface. Armağan *et al.* (2004) studied equilibrium of reactive azo dyes, color from textile effluents, adsorbed into clinoptilolite. They used a series of batch adsorption experiments to investigate the adsorption & reactive dyes into clinoptilolite. The adsorption results indicated that natural zeolite has a limited adsorption capacity for reactive dyes but can be distinctly improved by modifying its surfaces with quaternary amines with natural clinoptilolite comparison with a modified clinoptilolite for the adsorption densities of dyes, natural clinoptilolite yielded negative or slightly positive values, while those with modified clinoptilolite gave adsorption densities in the range of 2.9 to 7.6 mg/g. Englert and Rubio (2005) studied ammonia removal from aqueous solutions using a natural Chilean zeolite. The zeolitic-rich tuff sample was mainly composed of clinoptilolite and mordenite. Kinetics of ammonia removal appeared to proceed through ion-exchange and was rapid at neutral pH value, with removal capacities up to 0.68 meq NH^{4+}/g. The excellent equilibrium data fitting by Langmuir isotherm model. The results indicate a

significant potential for the Chilean natural zeolite as an adsorbent/ion-exchange material for wastewater treatment and water reuse applications.

Perlite is defined as a naturally occurring glassy volcanic siliceous rock which is inexpensive and easily available in Lopburi Province of Thailand and elsewhere around the world. Consequently, the scientist was attention to used perlite as materials for eliminate contaminants in wastewater. Mathialagan and Viraraghavan (2002) used perlite for removal of cadmium from aqueous solutions. The results found optimum pH for adsorption to be 6.0, the rate of cadmium adsorption by perlite was rapid in the first hour of the reaction time and cadmium concentration reached equilibrium in 6 h. The maximum removal of cadmium obtained from batch studies was 55% as well as using Freundlich isotherm model to define adsorption equilibrium. Koumanova and Peeva-Antova (2002) studied the adsorption of p-chlorophenol (p-CP) from aqueous solutions on bentonite and perlite. The results found rapid adsorption 20–30 min after the beginning for every experiment. After that, the concentration of p-CP in the liquid phase remained constant. The adsorption equilibrium of p-CP on bentonite and perlite was described by the Langmuir and the Freundlich models. A higher adsorption capacity was observed for bentonite (10.63 mg g^{-1}) compared to that for perlite (5.84 mg g^{-1}).

Diatomite is a siliceous rock made up largely from the skeletons of aquatic plants called diatoms that is found in Lampang province. The usefulness of diatomite is the same as perlite. Akyüz $et\ al.$ (2001) used natural diatomite from Kutahya-Alayunt (Anatolia, Turkey) adsorbed benzidine (bnz), 2,2′-bipyridyl (2,2′-bpy) and 4-4′-bipyridyl (4-4′-bpy). They used FTIR to investigate the nature of the surface species formed on diatomite after sorption. The vibrational results indicated the presence of chemisorbed species but no

physical sorbed species were detected. Summarization of this research indicated that most of the adsorbed 2,2´-bpy molecules coordinated to surface cations through ring nitrogens as bidentate ligands and some of the adsorbed 2,2´-bpy molecules formed anionic surface species. In this case, adsorbed 4,4´-bpy do not observe anionic surface species. The results showed that natural diatomite can be an adsorbent.

Water contamination resulting from dyeing and finishing in textile industry is a major concern. Discharging large amount of dyes in water resources accompanied with organics, bleaches, and salts can affect the physical and chemical properties of freshwater. If dyes are released into water it leads to water pollution. Therefore, researchers have tried to remove them from water. Erdem *et al.* (2005) studied adsorption of some textile dyes by diatomite. The study used batch adsorption techniques at 30ºC to adsorb these textile dyes onto diatomite earth samples. The adsorption behavior of textile dyes on diatomite samples was investigated using a UV–vis spectrophotometric technique. The experiment investigated the effect of particle size of diatomite, diatomite concentration, the effect of initial dye concentrations, and shaking time on adsorption. Adsorption coverage over the surface of diatomite was studied using two well-known isotherm models: Langmuir's and Freundlich's. These results suggest that the dye uptake process mediated by diatomite has potential for large-scale treatment of textile mill discharges. Values of the removal efficiency of the dyes ranged from 28.60 to 99.23%. The results showed that natural diatomite holds great potential to remove textile dyes from wastewater. Khraisheh *et al.* (2004) studied the effect of OH and silanol groups in the removal of methylene blue, reactive black (C-NN), and reactive yellow (MI-2RN) from aqueous solution by calcined and raw diatomite at 980ºC. This study demonstrated the

importance of the various functional groups on the mechanism of adsorption and also studied the role of pore size distribution in the dye adsorption. The results revealed that the removal of hydroxyl groups from the surface of diatomite leads to a decrease in the adsorption. Shawabkeh and Tutunji (2003) used diatomaceous earth (diatomite) to adsorb the basic dye, methylene blue, from an aqueous solution. This study investigated the effect of initial dye concentrations, adsorbent particle size and concentration, and agitation speed on adsorption and adsorption isotherms obtained at different solution temperatures, which revealed an irreversible adsorption with a capacity of 42 mmol dye/100 g diatomite reached within 10 min. This value slightly increases with increasing the solution temperature. From the results there was a better fit to the experimental data than that of Langmuir's and Freundlich's. It was found that the kinetics of adsorption of methylene blue onto the surface of diatomite at different operating conditions is best described by the pseudofirst-order model.

Additionally, natural zeolites are used in other applications such as gas separation, to improve catalysts, and also as a catalyst. Ackley *et al.* (2002) used natural zeolites including clinoptilolite, chabazite, mordenite, erionite, ferrierite and phillipsite, for gas separation. The results of the study indicated that these natural zeolites are particularly well suited for trace-gas removal.

In general, although natural zeolites are abundant and inexpensive, these attributes may not offset the effects of impurities and inconsistency of properties that have low efficiency to adsorb other ions relative to the more uniform synthetic zeolites. Therefore, researchers have tried to improve materials to have higher efficiency than from nature. Modification of the adsorptive properties of natural zeolites by ionexchange, thermal treatment and

structural changes to improve adsorption is interesting to study. Silva *et al.* (1996) used ammonium hexafluorosilicate treating NH$_4$MOR for dealumination. The experiment studied the influence of the treatment on the physicochemical characteristics and catalytic properties. The results showed a decrease in the adsorption rate and capacity for organic molecules and in activity and stability for m-xylene transformation. Vergani *et al.* (1997) studied modification of mordenite catalysts for isopropylation of biphenyl in continuous flow reactors. They used the combinations of acid extraction and calcinations to modify it. The results showed the best highly crystalline modified mordenite had a low sodium content, a Si/A1 ratio of about 70, a secondary pore volume in mesopores of about 0.15 ml/g and a surface area in mesopores of about 30 m2/g. Lee and Ha (1998) modified mordenites by dealumination with HCl/steam or HF treatment. For this study in HCl/steam-treated mordenites, the framework aluminum was mainly removed, while in HF-treated mordenites, the framework silicon and aluminum were simultaneously removed. HCl/steam-treated mordenites had lattice parameters smaller than on HF-treated mordenites at the same SiO$_2$/Al$_2$O$_3$ weight ratios. Also, HCl/steam-treated mordenites had a higher proportion of strong acidsites than HF-treated mordenites. The mordenites treated by HCl/steam and HF formed secondary mesopores of 3.7 nm in diameter. Kosanovic *et al.* (1998) used high-energy ball milling (mechanochemical amorphization) in order to investigate the processes of transformation of different types of zeolites, A, X, and synthetic mordenite. The formation of an amorphous aluminosilicate initially, followed by recrystallization of mordenite during prolonged heating, is performed by heating ammonium-exchanged synthetic mordenite. The amorphous precursor obtained by ball milling of the ammonium-exchanged synthetic mordenite remains amorphous during heating at 1000ºC. Müller *et al.* (2000) used thermal treatment, leaching with oxalic acid, and treatment

with SiCl$_4$ for dealumination of zeolites beta, mordenite, ZSM-5, and ferrierite. The results showed that dealumination of mordenite is thought to occur during the calcinations; it very easily dealuminated. Hernández-Guevara *et al.* (2000) used photoacoustic techniques and X-ray diffraction to study ternary compounds Zn$_x$Cd$_{1-x}$S ($0 \leq X \leq 1$) embedded in mordenite zeolite host. From the results, they found the thermal diffusivity, thermal effusivity and band-gap as functions of the *X* parameter. Mohamed (2002) studied the effect of acid dealmination of the Na–mordenite zeolite on the dispersion of added Mo. As a result, Mo/zeolite catalysts have been extensively employed in the petroleum industry for their valuable activities, e.g., hydrodesulfurization (HDS) and hydrodenitrogenation (HDN) reactions. The results of obtained Mo-dealuminated mordenites showed higher surface areas than those of Mo-free ones. The affinity of Mo encapsulated in dealuminated mordenites to water adsorption reflected varying interactions of water with Mo. Mohamed (2003) used Fe ion-exchanged mordenite catalyst for ethanol transformation. Park *et al.* (2003) studied occlusion of mordenite by non-nitrate salts such as KClO$_3$ and KH$_2$PO$_4$. The results demonstrated that KH$_2$PO$_4$ occluded mordenite about 2.1 % (w/w). This shows clearly that the occlusions of a variety of salts including non-nitrate salts could lead to further expansion of zeolite potential for salt occlusion. Chumbhalel *et al.* (2004) studied catalytic degradation of expandable polystyrene waste (EPSW) using mordenite and modified mordenites. They used hydrochloric acid treated mordenites at 98ºC and dried at 120ºC for 12 h. The results obtained H-mordenite zeolites with higher SiO$_2$/Al$_2$O$_3$ ratios. It is clear that dealumination by acid leaching of synthetic mordenite increases silica-to-alumina ratio without loss of framework structure and it reduces both weak and strong acid sites.

Because of the chemical components of mordenite have metals such as Fe, Ca, Na, and Mg (Manouchehri *et al.*, 2006) so the scientists were interesting to study effect of these metals involved adsorption on material surface and to extraction it from material for increase efficiency of material. Tuccillo *et al.* (1999) used hydrochloric acid 0.5 M to extract Fe from sediment. The results shown hydrochloric acid can dissolved poorly Fe oxide and small amounts of Fe in crystalline Fe oxide. Manouchehri *et al.* (2006) used ethylene diaminetetraacetic acid (EDTA) to extract trace and major elements such as Pb, Cu, Cd, Al, Ca, Mg, and Fe from soil. They used concentrations of EDTA varied from 0.002 to 0.05M. They used frame atomic adsorption spectrometry (FAAS) determined amount of cations concentration. At 0.05M concentration represents the excess of the reagent with respect to all extractable cations.

Zeolite as ion exchange

The advantage of zeolite as a promoter is that its acid and base properties can be modified through a simple procedure of ion exchange. The replacement of cations holds in their aluminosilicate anion framework by ions present in external solutions. Certain parameters control ion exchange properties of zeolite, i.e.:

1. The nature of both the competing ions with respect to their sizes and states of salvation inside and outside the zeolite.

2. The charge on zeolite framework coupled with framework geometry.

3. The temperature at exchange and the accessibility of sites can improve exchange kinetic.

4. The concentration of the external solution coupled with the presence or absence of ligands other than water molecules.

Zeolite as molecular sieves

When the zeolites are heated, the water is also removed and the voids created within the framework can take in other molecules. This process is called 'sorption' and the zeolites are said to 'sorb' molecules into their void volume, in other words, they act as 'sorbents'. That is to say, the sorbing molecules are described as 'guests' within the zeolite 'host'. From their geometry comes the ability of zeolites to separate mixtures of molecules on the basis of their effective sizes.

The stabilities of zeolite structures

1. **Thermal stability**

The commonly observed transformation of the zeolite structure is that promoted by water loss. This can cause a change from one zeolite structure to another, structure collapse to an amorphous phase or recrystallization to non-zeolitic materials. The critical water losses can occur over a wide temperature range.

2. **Hydrothermal stability**

The zeolites are formed in nature when they are exposed to water vapour at increased temperatures and/or pressures. Study of hydrothermal stability is of great importance to the regeneration processes used in

association with the use of synthetic zeolites as catalysts, molecular sieves and dying agents.

3. Stability to acid

The reaction of zeolites with moderate acid molarities demonstrates that the first stage is a cation exchange whereby hydronium ion replaces the indigenous cations. It can be carried out even in zeolite able to link-to the hydrolysis phenomenon. If the zeolites are heated, water is lost and they form hydrogen zeolite, which are stable and are desirable catalysts.

4. Stability to alkali

The hydroxyl species in solution is a critical factor in some zeolite transformations. The pH of the gel precursor in syntheses determines products and so it is to be expected that alkaline treatment of existing crystalline zeolites might create structure changes.

5. Stability to ionizing radiation

Zeolite structures have demonstrated to be remarkably resistant to radiation and prolonged exposure to high neutron and gramma rays produces a negligible effect on the zeolite matrix. High beta ray is equally ineffectual. Clearly, these are the properties needed for the use of zeolites to treat aqueous nuclear waste.

MATERIALS AND METHODS

Materials

1. Reagents

Anhydrous potassium dihydrogen phosphate (KH_2PO_4) from BDH (England) used as a synthesis orthophosphate solution for the study of adsorption and desorption. Potassium chloride (KCl) was used as electrolyte and obtained from Merck (Germany).

In order to measure orthophosphate concentration, potassium antimonyl tartrate ($K(SbO)C_4H_4O_6.1/2H_2O$) and ammonium molybdate ((NH_4)$_6Mo_7O_{24}.4H_2O$) were obtained from CARLO ERBA (Italy), ascorbic acid ($C_6H_8O_6$) was obtained from Ajex (Australia) and sulfuric acid (H_2SO_4) was purchased from Merck (Germany).

In addition, diversified materials as the adsorbents were used in this work. Activated granular natural zeolite was purchased from Kaset Center Company (Thailand). Perlite and diatomite were received from Department of Mineral Resource and ball clay and kaolin were received from Thailand Institute of Scientific and Technological Research (TISTR).

2. Apparatus

All adsorbents were calcined in a furnace (Lenton Thermal Desings). Nitrogen adsorption and adsorption measurement of adsorbent particles used a volumetric adsorption analyzer (Autosorb1) from TISTR. The specific surface area (S_{BET}) was calculated using the standard Brunauer-Emmett-Teller (BET)

method. The pore volume and pore width were calculated using the Barrett-Joyner-Halenda (BJH) method. For the characterization of adsorbent, the morphology was examined using scanning elecrtron microscope (SEM, JSM-6340F, JEOL, Japan), from TISTR. The chemical composition of an adsorbent was analyzed by energy dispersive X-ray spectroscopy (EDS). The chemical composition of adsorbents was in the oxide form of elements such as SiO_2, Al_2O_3. The X-ray diffraction (XRD, 6000RC, Japan) from TISTR was the equipment used to determine the structure of adsorbents. Fourier transform infrared spectrometer (FTIR, Perkin Elmer, System 2000, Germany) was used to identify the form of chemical compositions in natural zeolite structure and orthophosphate adsorption. Atomic Absorption Spectrophotometer (AAS, Perkin Elmer, 1100B, Germany) was used to determine amount of metal ions dissolved from the natural zeolite.

Orthophosphate adsorption measurements were done using a clifton shaking bath to shake the flasks and an ultracentrifuge (Hermle Z323, Germany) to centrifuge sample solutions. Orthophosphate concentration was determined by Ion chromatography (IC, Metrohm 761 Compact, Herisau, Switserland) and UV/Visible spectrophotometer (Model Genesys 5).

The zeta potential (ζ) of adsorbents was measured using a zeta sizer from TISTR.

Methods

1. Characterization

1.1 Analysis of surface area, pore volume, and pore size

The surface area was estimated by the Brunauer-Emmett-Teller (BET) method. The pore volume and pore size using the BJH method and nitrogen adsorption/desorption method. Each run was performed with 0.02-1.00 g of natural zeolite which was pretreated at 300 °C under vacuum.

1.2 Morphology of adsorbents

Scanning electron microscope (SEM) was used to investigate the natural zeolite morphology.

1.3 Analysis of the chemical composition of adsorbents

The surface chemical composition of adsorbents was analyzed using energy dispersive x-ray spectroscopy (EDS).

1.4 Analysis of the structure of adsorbents

The X-ray diffraction experiment (XRD) was performed on X-ray diffractometer operated at 30 kV and 30 mA using CuK_{α} radiation. Data were collected in the 2θ range of 2-80° and scan rate of 2°/minutes at room temperature.

1.5 Chemical bond analysis

The FT-IR spectra of natural zeolite and adsorbed orthophosphate on the natural zeolite surface were collected by taking 32 scans at 2 cm^{-1} resolution. The spectra were changed from 4000 to 400 cm^{-1} and for all samples were taken support in KBr.

2. Calcination of adsorbents

Prior to the study of orthophosphate adsorption, the natural zeolite was calcined in a tube furnace in order to study the effect of temperature on the adsorption. Calcination with the heating rate of 3.5°C/minute to the temperatures of 150, 300, 450, 600, 750, and 900°C, then left for 5 hours. After calcination, the natural zeolite was characterized and used to study orthophosphate adsorption. A schematic drawing of the procedure was shown in Figure 8.

```
┌─────────────────────────┐
│        adsorbent        │
└─────────────────────────┘
             │
             ▼
┌───────────────────────────────────────┐
│  calcine with heating rate 3.5°C/minute │
│         to various temperatures         │
└───────────────────────────────────────┘
             │
             ▼
┌───────────────────────────────────────┐
│    leave for 5 hours after temperature set  │
└───────────────────────────────────────┘
         ↙                    ↘
┌──────────────────────────┐   ┌──────────────────────┐
│ study orthophosphate adsorption │   │      characterize      │
└──────────────────────────┘   └──────────────────────┘
```
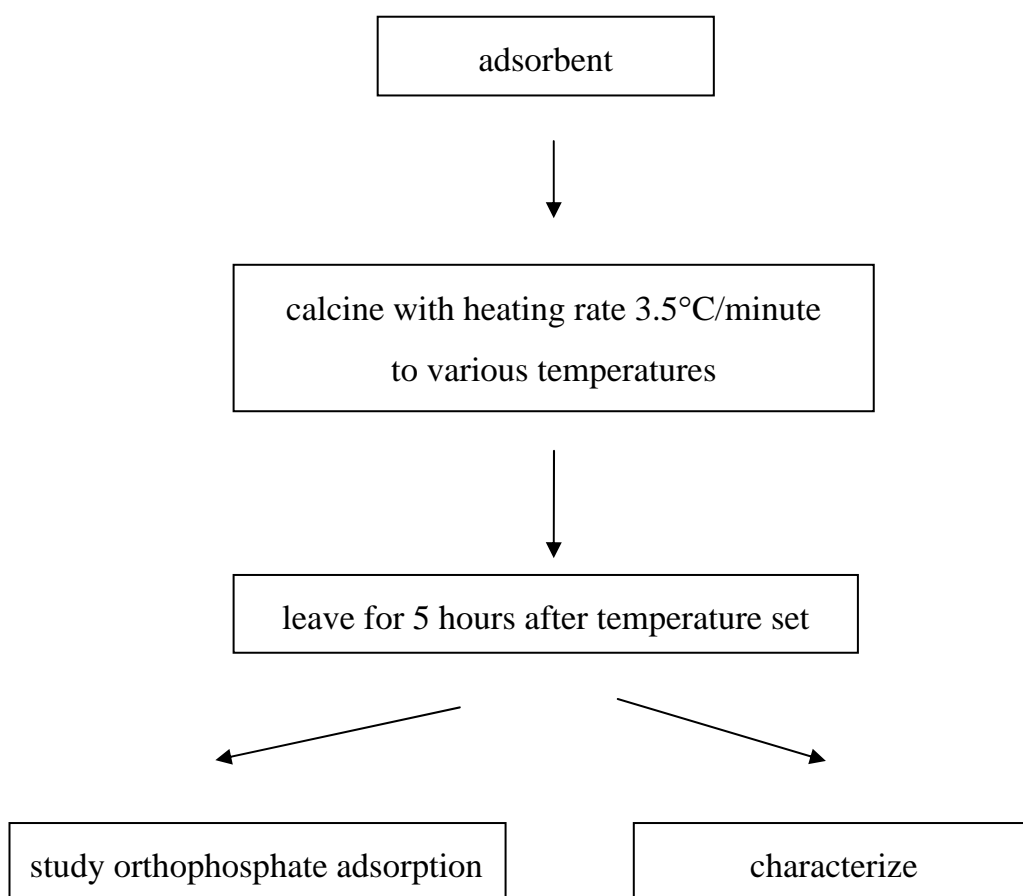
Figure 8 The scheme of natural zeolite calcination

3. **Preparation of orthophosphate solution**

The stock orthophosphate solution was prepared by dissolving 0.4393 g of anhydrous potassium dihydrogen phosphate (KH_2PO_4) with deionized water into 1,000 ml volumetric flask and adjusting to 1,000 ml. The stock solution has the concentration of 100 mg-P/L. Then, the stock solution was diluted to 5, 10, 20, and 30 mg-P/L.

4. <u>Measurement of orthophosphate concentration</u>

Because the phosphate in this study was in the orthophosphate form, the ascorbic acid method, one of colorimetric methods, was used for orthophosphate determination (Eaton, 1995). The reagents preparation of ascorbic acid method as shown in Appendix A.

4.1 The procedure of ascorbic acid method

Fifty ml of solution after orthophosphate adsorption by adsorbents were pipetted into a clean dry 125 ml erlenmeyer flask. Then, 1drop of phenolphthalein indicator was added. If a red color is developed, 5N H_2SO_4 solution was added drop wise to just discharge the color. Then, 8 ml of combined reagent was added and mixed thoroughly. The color absorbance of each sample was measured using UV/VIS spectrophotometer at wavelength (λ) 880 nm, using the reagent blank as the reference solution, at least 10 minutes after mixing but no longer than 30 minutes.

4.2 Calibration curve of orthophosphate determination

The stock solution was diluted to 0.2, 0.4, 0.6, 0.8, 1.0 and 1.2 mg-P/L. After preparation, orthophosphate concentration was measured following the measurement procedure of samples. Absorbance and orthophosphate concentration were plotted on y-axis and x-axis, respectively and gave a straight line passing through the origin.

5. Orthophosphate adsorption

By modifying the experimental procedure of Sakadevan and Bavor (1998), the experiments were performed in order to study the effect of orthophosphate concentrations and periods of shaking on the adsorption. A gram of natural zeolite was added to a 50 ml erlenmeyer flask. Then, KH_2PO_4 30ml at 5, 10, 20, and 30 mg-P/L concentration and three drops of 0.01M KCl was added into the flasks. The flasks were shaken in a shaking bath at the speed of 100 rpm at room temperature with the periods of shaking set at 20, 40, 60, 120, 180, and 240 minutes. At the end of the equilibration period, the samples were centrifuged at 10,000 rpm for 5 minutes. Centrifugates were measured for leftover orthophosphate concentration by colorimetric method (Andrew, 1995). A schematic drawing of the experimental procedure was shown in Figure 9.

```
┌─────────────────────────────────┐
│       a gram of adsorbent       │
└─────────────────────────────────┘
                 │
                 ▼
┌──────────────────────────────────────────────┐
│ add 30 ml of KH₂PO₄ at 5, 10, 20, and 30 mg-P/L │
└──────────────────────────────────────────────┘
                 │
                 ▼
┌─────────────────────────────────┐
│      add 3 drops of 0.01M KCl   │
└─────────────────────────────────┘
                 │
                 ▼
┌──────────────────────────────────────────────────┐
│     shake at speed 100 rpm, at room temperature   │
│  and periods of 20, 40, 60, 120, 180, and 240 minutes │
└──────────────────────────────────────────────────┘
                 │
                 ▼
┌──────────────────────────────────────┐
│   centrifuge at 10,000 rpm for 5 minutes │
└──────────────────────────────────────┘
                 │
                 ▼
┌──────────────────────────────────────────────────┐
│  measure the leftover orthophosphate concentration │
│                  in centrifugates                 │
└──────────────────────────────────────────────────┘
```
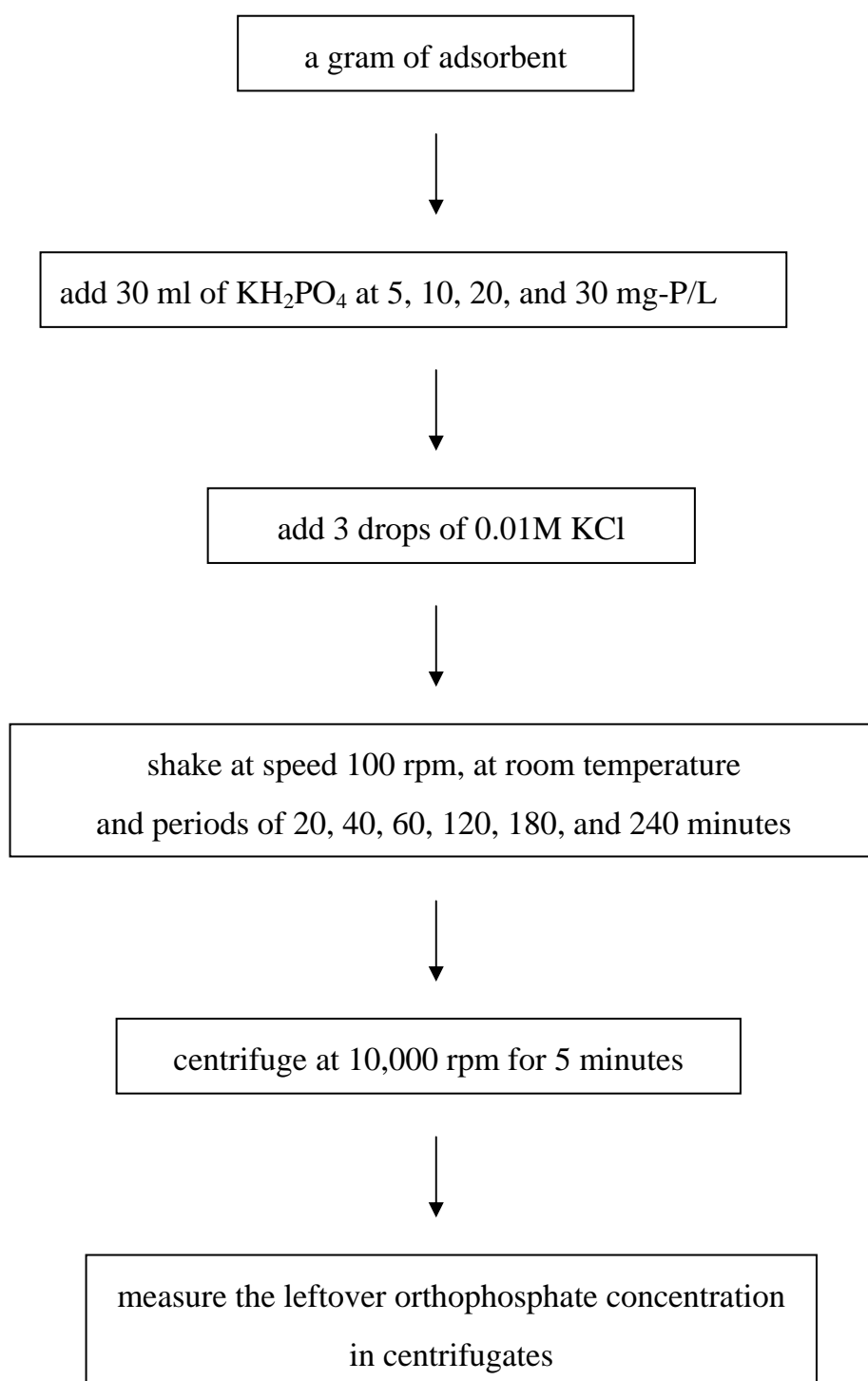
Figure 9 The scheme of orthophosphate adsorption procedure

6. <u>Desorption of adsorbed orthophosphate</u>

Desorption of orthophosphate was studied after obtaining the optimum adsorption condition and equilibrium periods for each initial orthophosphate concentrations. After the equilibrium adsorption on natural zeolite, the experiment was performed by having natural zeolite in 30 ml of deionized water and three drops of 0.01M KCl was added into the flasks. The flasks were shaken in a shaking bath at the speed of 100 rpm at room temperature with various periods of shaking. The measurement of orthophosphate concentration was the same method for adsorption experiment.

7. <u>Metal dissolution from natural zeolite</u>

7.1 Metals dissolution in 0.05M EDTA

0.05M EDTA was prepared by dissolving 9.306 g of EDTA salt (MW 372.24 g/mol) by deionized water into 500 ml volumetric flask and adjusting to 500 ml with deionized water.

The amount of 0.05M EDTA 30 ml was added into the flask with 1 g of natural zeolite before shaking the flasks in shaking bath at the speed of 100 rpm at room temperature for 4 hours. After that the suspension was centrifuged at 10,000 rpm for 5 minutes, and the centrifugate was collected. Natural zeolite was rewashed with 30 ml of deionized water. The suspension was recentrifuged for 2 hours before separating certrifugate from natural zeolite. Both certrifugates were combined and amount of Fe^{2+} determined by AAS. Natural zeolite was dried in the oven at 105ºC to use in the further orthophosphate adsorption and desorption study.

7.2 Metals dissolution in 0.5M HCl

The amount of 0.5M HCl 30 ml was added into the flask with 1 g of natural zeolite before shaking the flasks in shaking bath at the speed of 100 rpm at room temperature for 1 hour. After that the suspension was centrifuged at 10,000 rpm for 5 minutes and the centrifugate was collected. Natural zeolite was rewashed with 30 ml of deionized water. The suspension was recentrifuged for 1 hour before separating certrifugate from natural zeolite. Both certrifugates were combined and amount of Fe^{2+} determined by AAS. Natural zeolite was dry in the oven at 105ºC to use in the further orthophosphate adsorption and desorption study.

The metals dissolution in 0.5M HCl experiment was repeated with the shaking period of 5 hours before centrifugation. The centrifugate was collected to determine the amount of Fe^{2+} and Ca^{2+} by AAS.

7.3 Metals dissolution in deionized water

The amount of deionized water 30 ml was added into the flask with 1 g of natural zeolite before shaking the flasks in shaking bath at the speed of 100 rpm at room temperature for 5 hours. After that the suspension was centrifuged at 10,000 rpm for 5 minutes and the centrifugate was collected. The centrifugate was determined the amounts of Fe^{2+} and Ca^{2+} by AAS.

7.4 Metals dissolution in NaOH

The amount of NaOH 30 ml was added into the flask with 1 g of natural zeolite before shaking the flasks in shaking bath at the speed of 100

rpm at room temperature for 5 hours. After that the suspension was centrifuged at 10,000 rpm for 5 minutes and the centrifugate was collected. The certrifugate was determined the amount of Fe^{2+} and Ca^{2+} by AAS.

8. Zeta potential

The surface potential of natural zeolite was measured by zeta potential measurement. After the adsorbent preparation, 1 g of natural zeolite at different calcination temperature in deionized water was ground, then diluted 200 times. The zeta potential was measured at pH of solution and then added 1M NaOH to adjust its pH to 12. After that, 1M HCl was gradually added into the solution to decrease the pH to 2. The zeta potential was measured at every pH of the solution. After orthophosphate was adsorbed to equilibrium on 1 g of calcined natural zeolite at different temperature and the uncalcined one, the adsorbed natural zeolite particles in orthophosphate solution were then ground. The zeta potential measurement was followed the procedure of the natural zeolite indicated previously.

9. Orthophosphate adsorption on other adsorbents

In the preliminary study, the orthophosphate adsorption on other adsorbents, including perlite, diatomite, ball clay, and kaolin, was also investigated in this work. The adsorbent preparation of all other adsorbents had been followed the calcination procedure of natural zeolite as shown in Figure 8. The orthophosphate adsorption procedure was also as same as the method for natural zeolite as shown in Figure 9.

RESULTS AND DISCUSSION

1. The preliminary orthophosphate adsorption study

At the beginning of this work, orthophosphate adsorption on the different natural adsorbents, diatomite, perlite, kaolin, natural zeolite, and ball clay, was studied. These natural adsorbents are inexpensive and can be found available everywhere in Thailand.

Diatomite is a type of soil, it is occurred from the sediment of carcass and vegetable and can be found in the north of Thailand such as Lumpang province. In nature, it is white, light, porous, and dissolvable in water. After calcination at 750ºC, it turns to be hard and undissolvable in water. To study the adsorption, the orthophosphate concentration of 5 and 30 mg-P/L with the shaking time of 3 and 4 hours, respectively, the results were shown in Appendix B. The orthophosphate adsorption was about 9 % and 2% per 1 g diatomite.

Perlite is a rock, found at an extinct volcano in Lopburi province of Thailand. It is dark grey, heavy, high density, and undissolvable in water. With the same experimental conditions, the adsorption data was shown in Appendix B. The result showed the negative orthophosphate adsorption indicating that there could be orthophosphate released from perlite during experiment.

Kaolin has similar physical properties to diatomite but more crumbly, fragile, and heavy. In this work, kaolin was obtained from Chiangmai province. The uncalcined kaolin and the calcined one at 750ºC were used to study its

orthophosphate adsorption. With the same experimental conditions, the adsorption results were shown in Appendix B. The adsorption capability of both adsorbents was in the range of 7-17% per 1 g kaolin.

Ball clay is the sediment found in the north of Thailand. It is hard, light, dark color like charcoal but more dense. With the same experimental conditions, the adsorption data was shown in Appendix B. The maximum adsorption of both the uncalcined ball clay and the calcined one at 750ºC was in the range of 18-37% per 1 g ball clay.

The amount of orthophosphate adsorption on all adsorbent was summarized as shown in Table 7. Without calcination, ball clay had higher adsorption capability than kaolin and natural zeolite; after calcination at 750ºC, natural zeolite had the highest orthophosphate adsorption of 27.16 mg-P/L per gram adsorbent, which was equivalent to 90%, at initial orthophosphate concentration of 30 mg-P/L. From these results, natural zeolite came to ones' interest leading to the further study. Due to the low orthophosphate adsorption capability of diatomite, perlite, kaolin, and ball clay, the studies on their orthophosphate adsorption were discontinued.

Table 7 The orthophosphate adsorption on the adsorbents

Calcination temperature (°C)	Initial orthophosphate concentration (mg-P/L)	The amount of orthophosphate adsorption ((mg-P/L)/ 1g adsorbent) (% adsorption)				
		Natural zeolite	Diatomite	Perlite	Ball clay	Kaolin
Uncalcined	5	0.43 (8.60%)	-	-	1.72 (34.4%)	0.86 (17.20%)
	30	0.50 (1.67%)	-	-	5.18 (17.27%)	2.17 (7.23%)
750 ° C	5	4.38 (87.6%)	0.32 (6.40%)	-0.04	1.55 (31.00%)	0.70 (14.00%)
	30	27.16 (90.50%)	1.05 (3.50%)	-2.98	6.34 (21.13%)	3.30 (11.00%)

2. Characterization

2.1 Surface area, pore volume, and pore size

The surface area, pore volume, and pore size of mordenite after calcination at various temperatures were shown in Table 8. In BET measurement, the sample was outgased at 300ºC for 3 hours. In addition, the surface area and the micropore volume were calculated for each sample, using Barrett- Joyner- Halenda (BJH) method.

Table 8 indicated that natural zeolite was highly microporous due to high surface area and discrete pore size. When increasing the temperature of calcination, the surface area of natural zeolite was decreased. The calcination of natural zeolite was clearly affected the change in surface area and porosity,

which was shown by nitrogen adsorption isotherms in Appendix C. The isotherms showed the slightly rising of adsorption volumes when P/Po got close to 0.90 and then rapidly increasing from P/Po of 0.90 to 1.00 except at temperature of calcination 450ºC, which the adsorption volume was hardly changed. Additionally, the effect of calcination temperature indicated that when increasing temperature of calcination, the adsorption volumes were also increased. The surface area at multipoint of uncalcined natural zeolite was 126.20 m^2/g and after calcined at 150, 300, 450, 600, 750, and 900ºC were 126.80, 65.09, 34.58, 18.18, 18.25, and 2.68 m^2/g, respectively. When the temperature of calcination increased, the surface area tended to decrease and rapidly dropped at the temperature of calcination at 900ºC. The pore volume of uncalcined natural zeolite was 0.17 ml/g and decreased after calcination especially at the temperature of 450ºC, the pore volume was as low as 0.02 ml/g. The pore size of uncalcined natural zeolite was 19.40 Aº and tended to decrease after calcination at increasing temperature but rapidly increased at the calcination temperature of 900ºC. The results showed that the high calcination temperature made internal structure collapsed by removing water and organic compounds from the adsorbents and caused the surface area, pore size and pore volume to decrease. At the calcination temperature of 900ºC, the pore size was rapidly increased which could be resulted from the change of surface structure.

Table 8 Surface characterization of natural zeolite

Data	sample						
	uncalcined	calcination					
		150ºC	300ºC	450ºC	600ºC	750ºC	900ºC
surface area at multipoint (m^2/g)	126.20	126.80	65.09	34.58	18.18	18.25	2.68
surface area at single point (m^2/g)	126.26	124.80	64.97	34.54	18.11	18.16	2.66
pore volume (ml/g)	0.17	0.10	0.13	0.02	0.08	0.10	0.07
pore size (Aº)	19.40	21.19	14.31	14.37	14.25	14.34	30.64

2.2 Morphology of natural zeolite

The morphology of natural zeolite particles was shown in Figure10 and 11.
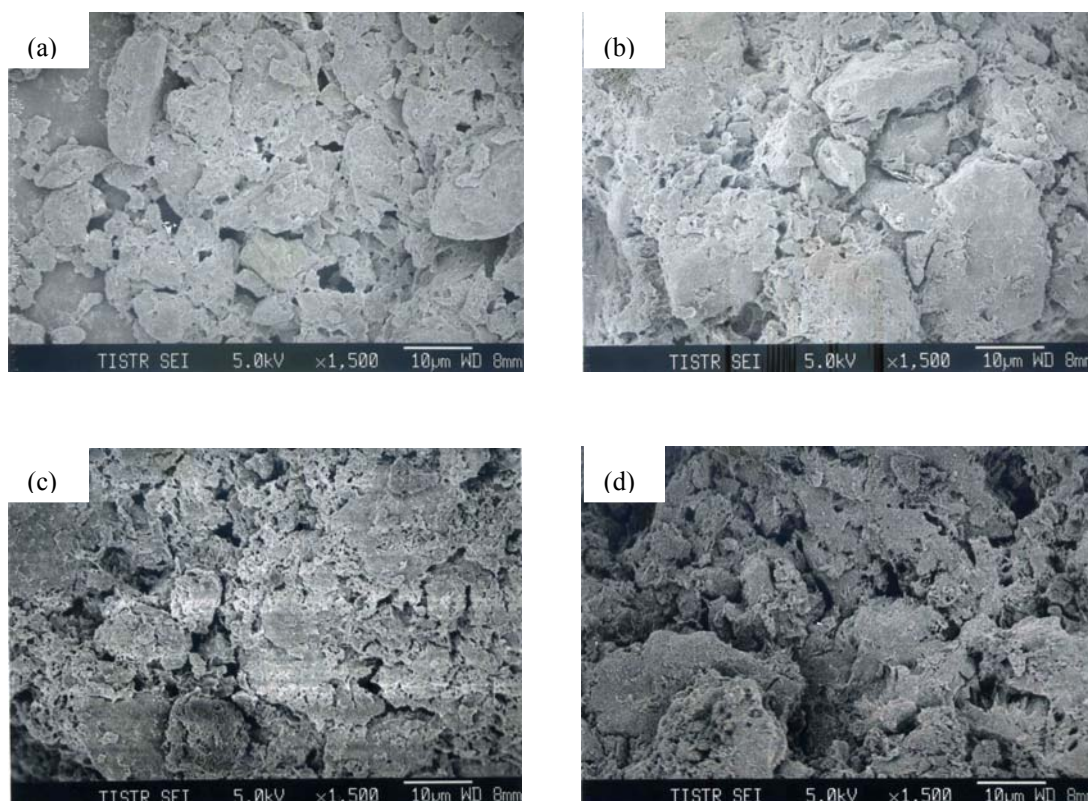
Figure 10 SEM image of natural zeolite (x 1,500): (a) uncalcined,
(b) calcination at 450ºC, (c) calcination at 600ºC, (d) calcination at
750ºC

From both figures, SEM images could not clearly reveal the difference in morphology between the calcined natural zeolites at various temperatures and the one without calcination. However, the different sample grain size seen in the images could be dependent on the grinding step in sample preparation.
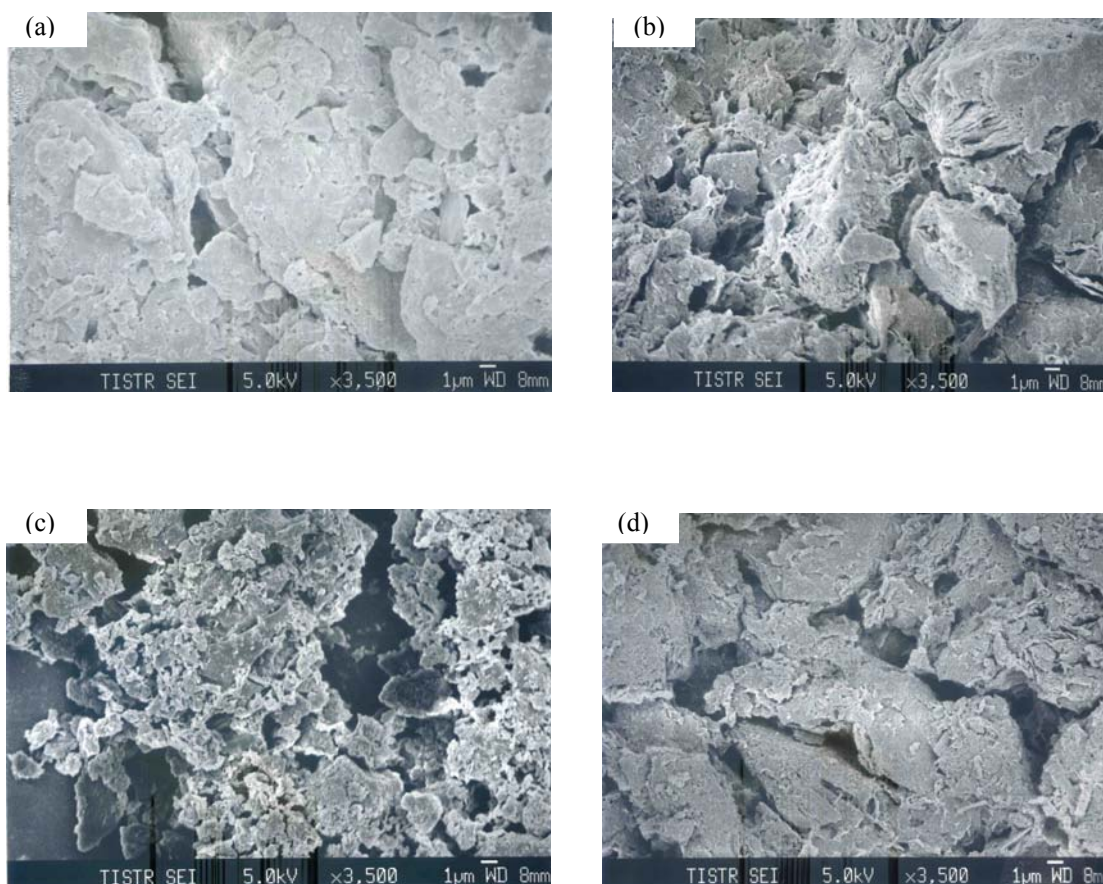
Figure 11 SEM image of mordenite (x 3,500): (a) uncalcined,
(b) calcination at 450ºC, (c) calcination at 600ºC, (d) calcination at
750ºC

2.3 The chemical composition on surface of natural zeolite

The chemical compositions on the surface of natural zeolite obtained by EDS were shown in Table 9. The uncalcined natural zeolite and the ones with calcination did not show much difference in surface composition. There were 60-80%wt SiO_2 and approximately 10%wt Al_2O_3 and the rest was approximately 10%wt of metal oxides. The chemical compositions of mordenite via EDS measurements were agreed with the study of Covarrubias *et al*. (2005) with 70.66%wt SiO_2, 12.69%wt Al_2O_3, and approximately 17%wt of

metal oxides. The different amount of chemical compositions on the surface of natural zeolite could affect the orthophosphate adsorption at the surface. There was a study of Yu (1997) stating that the Al-O sites of Al_2O_3 group at the surface could adsorb orthophosphate with the strong coordination adsorption.

Table 9 Chemical compositions on surface of natural zeolite

samples	components (%wt)						
	SiO_2	Al_2O_3	CaO	K_2O	FeO	Na_2O	MgO
uncalcined	65.07	10.89	18.76	1.99	1.26	1.07	0.96
uncalcined after adsorbed	81.15	10.91	3.57	1.43	1.02	1.42	0.50
calcination at 150ºC	77.57	12.02	3.64	2.17	2.16	1.21	0.83
calcination at 300ºC	79.64	11.27	3.45	1.79	1.88	1.09	0.66
calcination at 450ºC	78.75	11.28	4.77	1.67	1.68	1.07	0.77
calcination at 450ºC after adsorbed	59.31	9.03	27.26	1.29	1.32	0.88	0.91
calcination at 600ºC	78.52	11.69	3.75	1.92	1.72	1.32	0.76
calcination at 750ºC	71.65	13.70	6.50	3.04	2.82	1.02	0.94
calcination at 750ºC after adsorbed	77.28	10.87	6.00	2.22	1.56	0.91	1.15
calcination at 900ºC	78.19	11.29	5.04	1.58	1.31	1.48	0.84

2.4 The structure of natural zeolite

XRD provided information and was a recognized method for identifying crystalline mordenite. A crystal was a three-dimentional pattern of electron density. The internal electrons in crystal lattice determined the directions and intensities of scattered X-ray beams. Peaks of atoms in the crystal defined the symmetry of electron density distribution and size of unit cell in three-dimensional portion of crystal. The XRD information showed that the

natural zeolite used in this work was mordenite by having the major intensity at $2\theta = 11, 15, 20, 23, 26, 28, 29$, and $32°$. Therefore, natural zeolite used in this work would be called as mordenite from now on. The unit cell of mordenite was orthorhombic having axial: a=18.16 $A°$, b=20.45 $A°$, c=7.54 $A°$ and angular relationship: $\alpha=\beta=\gamma = 90°$. Molecular formula of mordenite was (Ca, Na_2, K_2) $Al_2Si_{10}O_{24}.7H_2O$. When increasing the temperature of calcination to 300°C, the major peaks was increased in height, and then decreased with the increasing temperature. The decrease in XRD intensity showed the decrease in mordenite structure; until at the calcination temperature of 900°C, structure of mordenite turned into aluminum silicate (Al_2SiO_5) of Kyanite and silicon oxide (SiO_2) by having the major intensity of $2\theta = 22, 27, 29$, and $51°$. The orthophosphate adsorption capability was possibly related to the crystal structure.
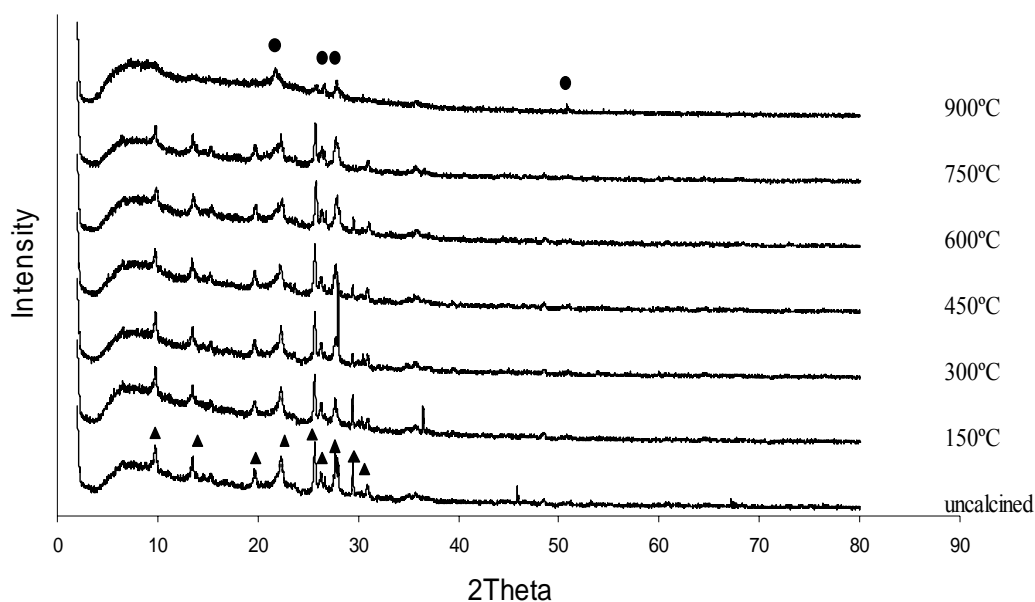
Figure 12 XRD patterns of the mordenite calcination at various temperatures
▲ mordenite , ● aluminum silicate of Kyanite and silicon oxide

2.5 Molecular structure by FTIR

In order to investigate the molecular structure of mordenite in term of functional groups, FTIR was used to study the mordenite before and after adsorption. FTIR spectra of mordenite at various calcination temperatures were given in Appendix F.

The wave numbers obtained from this work confirmed that there were Si-O, Al-O, SiO-H, and Si(OH)Al bonds presented in the structure of mordenite and after orthophosphate adsorption, there were PO_4^{3-}, $H\,PO_4^{2-}$, and $H_2\,PO_4^{-}$ presented in mordenite. The observed wave numbers were agreed to the experimental values from other studies as presented in Table 10. The information from FTIR results confirmed the presence of PO_4^{3-}, $H\,PO_4^{2-}$, and $H_2\,PO_4^{-}$ ions in the adsorbed mordenite, however, it could not show the adsorption sites where orthophosphate ions were attracted to Si, Al, or any other sites on the surface.

Table 10 Interpretation of mordenite at various conditions from FTIR spectra

Functional group	Wave number (cm⁻¹) (observed)	Wave number (cm⁻¹) (references)
νSi-O	1085-1052	1081-1059 [a]
νAl-O	790	785-775 [a]
SiO-H	3453-3439	~3480 [a]
Si(OH)Al	3638-3623	~3650-3648 [a]
PO_4^{3-}	1056	1006 [c]; 1048, 966, 569 [b]
$H\,PO_4^{2-}$	1056,875	1077, 989, 850 [b]; 1666, 677, 512 [c]
$H_2\,PO_4^{-}$	1056, 875	1160, 1074, 940, 870 [b]; 1621, 601 [c]

[a] Mohamed, M.M., *et al*. (2005)

[b] Arai, Y. and Sparks, D.L. (2001)

[c] Wu, P.X. and Liao, Z.W. (2005)

3. Adsorption of orthophosphate in prepared wastewater

In the measurement of orthophosphate adsorption, Spectronic G5 was used and the calibration of orthophosphate standard was performed. The calibration curve of orthophosphate concentration was shown in Appendix G.

3.1 Orthophosphate adsorption

3.1.1 The effect of temperature on calcination

Prior to the orthophosphate adsorption, the appropriate condition for the orthophosphate adsorption of calcination temperatures, orthophosphate concentrations, and shaking periods were studied. The measurement of orthophosphate in solutions was preceded by ascorbic method.

The orthophosphate adsorptions with the orthophosphate concentrations of 5, 10, 20, and 30 mg-P/L at various temperatures of uncalcined, 150, 300, 450, 600, 750, and 900ºC were studied. The relation between % adsorption and the period of shaking was plotted as shown in Figure 13, the data was shown in Appendix G. The results showed that uncalcined mordenite having % adsorption of 8% per 1g mordenite and slightly increased to 10-20 % per 1g mordenite when calcined at 150 and 300ºC at initial concentration of 5, 10, 20, and 30 mg-P/L. The % adsorption was negative values at 450 and 600ºC due to possibility of orthophosphate leaching from the bulk of mordenite. At the calcination temperatures of 450 and 600ºC, the pore

volume of mordenite was as low as 0.02 ml/g and relatively small of 0.08 ml/g, respectively, this could result in the low orthophosphate adsorption compared to the adsorption of mordenite at other calcination temperatures. The adsorption became as high as 91, 93, 92, and 89% per 1g mordenite when calcined at 750ºC at initial concentration of 5, 10, 20, and 30 mg-P/L, respectively. The adsorption was dependent on the calcination temperature of mordenite. Due to the increase in the calcination temperature, the crystal structure and chemical composition on surface of mordenite were changed. From Figure 13, it indicated that the appropriate temperature of calcination was 750ºC.
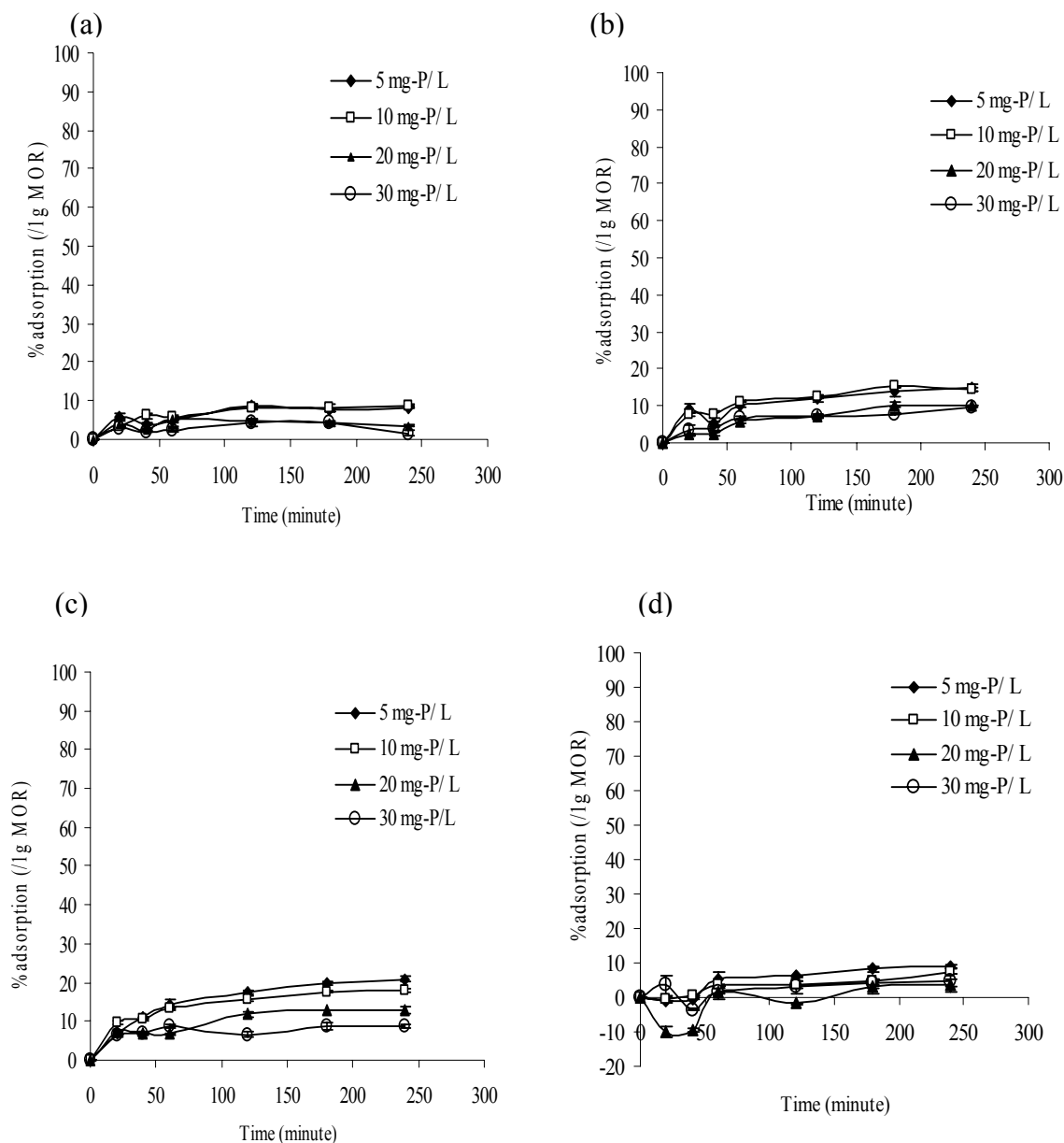
Figure 13 The effect of adsorbing time and concentration on the removal of
orthophosphate from aqueous solutions : (a) uncalcined
mordenite, (b) calcined at 150ºC, (c) calcined at 300ºC, (d) calcined
at 450ºC, (e) calcined at 600ºC, (f) calcined at 750ºC, (g) calcined at
900ºC

Figure 13 The effect of adsorbing time and concentration on the removal of
orthophosphate from aqueous solutions (Cont'd): (a) uncalcined
mordenite, (b) calcined at 150°C, (c) calcined at 300°C, (d) calcined
at 450°C, (e) calcined at 600°C, (f) calcined at 750°C, (g) calcined at
900°C

3.1.2 The effect of adsorbate concentration

To study the influence of the initial orthophosphate concentration on adsorption, the initial concentration was ranged from 5 to 30 mg-P/L. It was found that an increase of the initial concentration leads to the decrease in % adsorption capability. By decreasing the initial concentration, the percent orthophosphate adsorption was higher. The results between % adsorption and time at different temperatures for concentrations between 5 to 30 mg-P/L were shown in Figure 14. At the initial concentration of 5 mg-P/L, % adsorption of 750 and 900ºC were increasing rapidly to 80 % after 20 minutes and slightly increased to the maximum of 91 % per 1g mordenite after 60 minutes of shaking time, and then it tended to decrease slightly after 1 hour. For other calcination temperatures, % adsorption was approximately 5-15% per 1g mordenite, which was much lower than the ones calcined at 750 and 900ºC. At the initial concentration of 10, 20, and 30 mg-P/L, % adsorption of the calcined mordenite at 750ºC was decreased from 91% to 60% at the shaking time of 60 minutes. Because the orthophosphate molecules were quite large, at the initial concentration of 5 mg-P/L, the orthophosphate molecules in solution were able to adsorb on the surface with less interaction between itself and other orthophosphate molecules. As the initial concentration increased to 30 mg-P/L, there was higher interaction among the adsorbed orthophosphate molecules at the surface. The repulsion between orthophosphate molecules led to the decrease in amount of adsorption on mordenite surface.
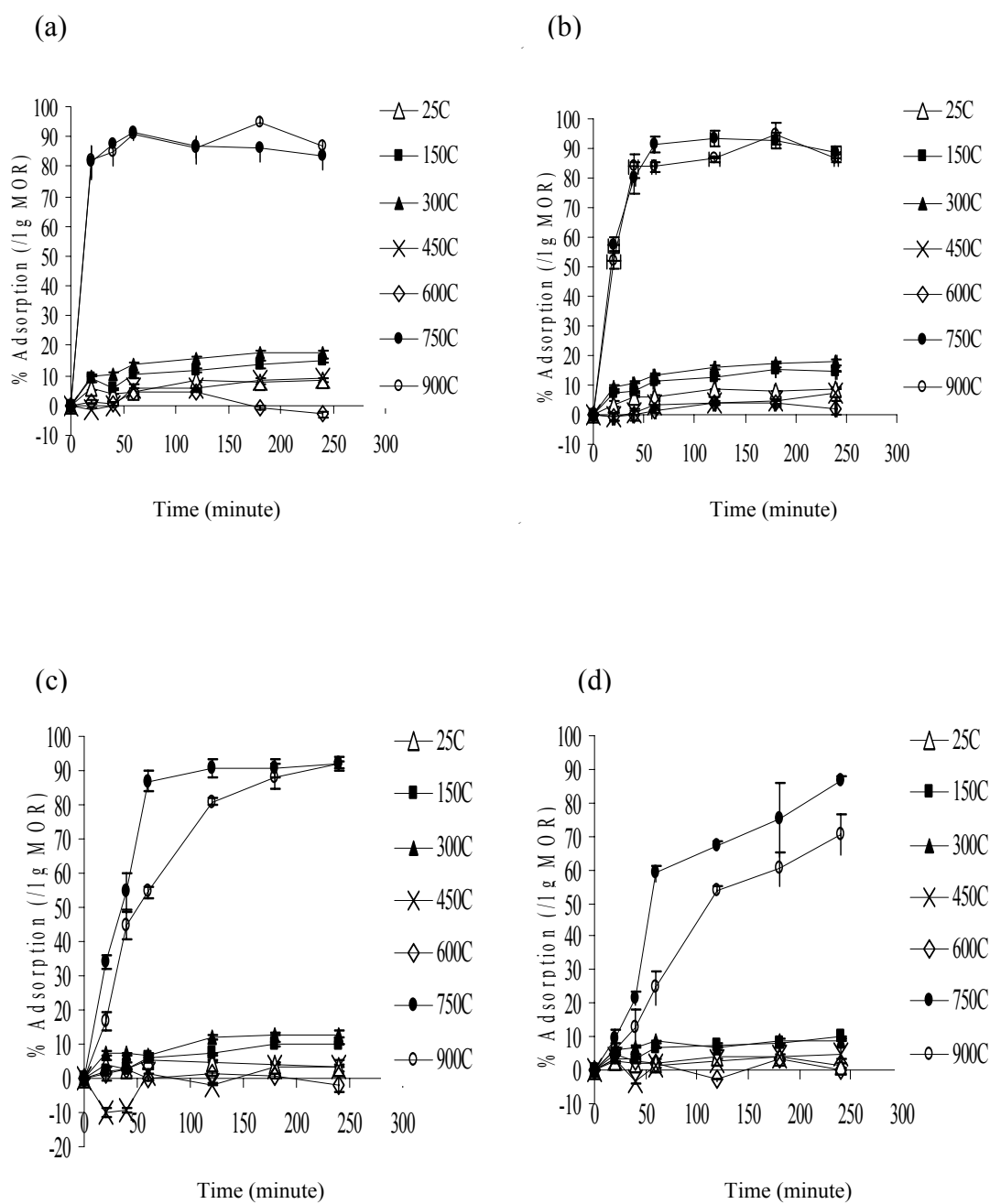
Figure 14 Initial orthophosphate concentration adsorption: (a) 5 mg-P/L, (b) 10 mg-P/L, (c) 20 mg-P/L, (d) 30 mg-P/L

3.1.3 The effect of adsorbing time

%Adsorption can be calculated from the difference between the initial orthophosphate concentration and the remaining orthophosphate concentration after being adsorbed on mordenite. From the previous results, it was shown that the adsorption capability was maximized at 750ºC. To study the appropriate time for adsorption to reach the equilibrium, the amount of adsorption was observed with the increase in adsorbing time until the amount of adsorption became consistent which implied that equilibrium was reached. The results on the adsorption at the calcination temperature of 750ºC could be seen in Figure 14. At initial concentration 5 mg-P/L, the amount of orthophosphate adsorption rapidly reached equilibrium in 1 hour with 91% adsorption and leveled off after 1 hour. At initial concentration of 10 mg-P/L, the amount of orthophosphate adsorption gradually approached the equilibrium in 2 hours with 93%adsorption. At the initial concentration of 20 mg-P/L, the amount of orthophosphate adsorption slightly increased to the equilibrium in 4 hours with 92% adsorption. At the initial concentration of 30 mg-P/L, orthophosphate adsorption rapidly increased to 60%in 1 hour then continued to slowly increase to the maximum adsorption in 5 hours with 89% adsorption, before it tended to decrease. To have the appropriate condition in orthophosphate adsorption, the results led to the adsorbing time of 5 hours and the calcination temperature of 750ºC at the initial orthophosphate concentration of 30 mg-P/L in the further experiments.

3.2 Adsorption isotherm

In this study, Langmuir and Freundlich adsorption isotherms were used to explain behaviors of several material adsorptions. The $C_e(x/m)$ versus

C_e were plotted on x-axis and y-axis, respectively and fitted with Langmuir isotherm from equation 8.

.

$$\frac{C_e}{X} = \frac{1}{bX_m} + \frac{C_e}{X_m} \quad \text{or} \quad \frac{C_e}{x/m} = \frac{1}{bX_m} + \frac{1}{X_m}C_e$$

The Langmuir adsorption isotherm at the calcination temperature of 750°C was shown in Figure 15, the data was plotted between $C_e(x/m)$ and C_e. Other calculation data was shown in Appendix H. The calculation variables from Langmuir adsorption isotherm, such as equation, correlation coefficient of determination (R^2), adsorption maximum, and binding energy were shown in Table 11. By fitting Langmuir adsorption isotherm in Figure 15, R^2 from 60 minutes of shaking time was 0.9965 and R^2 from the average shaking time was 0.9000. The maximum adsorption was increased with the shaking time from 20 minutes to 180 minutes and binding energy was found to decrease with shaking time from 60 minutes to 180 minutes.
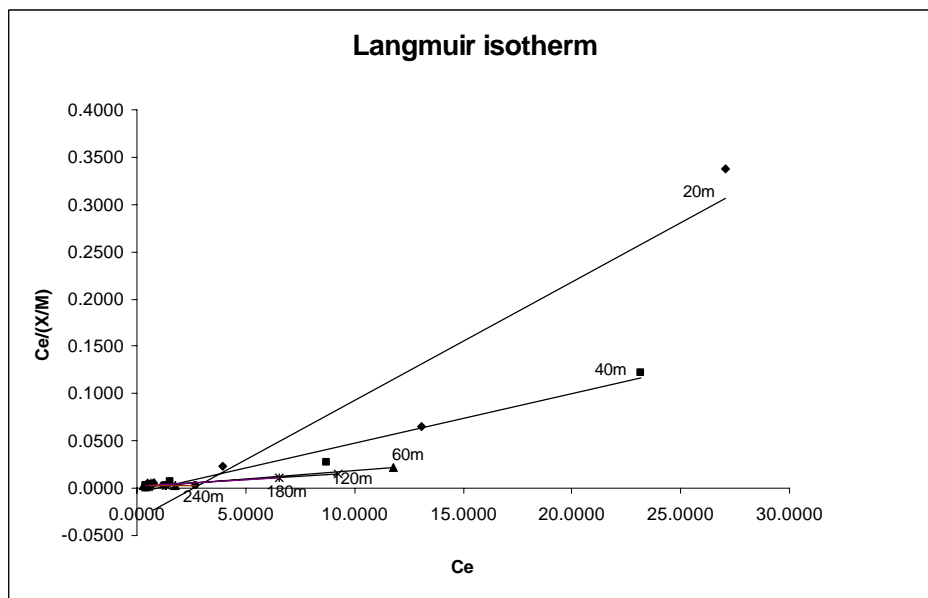
Figure 15 Langmuir adsorption isotherm calcination at 750°C

Table 11 The calculation variables from Langmuir adsorption isotherm

| Shaking time (minutes) | Langmuir isotherm | | | |
	Equation	R^2	Adsorption maximum (X_m) (mg-P/Kg)	Binding energy (b)
20	Y=0.0126x - 0.0327	0.9124	79.36	-0.38
40	Y=0.0053x - 0.0048	0.9717	188.68	-1.10
60	Y=0.0018x + 0.0010	0.9965	555.55	1.80
120	Y=0.0014x + 0.0019	0.9530	714.28	0.74
180	Y=0.0013x + 0.0020	0.8532	769.23	0.65
240	Y=-0.0001x + 0.0034	0.0071	-10000.00	-0.03

To study Freundlich adsorption, log (x/m) versus log C_e was plotted on y-axis and x-axis, respectively, as stated in equation 12.

$$\log\left(\frac{C_o - C_e}{m}\right) = \log K + \frac{1}{n}\log C_e \quad \text{or} \quad \log\left(\frac{x}{m}\right) = \log K + \frac{1}{n}\log C_e$$

Freundlich adsorption isotherm for the calcined mordenite at 750ºC was shown in Figure 16, the data was plotted between log x/m and log C_e. Other calculation data was shown in Appendix H. The calculation variables from Freundlich adsorption isotherm, such as equation, correlation coefficient of determination (R^2), K represented the capacity measurement of the adsorbent, and n represented the value of adsorption efficiency (Faust, 1987), were shown in Table 12. By fitting Freundlich adsorption isotherm in Figure 16, R^2 from 60 minutes of shaking time was 0.6971 and R^2 from the average shaking time was 0.5040. After the data at calculation 750ºC were fitting by Freundlich isotherm, the capacity of the adsorbent was increased with the shaking time from 20

minutes to 240 minutes and the value of adsorption efficiency was found to decrease with the shaking time from 20 minutes to 240 minutes.
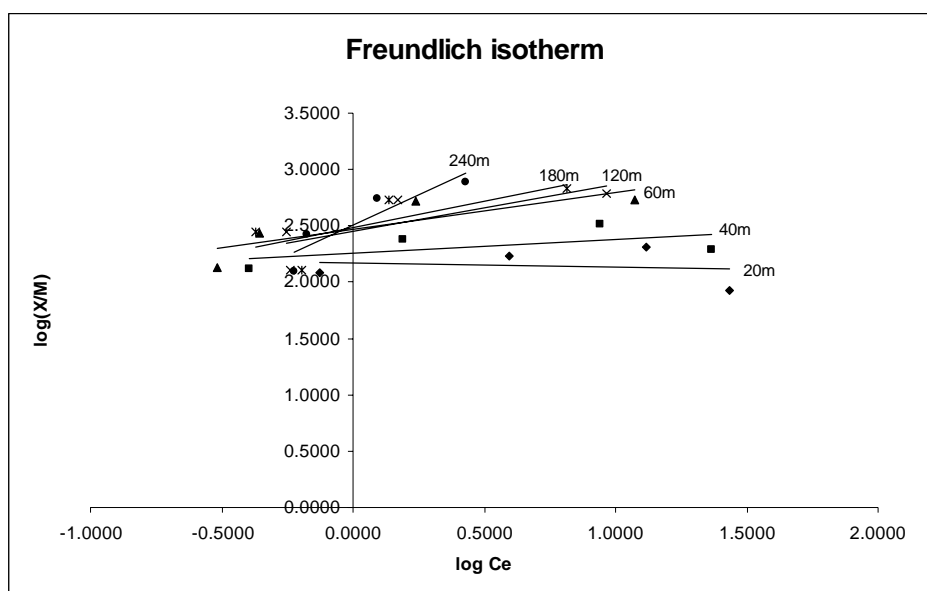
Figure 16 Freundlich adsorption isotherm calcination at 750ºC

Table 12 The calculation variables from Freundlich adsorption isotherm

Shaking time (minutes)	Freundlich isotherm			
	Equation	R^2	K	n
20	Y=-0.0376x + 2.1667	0.0229	146.79	-26.60
40	Y=0.1194x + 2.2599	0.3087	181.93	8.37
60	Y=0.3245x + 2.4671	0.6971	293.16	3.08
120	Y=0.4162x + 2.4504	0.5902	282.10	2.40
180	Y=0.4698x + 2.4833	0.5760	304.30	2.13
240	Y=1.0699x + 2.5047	0.8291	319.67	0.93

The Langmuir adsorption isotherm fitting approach linearity with R^2 of 0.9000 compared to the fitting on the Freundlich adsorption isotherm with R^2

of 0.5040. For these results, the orthophosphate adsorption behavior tended to follow Langmuir adsorption isotherm postulated a monolayer of orthophosphate on mordenite surface with chemisorption.

3.3 Desorption of adsorbed orthophosphate

The study of orthophosphate desorption from surface of mordenite at the selected calcination temperature of 750ºC was shown in Figure 17. The data was presented in Appendix I. In the experiment, the initial orthophosphate concentration was varied from 5-30 mg-P/L, and the desorbing time was varied from 2-6 hours due to the limitation on the shaking bath operation. At the initial orthophosphate concentration of 5 mg-P/L and desorption time of 6 hours, % desorption per 1g of mordenite was 1.48% in the first hour and decreased to 0.29 % per 1g of mordenite after 6 hours. At initial orthophosphate concentration of 10 mg-P/L, % desorption was 1.31% in the first hour and decreased to 1.14 % per 1g of mordenite after 5 hours. At initial orthophosphate concentration of 20 mg-P/L, % desorption was 1.53 % in the first hour and decreased to 0.49 % per 1g of mordenite after 3 hours. At initial orthophosphate concentration of 30 mg-P/L, % desorption was 0.39% in the first hour and 0.29 % per 1g of mordenite after 2 hours. The results showed that adsorbed orthophosphate was difficult to desorb from the surface of mordenite.   It could be resulted from the chemisorption by a strong chemical bond between the orthophosphate molecule and the surface followed the assumption of Langmuir adsorption isotherm.
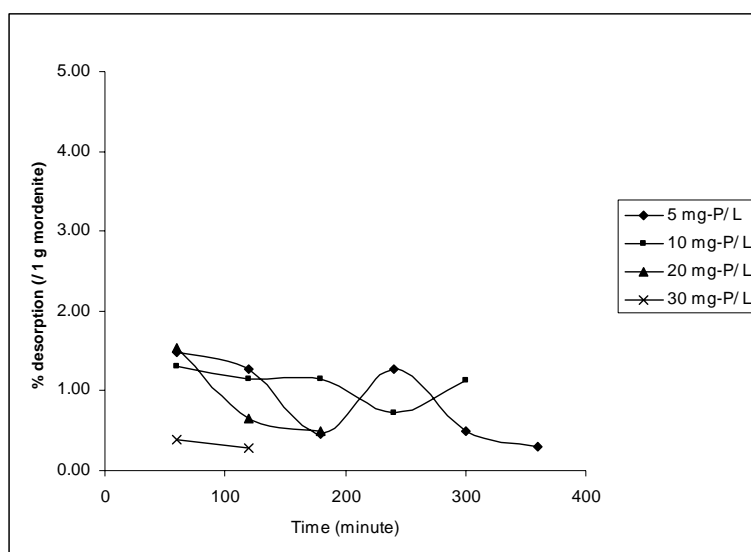
Figure 17 Desorption of orthophosphate after adsorbed on mordenite
calcination at 750ºC

4. Analysis amount of metal dissolution

4.1 Metal dissolution in 0.05M EDTA

After suspending mordenite in 0.05M EDTA, the concentration of
Fe^{2+} that dissolved from mordenite into 0.05M EDTA was analyzed by AAS.
The results indicated that the dissolved Fe^{2+} concentration was 2.09 ppm per 1 g
mordenite calcined at 750ºC. By using the EDTA-treated mordenite as an
adsorbent in orthophosphate adsorption, the results shown in Appendix J
indicated no orthophosphate adsorption on mordenite and it was possible for
orthophosphate to leach out from mordenite.

4.2 Metal dissolution in 0.5M HCl

After suspending in 0.5M HCl, the concentration of Fe^{2+} was measured by AAS. The results indicated that the dissolved Fe^{2+} concentration was 2.22 ppm per 1 g mordenite calcined at 750ºC. By using the acid-treated mordenite as an adsorbent in orthophosphate adsorption, the results shown in Appendix J indicated no orthophosphate adsorption on mordenite and it was possible for orthophosphate to leach out from mordenite at the initial orthophosphate concentration of 5 and 30 mg-P/L. However, at the initial concentration of 10 and 20 mg-P/L, orthophosphate was adsorbed on the treated mordenite in the amount of 0.57 and 1.98 mg-P/L per 1 g mordenite. Moreover, to identify the presence of Ca^{2+}, the concentration of Ca^{2+} was also measured by AAS. The results shown in Table 13 indicated that dissolved Ca^{2+} concentration was 159.69 ppm per 1 g uncalcined mordenite. The dissolution Ca^{2+} concentration decreased to 113.54 ppm per 1 g mordenite when calcination temperature increased to 600ºC and increased to 125.29 ppm per 1 g mordenite when calcination temperature was increased to 900ºC.

4.3 Metal dissolution in deionized water

After suspending in deionized water, the concentration of Fe^{2+} and Ca^{2+} were measured by AAS. The results shown in Table 13 indicated that the dissolved Fe^{2+} concentration was approximately 0.12-0.30 ppm per 1g mordenite at all calcination temperatures and without calcination. The dissolved Ca^{2+} concentration was approximately 2.66-4.01 ppm per 1 g mordenite at the calcination temperature of 150-600ºC and one without calcination. The Ca^{2+} concentration increased to 7.84 and 12.97 ppm per 1 g mordenite at the calcination temperature at 750 and 900ºC, respectively.

4.4 Metal dissolution in 0.01M NaOH

After suspending in 0.01M NaOH, the concentration of Fe^{2+} and Ca^{2+} were measured by AAS. The results shown in Table 13 indicated that the dissolved Fe^{2+} concentration was approximately 2.53-3.64 ppm per 1 g mordenite at 150-300ºC and the uncalcined. It decreased to less than 0.20 ppm per 1 g mordenite for calcination temperature at 600-900ºC. The dissolved Ca^{2+} concentration was approximately 0.09-0.16 ppm per 1 g mordenite at uncalcined and all calcination temperature.

From the literature review, there was possibility that Fe^{2+} and Ca^{2+} ions influenced orthophosphate adsorption. In basic solution, Fe^{2+} ions could dissolve from the bulk of mordenite into solution more than Ca^{2+}, which the increase in amount of Fe^{2+} could enhance orthophosphate adsorbed on the surface by coordination adsorption. In acidic solution, Ca^{2+} ions could dissolve from the bulk more than Fe^{2+}, which Ca^{2+} could have orthophosphate adsorbed on the surface by electrostatic adsorption. Therefore, the amount of both metal ions in solution had an effect on orthophosphate adsorption on mordenite surface.

Table 13 Metals dissolution in various solutions condition

Calcination temperature ($^{\circ}$C)	Metals dissolution in various solutions condition					
	Acidic solution (pH=2)		Neutral solution (pH=6)		Basic solution (pH=12)	
	$[Fe^{2+}]$ (mg/L)	$[Ca^{2+}]$ (mg/L)	$[Fe^{2+}]$ (mg/L)	$[Ca^{2+}]$ (mg/L)	$[Fe^{2+}]$ (mg/L)	$[Ca^{2+}]$ (mg/L)
Uncalcined	0.24	159.69	0.13	3.82	3.64	0.12
150 ºC	0.19	161.11	0.21	3.72	3.58	0.12
300 ºC	0.23	150.88	0.18	4.02	2.53	0.16
450 ºC	0.22	134.13	0.16	3.98	0.67	0.10
600 ºC	0.36	113.54	0.17	2.66	0.11	0.09
750 ºC	0.21	136.75	0.30	7.84	0.19	0.10
900 ºC	0.58	125.29	0.16	12.97	0.18	0.15

5. Zeta potential

As a result of the orthophosphate adsorption experiment, the adsorption tended to increase when increasing the calcination temperature. To extract more information on the orthophosphate capability at different calcination temperature, the orthophosphate adsorption behavior at the surface of mordenite was observed by the zeta potential measurement. The zeta potential before and after the orthophosphate adsorption on the uncalcined and calcined mordenite was investigated. The suspension was measured its initial pH and zeta potential before adjusting the pH. From the initial pH in the neutral or slightly basic range, the suspension was firstly adjusted its pH to 12 by NaOH and gradually decreased its pH of 12 to 2 by HCl. The zeta potential was calculated from equation 21.

$$\zeta = \frac{4\pi\eta}{\varepsilon} \times U \times 300 \times 300 \times 1000 \qquad (\text{eq.21})$$

Where ζ = zeta potential (mV)

η = viscosity of solution

ε = dielectric constant

$$U = \frac{\upsilon}{V/L}$$

v = speed of particle (cm/sec)

V = voltage (V)

L = the distance of electrode

The zeta potential was measured at each pH leading to the understanding on the adsorption behavior at the mordenite surface. And, to evaluate the proposed reaction at the surface, the equilibrium constant expressed in terms of activity, K^0, was considered.

$$H + L \rightleftharpoons HL \qquad\qquad \text{(eq.22)}$$

$$K^0 = \frac{(HL)}{(H)(L)}$$

The experiment was started on the uncalcined mordenite. After measuring the initial pH of 6.87 with the zeta potential of -15.14 as shown in Appendix K, the pH was adjusted to 12 by adding NaOH which caused the surface of mordenite to be deprotonated as shown in eq. 23 and the surface charge became more negatively charged.
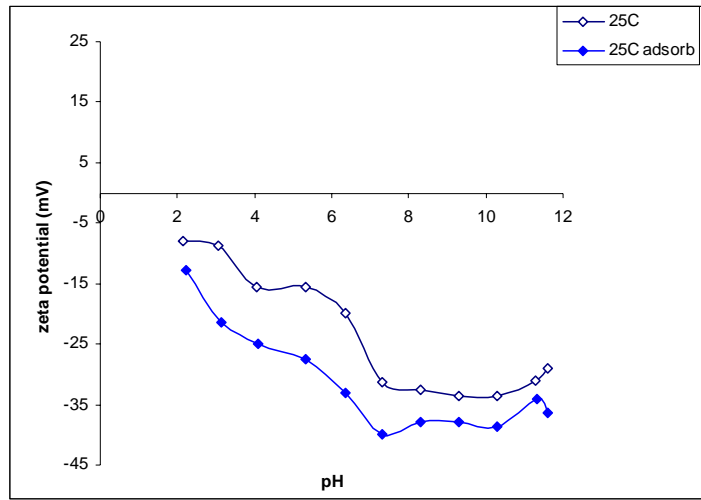
Figure 18 Zeta potential of uncalcined mordenite

$$Si\text{—}OH + OH^- \longrightarrow Si\text{—}O^- + H_2O \qquad (eq.23)$$
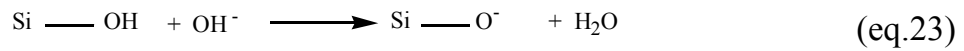
Then, iron ions in the form of Fe^{2+} and Fe^{3+}, which can be released from mordenite in basic solution as shown in the previous result of AAS, would play an important role. Since Fe^{3+} can be easily reduced to Fe^{2+} in the solution as shown in eq. 25, the iron ion referred in this work will be Fe^{2+}. As the pH of the solution became basic, Fe^{2+} attracted to the negative charge of the oxygen atom producing the ion complex at the surface. Due to the high concentration of OH^-, OH^- would deprotonate the complex and leave the complex with the negative charge to lower the zeta potential as shown in eq. 25.

$$Fe^{3+} + e^- \rightleftharpoons Fe^{2+} \qquad \log K^o = 13.04 \qquad (eq.24)$$

$$(eq.25)$$
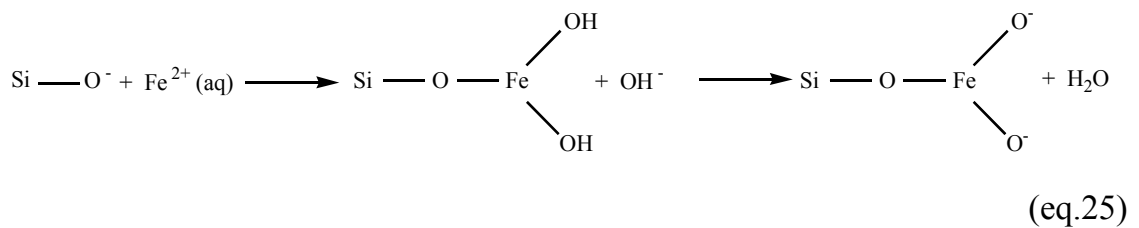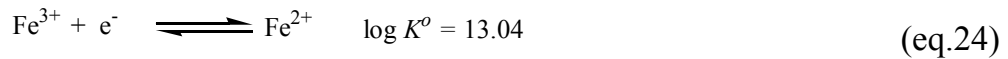
To observe the changes at the surface, the solution pH would be changed from basic to acidic.   From pH of 12, HCl was added in solution, the surface of mordenite was gradually protonated as showed in eq. 26

$$Si - O - Fe \underset{O^-}{\overset{O^-}{<}} + 2\,H^+ \longrightarrow Si - O - Fe \underset{OH}{\overset{OH}{<}}$$

(eq.26)
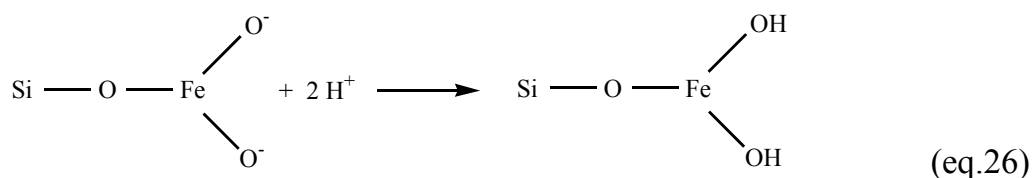
Along with the decreasing of pH, $Fe(OH)_2$ was dissociated from surface as shown in eq.27.

$$Si - O - Fe\,(OH)_2 + 2\,H^+ \rightleftharpoons Fe^{2+} + 2\,H_2O + Si - OH$$

(eq.27)
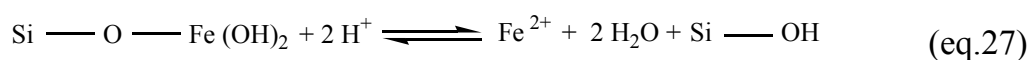
From the information on metal dissolution in HCl, the high amount of Ca^{2+} was released from mordenite into the acidic solution. Ca^{2+} would be closely around OH groups of Si atom at surface by electrostatic adsorption as shown in eq.28.   From the influence of Si-OH and Si-OH (Ca^{2+}) at surface, the zeta potential became higher positive with decreasing pH.

$$Si - OH + Ca^{2+} \rightleftharpoons Si - \underset{Ca^{2+}}{OH}$$

(eq.28)
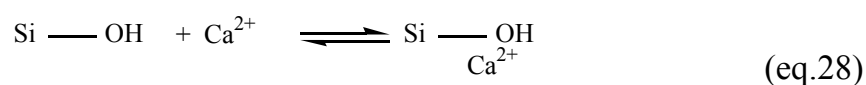
After orthophosphate adsorption, zeta potential at the initial pH of 5.49 was -13.5. When the pH was increased to 12, the behavior was followed eq.26 and orthophosphate ion was adsorbed by the coordinated adsorption of Fe^{2+} on the surface as shown in eq.29. For this reason, the zeta potential after adsorption was higher negatively charged than the one before adsorption.

$$
\text{Si} - \text{O} - \overset{\displaystyle \text{OH}}{\underset{\displaystyle \text{OH}}{\text{Fe}}} + H_2PO_4^- \longrightarrow \text{Si} - \text{O} - \text{Fe} - \text{O} - \overset{\displaystyle O}{\underset{\displaystyle \text{OH}}{\overset{\displaystyle \|}{P}}} \diagup \text{OH} + H_2O
$$

(eq.29)
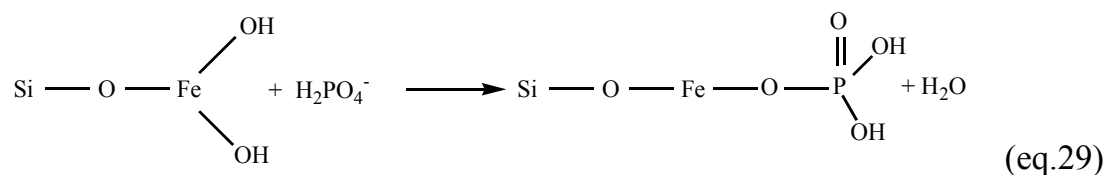
When pH gradually decreased to acidic, the negative charge was lower. An important cause was from the Ca^{2+} ion that covered around the OH group of Si as shown previously in eq.28 leading to the orthophosphate to adsorb on Si-OH(Ca^{2+}) by electrostatic adsorption as shown in eq.30.

$$
\text{Si} - \underset{\displaystyle Ca^{2+}}{\text{OH}} + H_2PO_4^- \longrightarrow \text{Si} - \underset{\displaystyle Ca^{2+} \; H_2PO_4^-}{\text{OH}} .
$$

(eq.30)
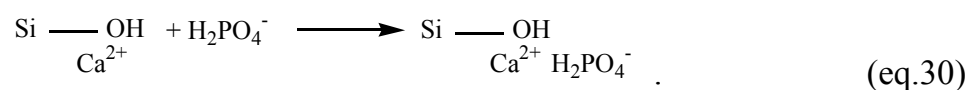
Because of the reaction in eq.29 and 30, the zeta potential was higher negatively charged than the one before adsorption and the negativity decreased when decreasing pH.
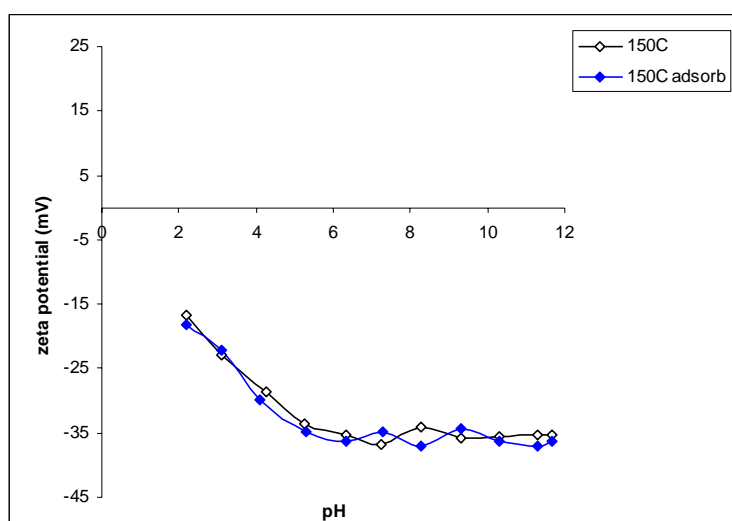
Figure 19 Zeta potential of mordenite calcined at 150ºC

For the calcined mordenite at 150ºC, the zeta potential before orthophosphate adsorption as shown in Figure 19 was quite similar to the zeta

potential of the uncalcined mordenite. The behavior was followed eq.23, 24, 25, 26, 27, and 28. After orthophosphate adsorption, the zeta potential was not different which can be implied that orthophosphate was not coordinately bound to the surface. The zeta potential of both before and after orthophosphate adsorption was the same.
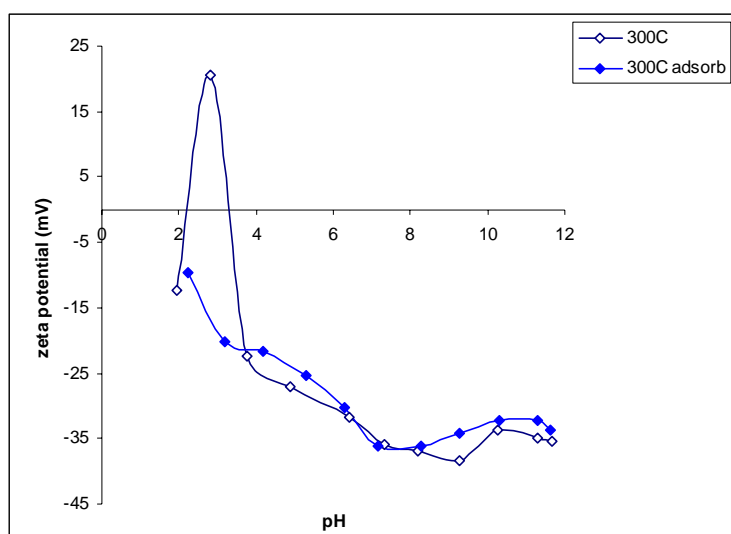
Figure 20 Zeta potential of mordenite calcined at 300ºC

For the calcined mordenite at 300ºC, the zeta potential before orthophosphate adsorption as shown in Figure 20 was quite similar to the zeta potential of the uncalcined mordenite until pH of 4. The behavior at the surface was still followed the eq.23, 24, 25, 26, 27, and 28. After that, the zeta potential was rapidly increased to zero at pH of 3.4 which equaled to the isoelectric point (IEP) of silica. It was point of zero net charge (PZNC). From Table 6, PZNC would be equal to zero when the effective surface charge equals the inner-sphere complex charge and the outer-sphere complex charge. It meant that at this point, the charge of all complexes cancelled out giving the net charge of zero. All Si atoms at the surface were protonated to be Si-OH. Then, when HCl was continued adding to the solution, H^+ would attract OH groups of Si at surface as shown in eq.31.

$$\text{Si} \longrightarrow \text{OH} + \text{H}^+ \longrightarrow \text{Si} \longrightarrow {}^+\text{OH}_2 \qquad \text{(eq.31)}$$
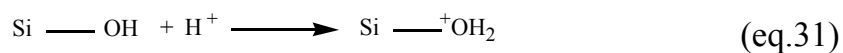
As long as the number of H^+ attracting the OH groups increased, the zeta potential was increased. When the OH groups were fully protonated, the zeta potential reached the maximum. Then, the counter ions of Cl^-, which are fully dispersed in solution, would come close to $Si-{}^+OH_2$ as shown in eq.32, have electrostatic anion adsorption, and decrease the zeta potential.

$$\text{Si} \longrightarrow {}^+\text{OH}_2 + \text{Cl}^- \longrightarrow \text{Si} \overset{\text{Cl}^-}{\longrightarrow} {}^+\text{OH}_2 \qquad \text{(eq.32)}$$
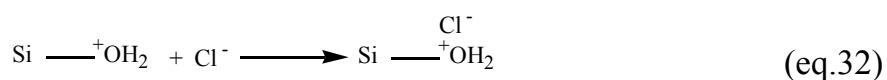
At pH 3.4, the zeta potential became zero. This pH equaled PZNC and corresponded to IEP of silica. It was implied that there were a lot of silica at the surface of the calcined mordenite at $300^{\circ}C$.

After orthophosphate adsorption, the zeta potential was quite similar to the zeta potential of the uncalcined mordenite. At pH 4-12, the zeta potential was not more or less different from the one before adsorption. It could be implied that orthophosphate was not coordinately bound to the surface after adsorption.
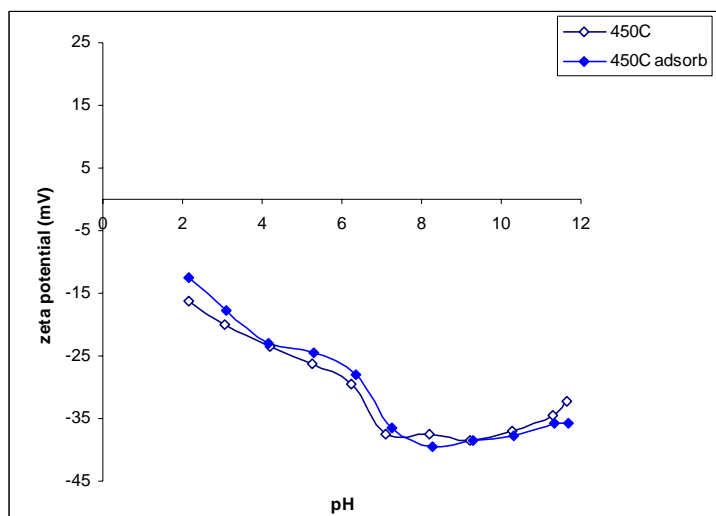
Figure 21 Zeta potential of mordenite calcined at 450ºC

For the calcined mordenite at 450ºC, the zeta potential before
orthophosphate adsorption as shown in Figure 21 was quite similar to the zeta
potential of the uncalcined mordenite and the calcined one at 150ºC. The
behavior was followed eq.23, 24, 25, 26, 27, and 28. After orthophosphate
adsorption, the zeta potential was not different which can be implied that
orthophosphate was not coordinately bound to the surface. The zeta potential of
both before and after orthophosphate adsorption was the same.
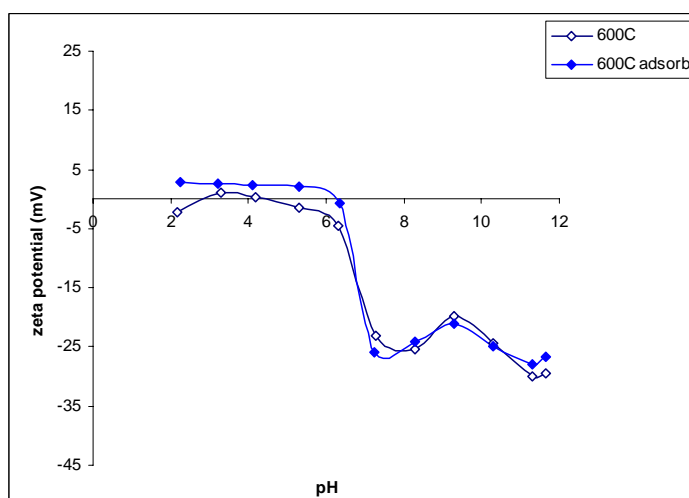
Figure 22 Zeta potential of mordenite calcined at 600ºC

For the calcined mordenite at 600ºC, the zeta potential before orthophosphate adsorption as shown in Figure 22 performed the fluctuation of surface charge when pH of the solution decreased from pH 12 to 8. After pH of 8, the zeta potential was rapidly increased to approach zero charge, which corresponded to PZNC. The zeta potential showed that at this calcination temperature, the surface of the particle tended to change its character. By looking at the zero charge pH of 4.2, it seemed that the increase of the zero charge pH was arised from the migration of Al to the surface. It could be said that PNZC was dependent on the surface composition and it's IEP ($IEP_{Si} = 2-3$ and $IEP_{Al} = 9$ (Sposito, 1989)) at the point when PZC was equaled to PNZC. When the zero charge pH was increased from 3.4 to 4.2, at the calcination temperature of 300 and 600ºC, respectively, the surface composition was changed from fully Si to Si with slightly Al. The behavior at the surface was followed eq.23, 25, and 26. In addition, Al would have the same behavior as Si as shown in the following equations.

In the basic solution, Al on the surface of mordenite was deprotonated as shown in eq.33.

$$Al-OH + OH^- \longrightarrow Al-O^- + H_2O \qquad (eq.33)$$
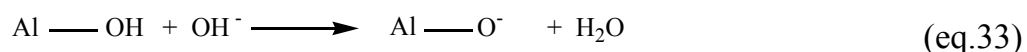
And, along with the deprotonation, the released Fe^{2+} ions could attract to the negative charge of oxygen as shown in eq.34.

$$Al-O^- + Fe^{2+}(aq) \longrightarrow Al-O-Fe\begin{smallmatrix}OH\\\\OH\end{smallmatrix} + OH^- \longrightarrow Al-O-Fe\begin{smallmatrix}O^-\\\\O^-\end{smallmatrix} + H_2O$$

$$(eq.34)$$
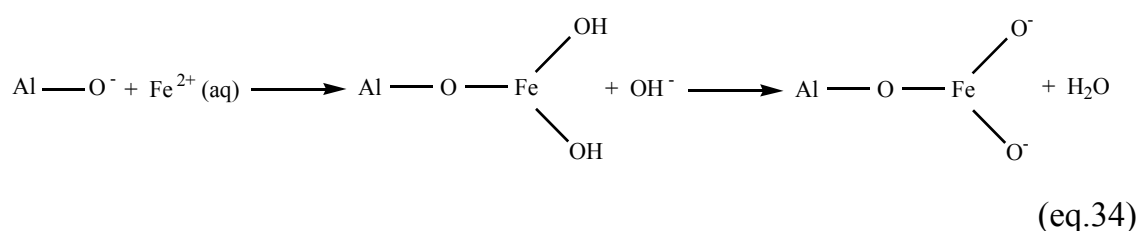
When HCl was added to solution in order to decrease the pH solution, the surface of mordenite became protonated as shown in eq.35 and 36.

$$Al - O - Fe \left\langle \begin{matrix} O^- \\ O^- \end{matrix} \right. + 2H^+ \longrightarrow Al - O - Fe \left\langle \begin{matrix} OH \\ OH \end{matrix} \right. \qquad (eq.35)$$

$$Al - O^- + H^+ \rightleftharpoons Al - OH \qquad (eq.36)$$
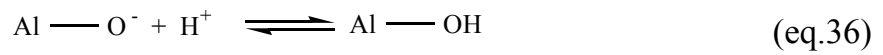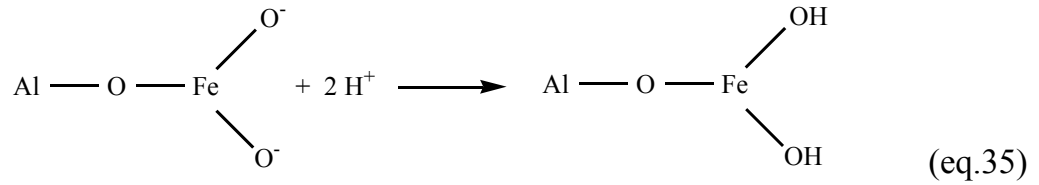
At the decreased pH, iron oxides could dissociate from surface as shown in eq.37.

$$Al - O - Fe(OH)_2 + 2H^+ \rightleftharpoons Fe^{2+} + 2H_2O + Al - OH \qquad (eq.37)$$
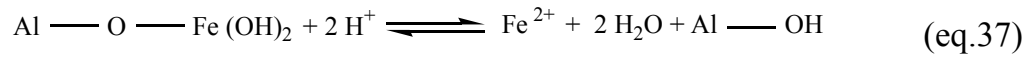
In the acidic solution, ion H^+ would attract OH groups of Al leading the counter ions Cl^- to come close to $Al-^+OH_2$ and decrease the zeta potential as shown in eq.38 and 39. Besides, the released Ca^{2+} from the mordenite surface could attract the OH group of Al by electrostatic adsorption as shown in eq.40.

$$Al - OH + H^+ \longrightarrow Al - {}^+OH_2 \qquad (eq.38)$$

$$Al - {}^+OH_2 + Cl^- \longrightarrow Al - {}^+OH_2 \cdots Cl^- \qquad (eq.39)$$

$$Al - OH + Ca^{2+} \rightleftharpoons Al - OH \cdots Ca^{2+} \qquad (eq.40)$$
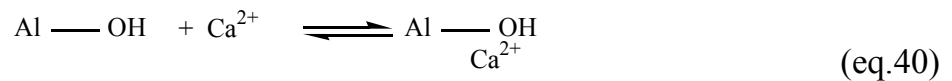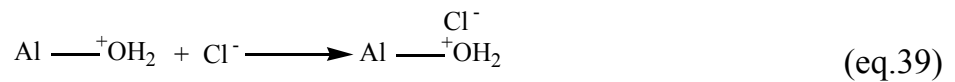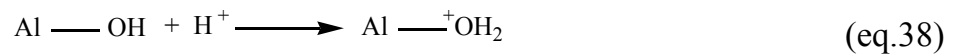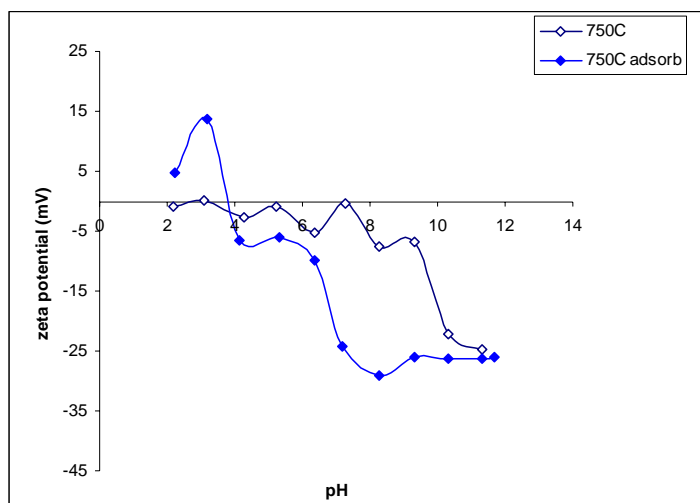
Figure 23 Zeta potential of mordenite calcined at 750ºC

For the calcined mordenite at 750ºC, the zeta potential before orthophosphate adsorption as shown in Figure 23 was approaching zero charge at the pH of 7.2 indicating that the increasing number of Al migrated to the surface of mordenite. After that the zeta potential became fluctuated and approached zero charge again at pH of 5.2 and 3.0 which could be resulted from the competed reaction on the surface between eq.28 and 39.

After orthophosphate adsorption in the basic solution, the zeta potential became more negative than the one before adsorption. It could be resulted from the increase in amount of Al in the surface composition. At the surface, beside the orthophosphate adsorption on Si by following eq. 29, Al also had a high capability to coordinately bind to orthophosphate as shown in eq.41 and 42. This resulted in the high negativity in zeta potential in pH 6-12.

$$\text{Al} - \text{OH} + \text{H}_2\text{PO}_4^- \longrightarrow \text{Al} - \text{O} - \overset{\overset{\displaystyle O}{\|}}{\underset{\displaystyle \text{OH}}{P}} \diagup \text{OH} + \text{OH}^- \qquad \text{(eq.41)}$$

$$\text{Al}-\text{O}-\text{Fe}\begin{array}{c}\text{OH}\\ \\ \text{OH}\end{array} + \text{H}_2\text{PO}_4^- \longrightarrow \text{Al}-\text{O}-\text{Fe}-\text{O}-\overset{\overset{\text{O}}{\|}}{\underset{\text{OH}}{\text{P}}}-\text{OH} + \text{H}_2\text{O}$$

(eq.42)
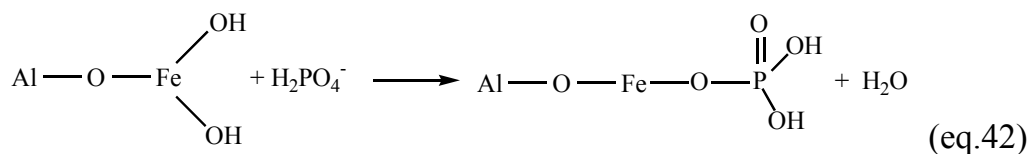
As the pH continued to decrease, the protonation proceeded. At the pH of 3.8, the zeta potential charge became more positive due to the increase in number of Si-$^+$OH$_2$ and Al-$^+$OH$_2$ presented at the surface until it reached the maximum. The positive charge at O would lead the counter ions of Cl$^-$, which are fully dispersed in system, to come close to Si-$^+$OH$_2$ and Al-$^+$OH$_2$ and decrease the zeta potential as shown in eq.32 and 39.
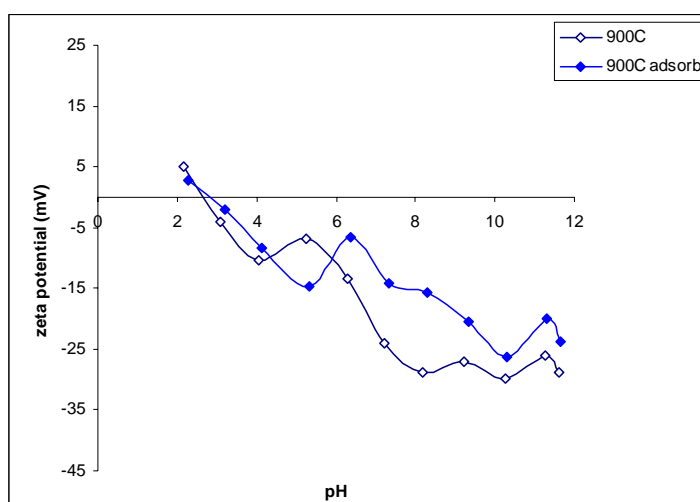
Figure 24 Zeta potential of mordenite calcined at 900ºC

From XRD pattern as shown in Figure 12, it was shown that the structure of the calcined mordenite at 900ºC was transformed into the aluminum silicate (Al$_2$SiO$_5$) of Kyanite and silicon oxide (SiO$_2$). The zeta potential before orthophosphate adsorption as shown in Figure 24 tended to become less negative as decreasing pH of the solution. The behavior on the surface was

followed the reaction of SiO⁻ and AlO⁻ as shown in eq.25-28, 31, and 34-38. At the pH of 2.6, the zeta potential became zero which corresponded to the IEP of silica. This indicated that the main surface composition was Si.

After orthophosphate adsorption, the zeta potential was less negative at the pH 6.3-12. It could be implied that as the pH was decreased, there were other cations, such as K^+ and Na^+, attracted to the O^- at the surface. K^+ and Na^+ would compete with H^+ and electrostatically bind to O^- as shown in eq.43-44.

$$Si-O-Fe\underset{O^-}{\overset{O^-}{\Big<}} + H^+, K^+, Na^+ (aq) \rightleftharpoons Si-O-Fe\underset{O^-K^+or\,H^+}{\overset{O^-Na^+or\,H^+}{\Big<}} \qquad (eq.43)$$

$$Si-O^- + H^+, K^+, Na^+ (aq) \rightleftharpoons Si-O^-_{Na^+or\,H^+} \quad or \quad Si-O^-_{K^+or\,H^+} \qquad (eq.44)$$
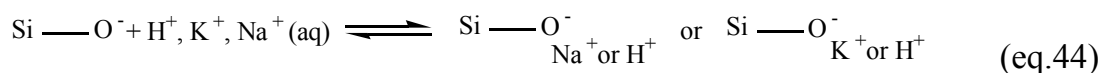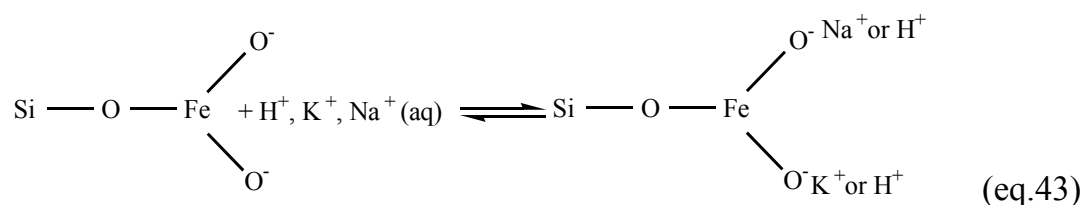
Due to Na^+ and K^+ having larger size than H^+, the $H_2PO_4^-$ adsorption would be in a distance from O^- as shown in eq.45-46. $H_2PO_4^-$ would be around Na^+ and K^+ and away in the diffuse layer. Because the zeta potential was measured the surface potential at the surface of shear, the effect of the negative charge on $H_2PO_4^-$ on the zeta potential would be less, whereas the effect charge on Na^+ and K^+ increased. This would result in less negativity in the zeta potential.

$$Si-O-Fe\underset{O^-K^+}{\overset{O^-Na^+}{\Big<}} + 2\,H_2PO_4^- (aq) \rightleftharpoons Si-O-Fe\underset{O^-K^+\,H_2PO_4^-}{\overset{O^-Na^+\,H_2PO_4^-}{\Big<}} \qquad (eq.45)$$

$$\text{Si}\text{---}\underset{\text{Na}^+}{\text{O}^-} \text{ or } \text{Si}\text{---}\underset{\text{K}^+}{\text{O}^-} + 2\,\text{H}_2\text{PO}_4^-\text{ (aq)} \rightleftharpoons \text{Si}\text{---}\underset{\text{Na}^+\,\text{H}_2\text{PO}_4^-}{\text{O}^-} \text{ or } \text{Si}\text{---}\underset{\text{K}^+\,\text{H}_2\text{PO}_4^-}{\text{O}^-} \quad \text{(eq.46)}$$
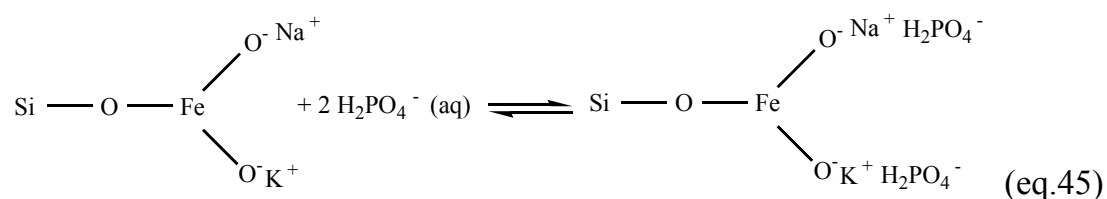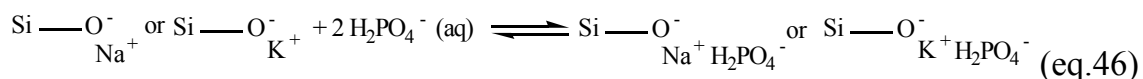
To understand the adsorption capability on mordenite at different calcination temperatures, the information on zeta potential was evaluated and compared to the results from the adsorption experiments. The zeta potential study was not able to explain the orthophosphate adsorption behavior at the calcination temperature of 150ºC. From the adsorption experiment, calcined mordenite at 150ºC could adsorb orthophosphate in the amount of 1-3 mg-P/L but there was not clearly different in zeta potential values of before and after orthophosphate adsorption. At the calcination temperatures of 450ºC and 600ºC, the results from adsorption experiment showed a small orthophosphate adsorption of less than 1 mg-P/L which agreed with the zeta potential values of before and after orthophosphate adsorption. Moreover, the small orthophosphate adsorption at 450ºC could be affected by the considerably small pore volume shown in Table 8. At the calcination temperature of 750ºC and the uncalcined, the information from zeta potential could explain the adsorption behavior which was fully agreeable to the adsorption experiment. The information from zeta potential was proposed in order to explain the adsorption behavior at the calcination temperature of 900ºC which was disagreeable to the adsorption experiment because the surface was adsorbed with cations such as Na^+ and K^+.

However, pH of the orthophosphate adsorption experiment was in the range of pH 6-11. Thus, the information retrieved from zeta potential measurement could explain the orthophosphate adsorption behavior in the range of pH 6-11. The adsorption was in the range of chemisorption.

CONCLUSION

After investigating the orthophosphate adsorption on natural adsorbents of natural zeolite, diatomite, perlite, kaolin, and ball clay, natural zeolite showed the highest % adsorption among the others. The structure of natural zeolite used in this work was identified its structure and composition. The XRD results showed the structure of mordenite, $(Ca, Na_2, K_2) Al_2Si_{10}O_{24}.7H_2O$, and the structure tended to change to aluminum silicate (Al_2SiO_5) of kyanite and silicon oxide (SiO_2) at the calcination temperature of 900ºC. For surface characterization, after increasing calcination temperature, it was indicated that surface area at multiple point of mordenite tended to decrease from $126.20 m^2/g$ for one without calcination to $2.66 m^2/g$ for one calcined at 900ºC. SEM was not able to inform the difference in morphology after calcination at various temperatures. The chemical composition on surface obtained from EDS for all calcination temperatures, before and after adsorption, had 60-80%wt SiO_2, approximately 10%wt Al_2O_3, and 10%wt of other metal oxides. These results indicated that SiO_2 was the major composition and Al_2O_3 was the minor one on surface. Moreover, there were also traces of metal oxide (Ca^{2+}, Fe^{2+}, Na^+, K^+) on their surface.

In the orthophosphate adsorption study, the results showed the maximum adsorption on the calcined mordenite at 750ºC. The equilibrium adsorptions were 1, 2, 4, and 5 hr at initial orthophosphate concentration of 5, 10, 20, and 30 mg-P/L, respectively. The orthophosphate adsorption capacity of the calcined mordenite at 750ºC was 91, 93, 92, and 89% per 1g mordenite for initial orthophosphate concentration of 5, 10, 20, and 30 mg-P/L, respectively. The adsorption results were fitted with Langmuir

isotherm with $R^2 = 0.8532$ giving the maximum adsorption of 769.23 mg-P/Kg adsorbent. Therefore, the behavior of orthophosphate adsorption in this work was monolayer. The adsorption occurs on specific sites with chemical adsorption and the orthophosphate molecules cannot migrate across the surface or interact with adjacent molecules.

To explain the orthophosphate adsorption behavior, FTIR was used to investigate the bonding between orthophosphate and the surface of mordenite. The FTIR results showed Si-O, Al-O, SiO-H, and Si(OH)Al bonds on mordenite and there were PO_4^{3-}, $H PO_4^{2-}$, and $H_2 PO_4^{-}$ at the surface. However, the results could not inform the site where orthophosphate was bound to. Therefore, zeta potential measurement was used to further observe the adsorption behavior.

The zeta potential results could give the information on adsorption behavior at the surface on the uncalcined mordenite and the calcined ones at some temperatures. The results indicated that the high dissolution of Ca^{2+} in the acidic solution and the high dissolution of Fe^{2+} in basic solution had an effect on the orthophosphate adsorption.

At the surface, the dissolved Fe^{2+} could help Al and Si to adsorb orthophosphate by coordination adsorption and the Ca^{2+} could increase the orthophosphate adsorption by electrostatic adsorption. On the surface of the uncalcined mordenite, the zeta potential showed that the Si-OH was dominated and the orthophosphate adsorption was occurred at Si-OH sites. After the mordenite was calcined, the zeta potential of the calcined mordenite at 600 and 750ºC clearly showed the increase in Al-O groups at the surface. At the calcination temperature of 750ºC, orthophosphate could adsorb not only on

Si-O sites but also on Al-O sites which significantly increased the adsorption capability. With the presence of Fe^{2+}, the zeta potential of the calcined mordenite at 750ºC showed the highest orthophosphate adsorption capability which agreed to the results from orthophosphate adsorption experiment.

At the calcination temperature of 900ºC, the structure of mordenite was changed and the surface properties were altered. The zeta potential showed that the adsorbed orthophosphate groups were attracted by electrostatic adsorption in the distance to the surface. The information from zeta potential could be used to propose the adsorption behavior on the uncalcined mordenite and the calcined ones at 450, 600, 750, and 900ºC. However, the results could not clearly explain the adsorption of the calcined mordenite at 150 and 300ºC. There should be further investigations on surface adsorption behavior in order to clarify the adsorption behavior of the calcined mordenite at 150 and 300ºC.

LITERATURE CITED

Ackley, M.W., S.U. Rege, and H. Saxena. 2003. Application of natural zeolites in the purification and separation of gases. **Microporous and Mesoporous Materials**. 61: 25–42.

Adams, W. A., S. N. Gafoor, and M. I. Karim. 1987. Composition and properties of poorly ordered minerals in Welsh soils. II. Phosphate adsorption and reactivity towards NaF solution. **Journal of Soil Science**. 38: 95-103.

Ahmad, I., J. A. Anderson, T. J. Dines, and C. H. Rochester. 1998. Infrared Study of Acetophenone Adsorption on Mordenite and Dealuminated Mordenite. **J. Colloid Interface Sci**. 207: 371–378.

Akay, G., B. Keskinler, A. Çakici, and U. Danis. 1998. Phosphate removal from water by red mud using crossflow microfiltration. **Wat. Res.** 32: 717-726.

Akyüz, S., T. Akyüz, and N.M. Ozer. 2001. FT-IR spectroscopic investigations of benzidine and bipyridyls adsorbed on diatomite from Anatolia. **J. Mol. Struct**. 565-566: 493-496.

Arai, Y. and D.L. Sparks. 2001. ATR-FTIR Spectroscopic Investigation on Phosphate Adsorption Mechanisms at the Ferrihydrite-Water Interface. **J. Colloid Interface Sci**. 241: 317–326.

Armağan, B., M. Turan, and M.S. Çelik. 2004. Equilibrium studies on the adsorption of reactive azo dyes into zeolite. **Desalination**. 170: 33-39.

Barrow, N. J., 1984. Modeling the effects of pH on phosphate sorption by soils. **Journal of Soil Science**. 35: 283-297.

Boari, G., and L. Liberty. 1975. Selective renovation of eutrophic wastes phosphate removal. **Wat. Res.** 10: 421-428.

Boisvert, J.-P, T.C. To, A. Berrak, and C. Jolicoeur. 1997. Phosphate adsorption in flocculation processes of aluminum sulphate and poly-aluminium-silicate-sulphate. **Wat. Res.** 31: 1939-1946.

Bortone, G., F. Malaspina, L. Stante, and A. Tilche. 1994. Biological nitrogen and phosphorus removal in an anaerobic/anoxic sequencing batch reactor with separated biofilm nitrification. **Water Sci and Tech**. 30: 303-313.

Burton, F.L. and H.D. Stensel. 2003. **Wastewater Engineering: Treatment and Reuse**. Metcalf & Eddy, Inc, North America.

Chumbhalel, V.R., J.S. Kim, S.B. Lee, and M.J. Choi. 2004. Catalytic degradation of expandable polystyrene waste (EPSW) over mordenite and modified mordenites. **Journal of Molecular Catalysis A: Chemical**. 222: 133–141.

Clark, S., R. Pitt, J. Easton, O. Mirov, and K. Parmer. 1997. Pollution Rrmoval Capacity of Stromwater Filtration Media – Breakthrugh Teste. **Poster presentation at Water Environment Federation Conference – 70th Annual Conference and Exposition**. Chicago, IL. October 18-22.

Covarrubias, C., R. García, R. Arriagada, J. Yánez, and M.T. Garland. 2005. Cr(III) exchange on zeolites obtained from kaolin and natural mordenite. **Microporous and Mesoporous Materials**. 88: 220–231.

Deka, R. C., and R. Vetrivel. 1998. Adsorption Sites and Diffusion Mechanism of Alkylbenzenes in Large Pore Zeolite Catalysts as Predicted by Molecular Modeling Techniques. **J. Catal**. 174: 88-97.

Doğan, M., and M. Alkan. 2003. Adsorptiion kinetics of methyl violet onto perlite. **Chemosphere.** 50: 517-528.

Doğan, M., M. Alkan, A. Tűrkyilmas, and Y. Őzdemir. 2004. Kinetics and mechanism of removal of methylene blue by adsorption onto perlite. **J. Hazard. Mater**. B109: 141-148.

Doula, M., A. Ioannou, and A. Dimirkou. 2002. Copper Adsorption and Si, Al,Ca, Mg, and Na Release from Clinoptilolite. **J. Colloid Interface Sci**. 245: 237–250.

Dyer, A., 1988. **An Introduction to Zeolite Molecular Sieves**. John Wiley & Son Ltd, United state of America.

Eaton, A.D., L.S. Clesceri, and A.E. Greenberg. 1995. **Standard Method for Examination of Water and Wastewater**. United Book Press Inc., Baltimore, Maryland, USA.

Englert, A.H., and J. Rubio. 2005. Characterization and environmental application of a Chilean natural zeolite. **Int. J. Miner. Process**. 75: 21– 29.

Erdem, E., G. Çölgeçen, and R. Donat. 2005. The removal of textile dyes by diatomite earth. **J. Colloid Interface Sci**. 282: 314–319.

Fause and S. Denton. 1987. **Adsorption Processes for water treatment**. Butterworth Publishers, USA.

Faust, S.D., and O.M. Aly. 1987. **Adsorption process for water treatment .** Butterworth Publishers, USA.

Fresenius, W., *et al*, 1989. **Waste Water Technology: Origin, collection, treatment, and analysis of waste water**. Springer Verlag Berlin Heidelberg, Geramany.

Gregory, J., and R.V. Dhond. 1972. Anion exchange equilibria involving phosphate, sulphate, and chloride. **Water Research Pergamon Press**. 6: 695-702.

Hayakawa, K., T. Morita, M. Ariyoshi, T. Maeda, and I. Satake. 1996. Adsorption of Cationic Surfactants on Hydrophobic Mordenites of Different Si/Al Ratio. **J. Colloid Interface Sci**. 177: 621-627.

Henri, R., 1996. **Chemical Water Treatment: Principles and Practice**. VCH Publishers, Inc, UK.

Hernández-Guevara, A., A. Cruz-Orea, O.H. Vigil, H. Villavicencio, and F. Sánchez-Sinencio. 2000. Thermal and optical characterization of $Zn_xCd_{1-x}S$ embedded in a zeolite host. **Materials Letters**. 44: 330–335.

Hiemenz, P.C. and R. Rajagopalan. 1997. Principles of Colloid and Surface Chemistry. 3rd ed. Marcel Dekker, Inc. New York. United State of America.

Hong, Y., and J.J. Fripiat. 1995. Microporous characteristics of H-Y, H-ZSM-5 and H-mordenite dealuminated by calcination. Microporous Material. 4: 323-334.

Hrenović, J., D. Tibljaš, H. Büyükgüngör, and Y. Orhan. 2003. Influence of Support Materials on Phosphate Removal by *A. calcoaceticus*. **Food Technol. Biotechnol**. 41: 331–338.

Inglezakis, J., A. Zorpas, and D. Loizidou. 2003. Simultaneous removal of metals Cu^{2+}, Fe^{3+} and Cr^{3+} with anions SO_4^{2-} and HPO_4^{2-} using clinoptilolite. **Microporous and Mesoporous Material**. 61: 167-171.

Jφrgensen, S. E., 1973. A new method of removing phosphorus to produce a ready fertilizer. **Wat. Res**. 7: 249-254.

Khraisheh, M.A.M., M.A. Al-Ghouti, S.J. Allen, and M.N. Ahmad. 2004. Effect of OH and silanol groups in the removal of dyes from aqueous solution using diatomite. **Wat. Res**. 13: 65-73.

Korkuna, O., R. Leboda, J. Skubiszewska-Zięba, T. Vrublevs'ka, V.M. Gun_ko, and J. Ryczkowski. 2005. Structural and physicochemical properties of natural zeolites: clinoptilolite and mordenite. **Microporous and Mesoporous Materials**. 87: 243–254.

Kosanovic, C., B. Subotic, and I. Smit. 1998. Thermally induced phase transformations in cation-exchanged zeolites 4A, 13X and synthetic mordenite and their amorphous derivatives obtained by mechanochemical treatment. **Thermochimica Acta**. 317: 25-37.

Koumanova, B., and P. Peeva-Antova. 2002. Adsorption of *p*-chlorophenol from aqueous solutions on bentonite and perlite. **J. Hazard. Mater**. A90: 229–234.

Lee, K.H., and B.H. Ha. 1998. Characterization of mordenites treated by HCl/steam or HF. **Microporous and Mesoporous Materials**. 23: 211–219.

Liberti, L., and G. Boari. 1979. Phosphate and ammonia recovery from secondary effluents by selective ion exchange with production of a slow release fertilizer. **Wat. Res**. 13: 65-73.

Liberti, L., G. Boari, D. Petruzzelli, and R. Passino. 1981. Nutrient removal and recovery from wastewater by ion exchange. **Wat. Res**. 15: 337-342.

Liberti, L., and R. Passino. 1981. Anion exchange process to recover nutrients from sewage. **Resources and Conservation**. 6: 263-273.

Liberti, L., N. Limoni, A. Lopez, R. Passino, and G. Boari. 1986. The 10 m^3h^{-1} RIM-NUT demonstration plant at west bari for removing and recovering N and P from wastewater. **Wat. Res**. 20: 735-739.

Lindsay, W. L., 1979. **Chemical Equilibria in Soils**. John Wiley & Sons, Inc. United state of America.

Liu, R. X., J. L. Guo, and H. X. Tang. 2002. Adsorption of fluoride, phosphate, and arsenate ions on a new type of ion exchange fiber. **J.Coll. Int. Sci**. 248: 268-274.

Manouchehri, N., S. Besancon, and A. Bermond. 2006. Major and trace metal extraction from soil by EDTA: Equilibrium and kinetic studies. **Analytica Chimica Acta.** 559: 105-112.

Mathialagan, T. and T. Viraraghavan. 2002. Adsorption of cadmium from aqueous solutions by perlite. **J.Hazard. Mater**. B94: 291–303.

McCash, E.M., 2001. **Surface Chemistry**. Oxford University Press Inc., New York.

Metaxas, M., V. Kasselouri-Rigopoulou, P. Galiatsatou, C. Konstantopoulou, and D. Oikonomou. 2003. Thorium removal by different adsorbents. **J. Hazard. Mater**. B97: 71–82.

Mohamed, M.M., and T.M. Salama. 2002. Effect of Mordenite Dealumination on the Structure of Encapsulated Molybdenum Catalysts. **J. Coll. Int. Sci**. 249: 104–112.

Mohamed, M.M., 2003. Catalytic properties of Fe ion-exchanged mordenite toward the ethanol transformation: influence of the methods of preparation. **Journal of Molecular Catalysis A: Chemical** 200: 301–313.

Mohamed, M.M., T.M. Salama, I. Othman, and I.A. Ellah. 2005. Synthesis of high silica mordenite nanocrystals using *o*-phenylenediamine template. **Microporous and Mesoporous Materials**. 84: 84-96.

Moreau, F., P. Ayraulta, N.S. Gnepa, S. Lacombeb, E. Merlenb, and M. Guisneta. 2002. Influence of Na exchange on the acidic and catalytic properties of an HMOR zeolite. **Microporous and Mesoporous Materials**. 51: 211-221.

Müller, M., G. Harvey, and R. Prins. 2000. Comparison of the dealumination of zeolites beta, mordenite, ZSM-5 and ferrierite by thermal treatment, leaching with oxalic acid and treatment with $SiCl_4$ by ^1H, ^{29}Si and ^{27}Al MAS NMR. **Microporous and Mesoporous Materials**. 34: 135–147.

Özacar, M., and I.A. Şengil. 2003. Enhancing phosphate removal from wastewater by using polyelectrolytes and clay injection. **J.Hazard. Mater**. B100 (2003) 131–146.

Park, M., C.L. Choi, J.S. Kim, D.H. Lee, K.S. Kim, N.H. Heo, and J. Choi. 2003. Occlusion potential of zeolites for mixed and non-nitrate salts. **Microporous and Mesoporous Materials**. 62: 1–7.

Poborchii, V.V., A.V. Kolobov, H. Oyanagi, S.G. Romanov, and K. Tanaka. 1998. Raman and X-ray Absorption Study of Selenium Incorporated into the Channels of Mordenite: Dependence on the Ion Exchange and the Method of Incorporation. 10: 427-436.

Rouguerol, F., J. Rouguerol, and K. Sing. 1999. **Adsorption by Powder & Porous Solids: Principal, Methodology, and Applications**. Academic Press, UK.

Sakadevan, K., and H. J. Bavor. 1998. Phosphate adsorption characteristics of soils, slags, and zeolite to be used as substrates in constructed wetland systems. **Wat. Res.** 32: 393-399.

Sarioglu, M., 2005. Removal of ammonium from municipal wastewater using natural Turkish (Dogantepe) zeolite. **Separation and Purification Technology**. 41: 1–11.

Seida, Y., and Y. Nakano. 2002. Removal of phosphate by layered double hydroxides containing iron. **Wat. Res.** 36: 1306–1312.

Shawabkeh, R.A., and M.F. Tutunji. 2003. Experimental study and modeling of basic dye sorption by diatomaceous clay. **Applied Clay Science**. 24: 111- 120.

Silva, J.M., M.F. Ribeiro, F. RamBa Ribeiro, E. Benazzi, N.S. Gnep, and M. G&met. 1997. Influence of the treatment of mordenite by ammonium hexafluorosilicate on physicochemical and catalytic properties. **Zeolites**. 16: 275-280.

Simmonds, M.A., 1973. Experence with algal blooms and the removal of phosphorus from sewage. **Wat. Res.** 7: 255-264.

Sposito, G., 1989. **The Chemistry of Soils. Oxford University Press,** Inc. United States of America.

Subramanial, S., and T.C. Arnot. 2001. An Integrated Bioreactor/Adsorption Process for Phosphorus Recovery from Wastewater.

Tuccillo, M.E., I.M. Cozzarelli, and J.S. Herman. 1999. Iron reduction in the sediments of a hydrocarbon contaminated aquifer. **Applied Geochemistry.** 14 : 655-667.

Udomsinrod, K., 1996. **Water treatment**. Mitnarakanpim, Inc, Prakanong, khlongtoei, Bongkok.

Vergani, D., R. Prins, and H.W. Kouwenhoven. 1997. Isopropylation of biphenyl over dealuminated mordenite. **Appl. Catal. A: General**. 163: 71-81.

Wedler, G., 1976. **Chemisorption: An Experimental Approach**. Butterworth & co (Publishers) Ltd. London.

Wernert, V., O. Schäf, H. Ghobarkar, and R. Denoyel. 2005. Adsorption properties of zeolites for artificial kidney applications. **Microporous and Mesoporous Materials**. 83: 101–113.

Wu, P.X. and Z.W. Liao. 2005. Study on structural characteristics of pillared clay modified phosphate fertilizera and its increase efficiency mechanism. **J. Zhejiang Univ SCI**. 6B(3): 195-201.

Yu, T.R., 1997. **Chemistry of Varaiable Charge Soils**. Oxford University Press, Inc. United state of America.

Zhao, D., and A. K. Sengupta. 1998. Ultimate removal of phosphate from wastewater using a new class of polymeric ion exchangers. **Wat. Res**. 32: 1613-1625.

APPENDIX

Appendix A

Appendix A1 The reagents preparation for ascorbic acid method

a) Sulfuric acid solution, 5N: Prepared by diluting 70 ml of conc H_2SO_4 with deionized water to 500 ml.

b) Potassium antimonyl tartrate solution: Prepared by dissolving 1.3715g of K $(SbO)C_4H_4O_6.1/2H_2O$ and diluting to 500 ml with deionized water in volumetric flask. Stored in a glass-stoppered bottle.

c) Ammonium molybdate solution: Prepared by dissolving 20 g of $(NH_4)_6Mo_7O_{24}.4H_2O$ in 500 ml deionized water. Stored in a plastic bottle at 4°C.

d) Ascorbic acid solution, 0.1M: Prepared by dissolving 1.76 g of ascorbic acid in 100 ml deionized water. The solution was stable for about 1 week at 4°C.

e) Combined reagent: Mix all reagents above in the follow proportions for 100 ml of the combined reagent: 50 ml of 5N H_2SO_4, 5 ml of potassium antimonyl tartrate solution, 15 ml of ammonium molybdate solution, and 30 ml of ascorbic acid solution, with mixing after addition of each reagent.

All reagents must reach room temperature before being mixed and must be mixed in the given order. If turbidity forms in combined reagent, it was shaken and left to stand for a few minutes until the turbidity disappeared before proceeding. The combined reagent was stable for 4 hours.

Appendix B

Appendix Table B1 Data from experiment of uncalcined ball clay after orthophosphate adsorption

Phosphate concentration (mg-P/L)	Shaking time (minute)	pH	Ball clay weight (g)	Phosphate concentration (mg-P/L)			%adsorbed per 1g Ball clay	absorbance (average)
				Before adsorption	After adsorption	Amount adsorption		
5	20	5.64	1.0047	5.0106	4.3355	0.6751	13.4114	0.2764
	40	5.40	1.0054	5.0106	3.9707	1.0399	20.6439	0.2533
	60	5.47	1.0026	5.0106	3.7409	1.2697	25.2721	0.2388
	120	5.29	1.0012	5.0106	3.1885	1.8221	36.3215	0.2038
	180	5.29	1.0012	5.0106	3.1885	1.8221	34.0783	0.2103
	240	5.29	1.0066	5.0106	3.2919	1.7187	37.1039	0.2008
10	20	5.35	1.0026	10.0212	8.7019	1.3193	13.1295	0.2212
	40	5.28	1.0043	10.0212	8.2722	1.7490	17.3822	0.2103
	60	5.37	1.0034	10.0212	8.0267	1.9945	19.8339	0.2041
	120	5.21	1.0050	10.0212	7.1935	2.8277	28.0793	0.1830
	180	5.30	1.0026	10.0212	7.1935	2.8277	28.1426	0.1830
	240	5.30	1.0020	10.0212	6.7814	3.2398	32.2652	0.1726
20	20	5.14	1.0054	20.0424	18.4581	1.5843	7.8620	0.2342
	40	5.16	1.0033	20.0424	18.0635	1.9789	9.8391	0.2292
	60	5.19	1.0044	20.0424	16.7480	3.2944	16.3656	0.2126
	120	5.14	1.0042	20.0424	16.4060	3.6364	18.0696	0.2082
	180	5.17	1.0051	20.0424	15.2397	4.8027	23.8431	0.1934
	240	5.14	1.0052	20.0424	14.8889	5.1535	25.5835	0.1890
30	20	5.10	1.0030	30.0637	26.9296	3.1341	10.3938	0.3416
	40	5.09	1.0046	30.0637	26.4823	3.5814	11.8574	0.3359
	60	5.13	1.0071	30.0637	27.0436	3.0201	9.9744	0.3430
	120	5.07	1.0057	30.0637	25.6843	4.3794	14.4859	0.3258
	180	5.07	1.0058	30.0637	24.8950	5.1687	17.0939	0.3158
	240	5.05	1.0052	30.0637	24.8863	5.1774	17.1336	0.3157
blank	240	5.45	1.0026	0.0000	0.0282	-0.0282		0.0179

Appendix Table B2 Data from experiment of calcination ball clay at 750ºC

after orthophosphate adsorption

Phosphate concentration (mg-P/L)	Shaking time (minute)	pH	Ball clay weight (g)	Phosphate concentration (mg-P/L)			%adsorbed per 1g Ball clay	absorbance (average)
				Before adsorption	After adsorption	Amount adsorption		
5	20	5.65	1.0039	5.0277	4.5234	0.5043	9.9908	0.2877
	40	5.47	1.0020	5.0277	4.4199	0.6078	12.0657	0.2811
	60	5.56	1.0034	5.0277	4.2164	0.8113	16.0815	0.2682
	120	5.59	1.0034	5.0277	3.9726	1.0551	20.9160	0.2528
	180	5.93	1.0022	5.0277	3.7324	1.2953	25.7060	0.2376
	240	5.72	1.0029	5.0277	3.4798	1.5479	30.6971	0.2216
10	20	5.55	1.0029	10.0554	9.1116	0.9438	9.3582	0.2313
	40	5.46	1.0021	10.0554	8.8661	1.1893	11.8020	0.2251
	60	5.44	1.0022	10.0554	8.3268	1.7286	17.1531	0.2114
	120	5.52	1.0036	10.0554	7.9979	2.0575	20.3860	0.2031
	180	5.70	1.0037	10.0554	7.8050	2.2504	22.2980	0.1982
	240	5.66	1.0018	10.0554	7.3095	2.7459	27.2602	0.1857
20	20	5.25	1.0039	20.1107	18.8810	1.2297	6.0908	0.2394
	40	5.29	1.0022	20.1107	18.5214	1.5893	7.8842	0.2349
	60	5.33	1.0040	20.1107	17.8111	2.2996	11.3930	0.2259
	120	5.44	1.0018	20.1107	16.7851	3.3256	16.5071	0.2129
	180	5.47	1.0028	20.1107	16.0309	4.0798	20.2326	0.2033
	240	5.54	1.0027	20.1107	15.3468	4.7639	23.6248	0.1947
30	20	5.17	1.0029	30.1662	28.5188	1.6474	5.4447	0.3616
	40	5.19	1.0021	30.1662	27.7997	2.3665	7.8277	0.3524
	60	5.29	1.0016	30.1662	26.7473	3.4189	11.3153	0.3391
	120	5.38	1.0027	30.1662	25.3004	4.8658	16.0863	0.3208
	180	5.40	1.0047	30.1662	24.5286	5.6376	18.6007	0.3110
	240	5.45	1.0015	30.1662	23.8271	6.3391	20.9818	0.3021
blank	240	5.91	1.0013	0.0000	0.0175	-0.0175		0.0111

Appendix Table B3 Data from experiment of uncalcined kaolin after orthophosphate adsorption

| Phosphate concentration (mg-P/L) | Shaking time (minute) | pH | Kaolin weight (g) | Phosphate concentration (mg-P/L) | | | %adsorbed per 1g Kaolin | absorbance (average) |
				Before adsorption	After adsorption	Amount adsorption		
5	20	5.85	1.0092	5.0106	4.5770	0.4336	8.5715	0.2916
	40	5.53	1.0048	5.0106	4.4157	0.5949	11.8154	0.2813
	60	5.43	1.0045	5.0106	4.5034	0.5072	10.0761	0.2869
	120	5.31	1.0039	5.0106	4.3385	0.6721	13.3583	0.2764
	180	5.66	1.0021	5.0106	4.2350	0.7756	15.4466	0.2699
	240	5.29	1.0057	5.0106	4.1543	0.8563	16.9917	0.2648
10	20	5.38	1.0048	10.0212	9.2135	0.8077	8.0218	0.2341
	40	5.23	1.0022	10.0212	9.0688	0.9524	9.4821	0.2304
	60	5.13	1.0044	10.0212	9.0688	0.9524	9.4595	0.2304
	120	5.12	1.0063	10.0212	8.9855	1.0357	10.2706	0.2283
	180	5.24	1.0032	10.0212	8.6084	1.4128	14.0533	0.2188
	240	5.12	1.0025	10.0212	8.6216	1.3996	13.9335	0.2191
20	20	4.95	1.0054	20.0424	18.9347	1.1077	5.4959	0.2402
	40	4.90	1.0058	20.0424	18.5313	1.5111	7.4953	0.2351
	60	4.96	1.0039	20.0424	19.0837	0.9587	4.7651	0.2421
	120	4.89	1.0045	20.0424	18.8470	1.1954	5.9376	0.2391
	180	4.91	1.0039	20.0424	17.9963	2.0461	10.1690	0.2283
	240	4.80	1.0065	20.0424	18.0402	2.0022	9.9255	0.2289
30	20	4.78	1.0067	30.0637	29.2214	0.8423	2.7863	0.3706
	40	4.76	1.0023	30.0637	28.5374	1.5263	5.0655	0.3619
	60	4.79	1.0050	30.0637	28.1866	1.8771	6.2112	0.3574
	120	4.75	1.0028	30.0637	27.7043	2.3594	7.8255	0.3513
	180	4.73	1.0027	30.0637	28.0288	2.0349	6.7502	0.3554
	240	4.64	1.0040	30.0637	27.8972	2.1665	7.1774	0.3538
blank	240	5.81	1.0034	0.0000	0.0253	-0.0253		0.0160

Appendix Table B4 Data from experiment of calcination kaolin at 750ºC

after orthophosphate adsorption

Phosphate concentration (mg-P/L)	Shaking time (minute)	pH	Kaolin weight (g)	Phosphate concentration (mg-P/L)			%adsorbed per 1g Kaolin	absorbance (average)
				Before adsorption	After adsorption	Amount adsorption		
5	20	5.94	1.0052	5.0277	4.8312	0.1965	3.8874	0.3247
	40	5.85	1.0042	5.0277	4.7610	0.2667	5.2820	0.3202
	60	6.01	1.0057	5.0277	4.6874	0.3403	6.7316	0.3156
	120	5.87	1.0058	5.0277	4.5593	0.4684	9.2633	0.3074
	180	6.09	1.0025	5.0277	4.5120	0.5157	10.2318	0.3044
	240	5.98	1.0031	5.0277	4.3261	0.7016	13.9121	0.2927
10	20	5.73	1.0038	10.0554	9.4712	0.5842	5.7883	0.2474
	40	5.76	1.0018	10.0554	9.3133	0.7421	7.3667	0.2434
	60	5.84	1.0042	10.0554	9.3002	0.7552	7.4804	0.2431
	120	5.75	1.0018	10.0554	9.0152	1.0402	10.3264	0.2359
	180	5.91	1.0036	10.0554	8.8179	1.2375	12.2646	0.2309
	240	5.76	1.0069	10.0554	8.4846	1.5708	15.5145	0.2224
20	20	5.42	1.0065	20.1107	19.3677	0.7430	3.6697	0.2491
	40	5.49	1.0045	20.1107	19.2099	0.9008	4.4593	0.2471
	60	5.66	1.0028	20.1107	18.6661	1.4446	7.1627	0.2402
	120	5.49	1.0013	20.1107	18.1487	1.9620	9.7430	0.2337
	180	5.80	1.0054	20.1107	17.9909	2.1198	10.4850	0.2317
	240	5.59	1.0017	20.1107	17.5612	2.5495	12.6556	0.2262
30	20	5.31	1.0055	30.1662	28.7951	1.3711	4.5193	0.3686
	40	5.40	1.0045	30.1662	28.4969	1.6693	5.5088	0.3648
	60	5.49	1.0047	30.1662	27.8655	2.3007	7.5908	0.3568
	120	5.36	1.0045	30.1662	27.6725	2.4937	8.2290	0.3543
	180	5.53	1.0070	30.1662	27.4445	2.7217	8.9600	0.3514
	240	5.42	1.0038	30.1662	26.8657	3.3005	10.8996	0.3441
blank	240	6.26	1.0035	0.0000	0.2938	-0.2938		0.1861

Appendix Table B5 Data from experiment of calcination perlite at 750ºC

after orthophosphate adsorption

Phosphate concentration (mg-P/L)	Shaking time (minute)	Trial	pH	Perlite weight (g)	Phosphate concentration (mg-P/L)			%adsorbed per 1g perlite	absorbance (average)
					Before adsorption	After adsorption	Amount adsorption		
5	180	1	5.63	1.0380	5.0254	5.1283	-0.1029	-1.9726	0.3260
		2	5.64	1.0038	5.0254	5.1336	-0.1082	-2.1441	0.3263
		3	5.60	1.0445	5.0254	5.0915	-0.0661	-1.2587	0.3237
	240	1	6.27	1.0030	5.0254	5.0652	-0.0398	-0.7888	0.3220
		2	6.20	1.0261	5.0254	5.0704	-0.0450	-0.8731	0.3223
		3	6.23	1.0110	5.0254	5.0704	-0.0450	-0.8861	0.3223
30	180	1	5.78	1.0330	30.1525	31.4740	-1.3215	-4.2427	0.3990
		2	5.97	1.0391	30.1525	31.2109	-1.0584	-3.3781	0.3957
		3	5.59	1.0083	30.1525	31.3161	-1.1636	-3.8274	0.3970
	240	1	5.76	1.0145	30.1525	30.9741	-0.8216	-2.6860	0.3927
		2	5.75	1.0347	30.1525	31.3161	-1.1636	-3.7298	0.3970
		3	6.07	1.0077	30.1525	30.9215	-0.7690	-2.5309	0.3920
blank	240	1	6.28	1.0342	0.0000	0.0368	-0.0368		0.0233
		2	6.37	1.0068	0.0000	0.0053	-0.0053		0.0033
		3	6.37	1.0069	0.0000	0.0110	-0.0110		0.0070
		average				0.0177	-0.0177		0.0112

Appendix Table B6 Data from experiment of calcination diatomite at 750ºC

after orthophosphate adsorption

Phosphate concentration (mg-P/L)	Shaking time (minute)	Trial	pH	Diatomite weight (g)	Phosphate concentration (mg-P/L)			%adsorbed per 1g diatomite	absorbance (average)
					Before adsorption	After adsorption	Amount adsorption		
5	180	1	5.84	1.0093	5.0254	4.5346	0.4908	9.6765	0.3017
		2	5.61	1.0143	5.0254	4.4294	0.5960	11.6933	0.2950
		3	5.72	1.0150	5.0254	4.6030	0.4224	8.2811	0.3060
	240	1	6.00	1.0132	5.0254	4.8503	0.1751	3.4389	0.3217
		2	5.90	1.0039	5.0254	4.6556	0.3698	7.3297	0.3093
		3	5.95	1.0040	5.0254	4.5977	0.4277	8.4761	0.3057
30	180	1	5.44	1.0008	30.1525	29.6333	0.5192	1.7207	0.3783
		2	5.20	1.0025	30.1525	28.7124	1.4401	4.7640	0.3667
		3	5.49	1.0008	30.1525	30.3173	-0.1648	-0.5461	0.3870
	240	1	5.70	1.0056	30.1525	28.5020	1.6505	5.4434	0.3640
		2	6.00	1.0056	30.1525	29.2912	0.8613	2.8404	0.3740
		3	5.96	1.0003	30.1525	29.5017	0.6508	2.1577	0.3767
blank	240	1	6.12	1.0022	0.0000	0.1715	-0.1715		0.1087
		2	5.93	1.0057	0.0000	0.2336	-0.2336		0.1480
		3	5.94	1.0187	0.0000	0.2768	-0.2768		0.1753
		average				0.2273	-0.2273		

Appendix C
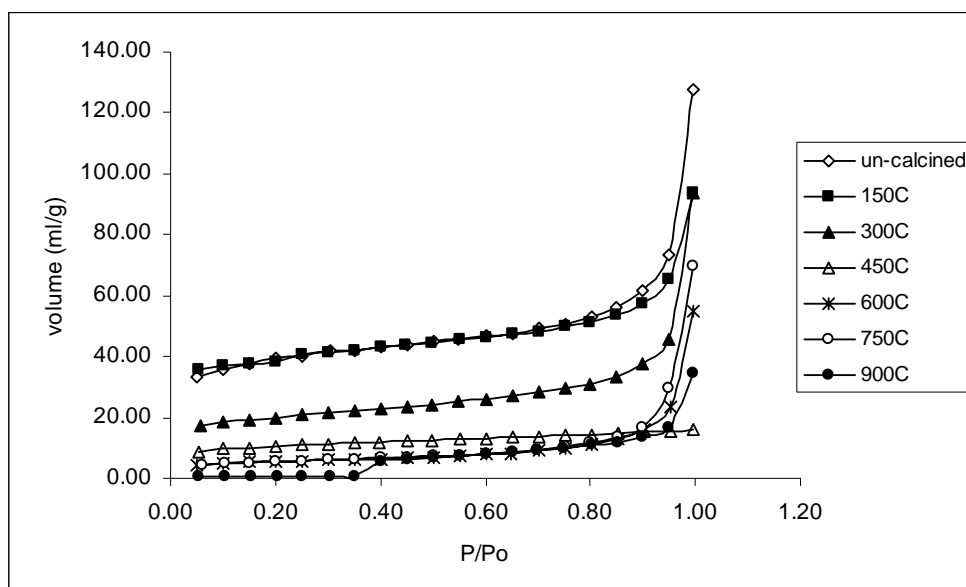
Appendix Figure C1 Nitrogen adsorption isotherms of the natural zeolite

calcination at various temperatures

Date: 02/06/2006

Quantachrome Corporation
Quantachrome Autosorb Automated Gas Sorption System Report
Autosorb for Windows® Version 1.19

Sample ID	Natural Zeolite 25				
Description	TISTR				
Comments					
Sample Weight	0.2047 g				
Adsorbate	NITROGEN	Outgas Temp	300.0 °C	Operator	Rungrueng
Cross-Sec Area	16.2 Å²/molecule	Outgas Time	3.0 hrs	Analysis Time	931.7 min
NonIdeality	6.580E-05	P/Po Toler	0	End of Run	01/18/2006
Molecular Wt	28.0134 g/mol	Equil Time	3	File Name	AS010327.RAI
Station #	1	Bath Temp.	77.40		

AREA-VOLUME-PORE SIZE SUMMARY

SURFACE AREA DATA

Multipoint BET...	1.262E+02	m²/g
Single Point BET...	1.262E+02	m²/g
BJH Method Cumulative Adsorption Surface Area...............	7.366E+01	m²/g
BJH Method Cumulative Desorption Surface Area...............	3.693E+01	m²/g
DH Method Cumulative Adsorption Surface Area...............	7.705E+01	m²/g
DH Method Cumulative Desorption Surface Area...............	3.905E+01	m²/g
DR Method Micro Pore Area..................................	1.818E+02	m²/g

PORE VOLUME DATA

Total Pore Volume for pores with Diameter less than 3868.3 Å at P/Po = 0.99503........................	1.975E-01	cc/g
BJH Method Cumulative Adsorption Pore Volume...............	1.664E-01	cc/g
BJH Method Cumulative Desorption Pore Volume...............	1.367E-01	cc/g
BJH Interpolated Cumulative Adsorption Pore Volume for pores in the range of 5000.0 to 0.0 Å Diameter...................	1.664E-01	cc/g
BJH Interpolated Cumulative Desorption Pore Volume for pores in the range of 5000.0 to 0.0 Å Diameter...................	1.367E-01	cc/g
DH Method Cumulative Adsorption Pore Volume...............	1.628E-01	cc/g
DH Method Cumulative Desorption Pore Volume...............	1.338E-01	cc/g
DR Method Micro Pore Volume................................	6.460E-02	cc/g
HK Method Cumulative Pore Volume...........................	5.822E-02	cc/g
SF Method Cumulative Pore Volume...........................	5.917E-02	cc/g

PORE SIZE DATA

Average Pore Diameter......................................	6.259E+01	Å
BJH Method Adsorption Pore Diameter (Mode)..................	1.940E+01	Å
BJH Method Desorption Pore Diameter (Mode)..................	3.816E+01	Å
DH Method Adsorption Pore Diameter (Mode)..................	1.940E+01	Å
DH Method Desorption Pore Diameter (Mode)..................	3.816E+01	Å
DR Method Micro Pore Width	8.112E+01	Å
DA Method Pore Diameter (Mode)............................	1.740E+01	Å
HK Method Pore Width (Mode)............................	1.492E+01	Å
SF Method Pore Diameter (Mode)............................	2.805E+01	Å

DATA REDUCTION PARAMETERS

Thermal Transpiration : ON
Effective Molecule Diameter (D) 3.5400
Effective Cell Stem Inner Diameter (d)
Last Po Acquired 788.55 mm Hg
Additional Initialization Information Not Available

BJH/DH Moving Average Size :

Interaction Constant (K) 2.9600 nm^3 x kJ/mol
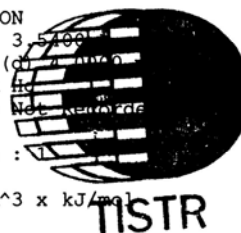
Appendix Figure C2 BET analysis of non calcination mordenite

Date: 06/16/2006

Quantachrome Corporation
Quantachrome Autosorb Automated Gas Sorption System Report
Autosorb for Windows® Version 1.19

Sample ID	Mrdenite 150				
Description	TISTR				
Comments					
Sample Weight	0.0997 g				
Adsorbate	NITROGEN	Outgas Temp	300.0 °C	Operator	Rungrueng
Cross-Sec Area	16.2 Å²/molecule	Outgas Time	3.0 hrs	Analysis Time	434.1 min
NonIdeality	6.580E-05	P/Po Toler	0	End of Run	05/31/2006 18
Molecular Wt	28.0134 g/mol	Equil Time	3	File Name	AS010467.RAW
Station #	1	Bath Temp.	77.40		

AREA-VOLUME-PORE SIZE SUMMARY

SURFACE AREA DATA

Multipoint BET...	1.248E+02	m²/g
Single Point BET...	1.262E+02	m²/g
BJH Method Cumulative Adsorption Surface Area..............	4.669E+01	m²/g
BJH Method Cumulative Desorption Surface Area..............	2.905E+01	m²/g
DH Method Cumulative Adsorption Surface Area..............	4.868E+01	m²/g
DH Method Cumulative Desorption Surface Area..............	2.970E+01	m²/g
DR Method Micro Pore Area..................................	1.767E+02	m²/g

PORE VOLUME DATA

Total Pore Volume for pores with Diameter less than 3634.9 Å at P/Po = 0.99470........................	1.450E-01	cc/g
BJH Method Cumulative Adsorption Pore Volume...............	1.034E-01	cc/g
BJH Method Cumulative Desorption Pore Volume...............	8.732E-02	cc/g
BJH Interpolated Cumulative Adsorption Pore Volume for pores in the range of 5000.0 to 0.0 Å Diameter...................	1.034E-01	cc/g
BJH Interpolated Cumulative Desorption Pore Volume for pores in the range of 5000.0 to 0.0 Å Diameter...................	8.732E-02	cc/g
DH Method Cumulative Adsorption Pore Volume................	1.013E-01	cc/g
DH Method Cumulative Desorption Pore Volume................	8.530E-02	cc/g
DR Method Micro Pore Volume................................	6.279E-02	cc/g
HK Method Cumulative Pore Volume...........................	5.840E-02	cc/g
SF Method Cumulative Pore Volume...........................	5.846E-02	cc/g

PORE SIZE DATA

Average Pore Diameter......................................	4.648E+01	Å
BJH Method Adsorption Pore Diameter (Mode).................	2.190E+01	Å
BJH Method Desorption Pore Diameter (Mode).................	3.815E+01	Å
DH Method Adsorption Pore Diameter (Mode).................	2.190E+01	Å
DH Method Desorption Pore Diameter (Mode).................	3.815E+01	Å
DR Method Micro Pore Width	6.280E+01	Å
DA Method Pore Diameter (Mode)............................	1.460E+01	Å
HK Method Pore Width (Mode)............................	1.462E+01	Å
SF Method Pore Diameter (Mode)............................	2.750E+01	Å

DATA REDUCTION PARAMETERS

Thermal Transpiration : ON
Effective Molecule Diameter (D) 3.5400 Å
Effective Cell Stem Inner Diameter (d) 4.0000
Last Po Acquired 798.09 mm Hg
Additional Initialization Information Not Recorded

BJH/DH Moving Average Size : 1

TISTR

Interaction Constant (K) 2.9600 nm^3 x kJ/mol

Appendix Figure C3 BET analysis of calcination mordenite at 150ºC

Date: 06/16/2006

Quantachrome Corporation
Quantachrome Autosorb Automated Gas Sorption System Report
Autosorb for Windows® Version 1.19

Sample ID   Mrdenite 300
Description   TISTR
Comments
Sample Weight   0.0863 g
Adsorbate   NITROGEN   Outgas Temp   300.0 °C   Operator   Rungrueng
Cross-Sec Area   16.2 Å²/molecule Outgas Time   3.0 hrs   Analysis Time   387.1 min
NonIdeality   6.580E-05   P/Po Toler   0   End of Run   06/01/2006 17
Molecular Wt   28.0134 g/mol   Equil Time   3   File Name   AS010468.RAW
Station #   1   Bath Temp.   77.40

AREA-VOLUME-PORE SIZE SUMMARY

SURFACE AREA DATA

Multipoint BET... 6.497E+01 m²/g
Single Point BET... 6.509E+01 m²/g
BJH Method Cumulative Adsorption Surface Area............... 4.028E+01 m²/g
BJH Method Cumulative Desorption Surface Area............... 5.406E+01 m²/g
DH Method Cumulative Adsorption Surface Area................ 4.168E+01 m²/g
DH Method Cumulative Desorption Surface Area................ 5.463E+01 m²/g
DR Method Micro Pore Area.................................... 9.303E+01 m²/g

PORE VOLUME DATA

Total Pore Volume for pores with Diameter
less than 4924.4 Å at P/Po = 0.99610........................ 1.447E-01 cc/g
BJH Method Cumulative Adsorption Pore Volume................ 1.299E-01 cc/g
BJH Method Cumulative Desorption Pore Volume................ 1.200E-01 cc/g
BJH Interpolated Cumulative Adsorption Pore Volume for pores
in the range of 5000.0 to 0.0 Å Diameter.................... 1.299E-01 cc/g
BJH Interpolated Cumulative Desorption Pore Volume for pores
in the range of 5000.0 to 0.0 Å Diameter.................... 1.200E-01 cc/g
DH Method Cumulative Adsorption Pore Volume................. 1.265E-01 cc/g
DH Method Cumulative Desorption Pore Volume................. 1.171E-01 cc/g
DR Method Micro Pore Volume................................. 3.306E-02 cc/g
HK Method Cumulative Pore Volume............................ 2.974E-02 cc/g
SF Method Cumulative Pore Volume............................ 3.009E-02 cc/g

PORE SIZE DATA

Average Pore Diameter.......................................
BJH Method Adsorption Pore Diameter (Mode)..............
BJH Method Desorption Pore Diameter (Mode)..............
DH Method Adsorption Pore Diameter (Mode)..............
DH Method Desorption Pore Diameter (Mode)..............
DR Method Micro Pore Width   .... Å
DA Method Pore Diameter (Mode).......................... 1.740E+01 Å
HK Method Pore Width   (Mode)........................... Å
SF Method Pore Diameter (Mode)........................... 2.796E+01 Å

DATA REDUCTION PARAMETERS

Thermal Transpiration : ON
Effective Molecule Diameter (D) 3.5400 Å
Effective Cell Stem Inner Diameter (d) 4.0000 mm
Last Po Acquired 792.47 mm Hg
Additional Initialization Information Not Recorded.

BJH/DH Moving Average Size : 1

Interaction Constant (K) 2.9600 nm^3 x kJ/mol

Appendix Figure C4 BET analysis of calcination mordenite at 300ºC

Date: 02/24/2006

Quantachrome Corporation
Quantachrome Autosorb Automated Gas Sorption System Report
Autosorb for Windows® Version 1.19

Sample ID   Mordenite450C
Description   TISTR
Comments
Sample Weight   0.3131 g
Adsorbate   NITROGEN   Outgas Temp   300.0 °C   Operator   Rungrueng
Cross-Sec Area   16.2 Å²/molecule Outgas Time   3.0 hrs   Analysis Time   309.4 min
NonIdeality   6.580E-05   P/Po Toler   0   End of Run   02/20/2006 20
Molecular Wt   28.0134 g/mol   Equil Time   3   File Name   AS010439.RAW
Station #   1   Bath Temp.   77.40

AREA-VOLUME-PORE SIZE SUMMARY

SURFACE AREA DATA

Multipoint BET... 3.458E+01 m²/g
Single Point BET.. 3.454E+01 m²/g
BJH Method Cumulative Adsorption Surface Area............... 2.342E+01 m²/g
BJH Method Cumulative Desorption Surface Area............... 1.327E+01 m²/g
DH Method Cumulative Adsorption Surface Area................ 2.458E+01 m²/g
DH Method Cumulative Desorption Surface Area................ 1.397E+01 m²/g
DR Method Micro Pore Area................................... 5.017E+01 m²/g

PORE VOLUME DATA

Total Pore Volume for pores with Diameter
less than 4925.7 Å at P/Po = 0.99610........................ 2.475E-02 cc/g
BJH Method Cumulative Adsorption Pore Volume................ 1.747E-02 cc/g
BJH Method Cumulative Desorption Pore Volume................ 1.052E-02 cc/g
BJH Interpolated Cumulative Adsorption Pore Volume for pores
in the range of 5000.0 to 0.0 Å Diameter.................... 1.747E-02 cc/g
BJH Interpolated Cumulative Desorption Pore Volume for pores
in the range of 5000.0 to 0.0 Å Diameter.................... 1.052E-02 cc/g
DH Method Cumulative Adsorption Pore Volume................. 1.743E-02 cc/g
DH Method Cumulative Desorption Pore Volume................. 1.049E-02 cc/g
DR Method Micro Pore Volume................................. 1.783E-02 cc/g
HK Method Cumulative Pore Volume............................ 1.578E-02 cc/g
SF Method Cumulative Pore Volume............................ 1.598E-02 cc/g

PORE SIZE DATA

Average Pore Diameter....................................... 2.862E+01 Å
BJH Method Adsorption Pore Diameter (Mode).................. 1.437E+01 Å
BJH Method Desorption Pore Diameter (Mode).................. 1.409E+01 Å
DH Method Adsorption Pore Diameter (Mode).................. 1.437E+01 Å
DH Method Desorption Pore Diameter (Mode).................. 1.409E+01 Å
DR Method Micro Pore Width .... 8.863E+00 Å
DA Method Pore Diameter (Mode)............................. 1.740E+01 Å
HK Method Pore Width   (Mode)............................. 1.448E+01 Å
SF Method Pore Diameter (Mode)............................. 2.713E+01 Å

DATA REDUCTION PARAMETERS

Thermal Transpiration : ON
Effective Molecule Diameter (D) 3.5400
Effective Cell Stem Inner Diameter (d) 4.0000
Last Po Acquired 515.50 mm Hg
Additional Initialization Information Not Reco

BJH/DH Moving Average Size : 1

Interaction Constant (K) 2.9600 nm^3 x kJ/mol

TISTR
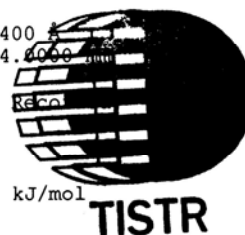
Appendix Figure C5 BET analysis of calcination mordenite at 450ºC

Date: 05/25/2006

Quantachrome Corporation
Quantachrome Autosorb Automated Gas Sorption System Report
Autosorb for Windows® Version 1.19

Sample ID	Mordenite 600C				
Description	TISTR				
Comments					
Sample Weight	0.0672 g				
Adsorbate	NITROGEN	Outgas Temp	300.0 °C	Operator	Rungrueng
Cross-Sec Area	16.2 Å²/molecule	Outgas Time	3.0 hrs	Analysis Time	308.2 min
NonIdeality	6.580E-05	P/Po Toler	0	End of Run	05/23/2006
Molecular Wt	28.0134 g/mol	Equil Time	3	File Name	AS010460.R?
Station #	1	Bath Temp.	77.40		

AREA-VOLUME-PORE SIZE SUMMARY

SURFACE AREA DATA

Multipoint BET... 1.779E+01 m²/g
Single Point BET... 1.777E+01 m²/g
BJH Method Cumulative Adsorption Surface Area............... 1.613E+01 m²/g
BJH Method Cumulative Desorption Surface Area.............. 3.081E+01 m²/g
DH Method Cumulative Adsorption Surface Area............... 1.677E+01 m²/g
DH Method Cumulative Desorption Surface Area.............. 3.116E+01 m²/g
DR Method Micro Pore Area.................................. 2.562E+01 m²/g

PORE VOLUME DATA

Total Pore Volume for pores with Diameter
less than 3495.4 Å at P/Po = 0.99449...................... 8.692E-02 cc/g
BJH Method Cumulative Adsorption Pore Volume............... 8.610E-02 cc/g
BJH Method Cumulative Desorption Pore Volume............... 8.763E-02 cc/g
BJH Interpolated Cumulative Adsorption Pore Volume for pores
in the range of 5000.0 to 0.0 Å Diameter.................. 8.610E-02 cc/g
BJH Interpolated Cumulative Desorption Pore Volume for pores
in the range of 5000.0 to 0.0 Å Diameter.................. 8.763E-02 cc/g
DH Method Cumulative Adsorption Pore Volume............... 8.394E-02 cc/g
DH Method Cumulative Desorption Pore Volume............... 8.550E-02 cc/g
DR Method Micro Pore Volume............................... 9.103E-03 cc/g
HK Method Cumulative Pore Volume.......................... 8.122E-03 cc/g
SF Method Cumulative Pore Volume.......................... 8.227E-03 cc/g

PORE SIZE DATA

Average Pore Diameter....................................... 1.955E+02 Å
BJH Method Adsorption Pore Diameter (Mode).................. 4.908E+01 Å
BJH Method Desorption Pore Diameter (Mode).................. 3.814E+01 Å
DH Method Adsorption Pore Diameter (Mode).................. 4.908E+01 Å
DH Method Desorption Pore Diameter (Mode).................. 3.814E+01 Å
DR Method Micro Pore Width .... 8.490E+01 Å
DA Method Pore Diameter (Mode)............................ 1.740E+01 Å
HK Method Pore Width   (Mode)............................ 1.473E+01 Å
SF Method Pore Diameter (Mode)............................ 2.768E+01 Å

DATA REDUCTION PARAMETERS

Thermal Transpiration : ON
Effective Molecule Diameter (D) 3.5400 Å
Effective Cell Stem Inner Diameter (d) 4.00 mm
Last Po Acquired 788.08 mm Hg
Additional Initialization Information Not Recorded

BJH/DH Moving Average Size : 1

Interaction Constant (K) 2.9600 nm^3 x kJ/mol

TISTR

Appendix Figure C6 BET analysis of calcination mordenite at 600ºC

Date: 02/24/2006

Quantachrome Corporation
Quantachrome Autosorb Automated Gas Sorption System Report
Autosorb for Windows® Version 1.19

Sample ID   Mordenite750C
Description   TISTR
Comments
Sample Weight   0.2296 g
Adsorbate   NITROGEN   Outgas Temp   300.0 °C   Operator   Rungrueng
Cross-Sec Area   16.2 Å²/molecule Outgas Time   3.0 hrs   Analysis Time   682.3 min
NonIdeality   6.580E-05   P/Po Toler   0   End of Run   02/16/2006 22
Molecular Wt   28.0134 g/mol   Equil Time   3   File Name   AS010438.RAW
Station #   1   Bath Temp.   77.40

AREA-VOLUME-PORE SIZE SUMMARY

SURFACE AREA DATA

Multipoint BET.. 1.825E+01 m²/g
Single Point BET... 1.816E+01 m²/g
BJH Method Cumulative Adsorption Surface Area.............. 1.440E+01 m²/g
BJH Method Cumulative Desorption Surface Area.............. 2.662E+01 m²/g
DH Method Cumulative Adsorption Surface Area.............. 1.461E+01 m²/g
DH Method Cumulative Desorption Surface Area.............. 2.715E+01 m²/g
DR Method Micro Pore Area.................................. 2.588E+01 m²/g

PORE VOLUME DATA

Total Pore Volume for pores with Diameter
less than 3264.0 Å at P/Po = 0.99410....................... 1.075E-01 cc/g
BJH Method Cumulative Adsorption Pore Volume............... 1.050E-01 cc/g
BJH Method Cumulative Desorption Pore Volume.............. 1.089E-01 cc/g
BJH Interpolated Cumulative Adsorption Pore Volume for pores
in the range of 5000.0 to 0.0 Å Diameter................... 1.050E-01 cc/g
BJH Interpolated Cumulative Desorption Pore Volume for pores
in the range of 5000.0 to 0.0 Å Diameter................... 1.089E-01 cc/g
DH Method Cumulative Adsorption Pore Volume............... 1.020E-01 cc/g
DH Method Cumulative Desorption Pore Volume............... 1.062E-01 cc/g
DR Method Micro Pore Volume................................ 9.196E-03 cc/g
HK Method Cumulative Pore Volume........................... 8.016E-03 cc/g
SF Method Cumulative Pore Volume........................... 8.139E-03 cc/g

PORE SIZE DATA

Average Pore Diameter...................................... 2.357E+02 Å
BJH Method Adsorption Pore Diameter (Mode)................. 1.434E+01 Å
BJH Method Desorption Pore Diameter (Mode)................. 3.822E+01 Å
DH Method Adsorption Pore Diameter (Mode)................. 1.434E+01 Å
DH Method Desorption Pore Diameter (Mode)................. 3.822E+01 Å
DR Method Micro Pore Width   .... 9.250E+01 Å
DA Method Pore Diameter (Mode)............................ 1.740E+01 Å
HK Method Pore Width   (Mode)........................... 1.473E+01 Å
SF Method Pore Diameter (Mode)............................ 2.768E+01 Å

DATA REDUCTION PARAMETERS

Thermal Transpiration : ON
Effective Molecule Diameter (D) 3.5410
Effective Cell Stem Inner Diameter (d)
Last Po Acquired 792.18 mm He
Additional Initialization Information Not Re

BJH/DH Moving Average Size : 1

Interaction Constant (K) 2.9600 nm^3 x kJ/mol

TISTR

Appendix Figure C7 BET analysis of calcination mordenite at 750ºC

Date: 06/16/2006

Quantachrome Corporation
Quantachrome Autosorb Automated Gas Sorption System Report
Autosorb for Windows® Version 1.19

Sample ID   Mrdenite 900
Description   TISTR
Comments
Sample Weight   0.1037 g
Adsorbate   NITROGEN   Outgas Temp   300.0 °C   Operator   Rungrueng
Cross-Sec Area   16.2 Å²/molecule Outgas Time   3.0 hrs   Analysis Time 296.2 min
NonIdeality   6.580E-05   P/Po Toler   0   End of Run   06/07/2006 19
Molecular Wt   28.0134 g/mol   Equil Time   3   File Name   AS010469.RAW
Station #   1   Bath Temp.   77.40

AREA-VOLUME-PORE SIZE SUMMARY

SURFACE AREA DATA

Multipoint BET... 2.661E+00 m²/g
Single Point BET... 2.678E+00 m²/g
BJH Method Cumulative Adsorption Surface Area.............. 3.266E+01 m²/g
BJH Method Cumulative Desorption Surface Area.............. 4.306E+01 m²/g
DH Method Cumulative Adsorption Surface Area............... 3.361E+01 m²/g
DH Method Cumulative Desorption Surface Area............... 5.536E+01 m²/g
DR Method Micro Pore Area.................................. 3.970E+00 m²/g

PORE VOLUME DATA

Total Pore Volume for pores with Diameter
less than 408.1 Å at P/Po = 0.95055....................... 2.599E-02 cc/g
BJH Method Cumulative Adsorption Pore Volume............... 6.663E-02 cc/g
BJH Method Cumulative Desorption Pore Volume............... 7.027E-02 cc/g
BJH Interpolated Cumulative Adsorption Pore Volume for pores
in the range of 5000.0 to 0.0 Å Diameter.................. 6.663E-02 cc/g
BJH Interpolated Cumulative Desorption Pore Volume for pores
in the range of 5000.0 to 0.0 Å Diameter.................. 7.027E-02 cc/g
DH Method Cumulative Adsorption Pore Volume................ 6.522E-02 cc/g
DH Method Cumulative Desorption Pore Volume................ 7.533E-02 cc/g
DR Method Micro Pore Volume................................ 1.411E-03 cc/g
HK Method Cumulative Pore Volume........................... 1.326E-03 cc/g
SF Method Cumulative Pore Volume........................... 1.346E-03 cc/g

PORE SIZE DATA

Average Pore Diameter...................................... 3.908E+02 Å
BJH Method Adsorption Pore Diameter (Mode)............... ‎   Å
BJH Method Desorption Pore Diameter (Mode)............... ‎   Å
DH Method Adsorption Pore Diameter (Mode)............... ‎   Å
DH Method Desorption Pore Diameter (Mode)............... ‎   Å
DR Method Micro Pore Width .... ‎   Å
DA Method Pore Diameter (Mode).......................... ‎   Å
HK Method Pore Width   (Mode)......................... ‎   Å
SF Method Pore Diameter (Mode).......................... ‎ 3.708E+01 Å

DATA REDUCTION PARAMETERS

TISTR

Thermal Transpiration : ON
Effective Molecule Diameter (D) 3.5400 Å
Effective Cell Stem Inner Diameter (d) 4.0000 mm
Last Po Acquired 791.10 mm Hg
Additional Initialization Information Not Recorded.

BJH/DH Moving Average Size : 1

Interaction Constant (K) 2.9600 nm^3 x kJ/mol
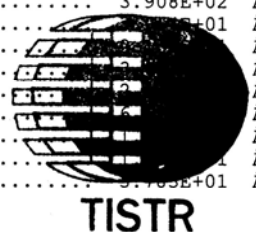
Appendix Figure C8 BET analysis of calcination mordenite at 900ºC

Appendix D

```
SEMQuant results. Listed at 11:03:01 PM on 28/2/06
Operator: Chaweewan
Client: none
Job: Job 2006_1
Spectrum label: 25 C ADSORB

System resolution =  76 eV

Quantitative method: ZAF ( 3 iterations).
 Analysed elements combined with: O ( Valency: -2)
 Method : Stoichiometry Normalised results.
 Nos. of ions calculation based on  32 anions per formula.

 3 peaks possibly omitted: -0.02, 0.24, 8.02 keV

Standards :
 Na K       NaCl 8/27/02
 Mg K       mgo sem 3/13/98
 Al K       Al 5/22/02
 Si K       sic_c 3/19/98
 K  K       KBr 5/22/02
 Ca K       CaSiO 8/27/02
 Fe K       Fe 8/27/02
```

Elmt	Spect. Type	Element %	Atomic %		Compound %	Nos. of ions
Na K	ED	1.05	0.94	Na2O	1.42	0.47
Mg K	ED	0.30	0.26	MgO	0.50	0.13
Al K	ED	5.77	4.38	Al2O3	10.91	2.17
Si K	ED	37.94	27.67	SiO2	81.15	13.72
K K	ED	1.19	0.62	K2O	1.43	0.31
Ca K	ED	2.55	1.30	CaO	3.57	0.65
Fe K	ED	0.79	0.29	FeO	1.02	0.
O		50.41	64.54			
Total		100.00	100.00		100.00	

```
* = <2 Sigma

Fit Indices
--------------------
Na K     25.4
Mg K      2.4
Al K      0.8
Si K      2.6
K  K      0.1
Ca K      0.1
Fe K      0.3
O  Ka     0.0
```
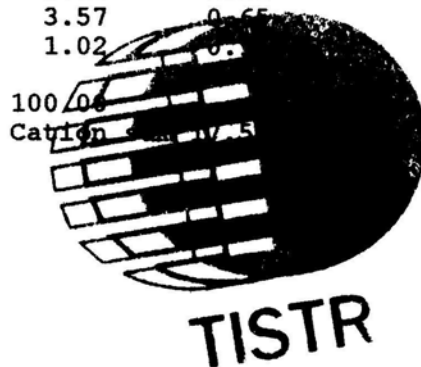
Appendix Figure D1 Chemical composition analysis of non calcinations

mordenite

```
SEMQuant results. Listed at 15:23:29 PM on 19/5/06
Operator: Chaweewan
Client: none
Job: Job 2006_1
Spectrum label: 1500 C

System resolution =  77 eV

Quantitative method: ZAF ( 3 iterations).
 Analysed elements combined with: O ( Valency: -2)
 Method : Stoichiometry Normalised results.
 Nos. of ions calculation based on  32 anions per formula.

 3 peaks possibly omitted: -0.02, 0.24, 8.04 keV

Standards :
 Na K       NaCl 8/27/02
 Mg K       mgo sem 3/13/98
 Al K       Al 5/22/02
 Si K       sic_c 3/19/98
 K  K       KBr 5/22/02
 Ca K       CaSiO 8/27/02
 Ti K       Ti 5/22/02
 Fe K       Fe 8/27/02
```

Elmt	Spect. Type	Element %	Atomic %		Compound %	Nos. of ions
Na K	ED	0.90	0.81	Na2O	1.21	0.40
Mg K	ED	0.50	0.42	MgO	0.83	0.21
Al K	ED	6.36	4.88	Al2O3	12.02	2.43
Si K	ED	36.26	26.69	SiO2	77.57	13.31
K K	ED	1.81	0.95	K2O	2.17	0.48
Ca K	ED	2.60	1.34	CaO	3.64	0.67
Ti K	ED	0.24	0.10	TiO2	0.39	0.05
Fe K	ED	1.68	0.62	FeO	2.16	0.31
O		49.66	64.18			32.00
Total		100.00	100.00		100.00	
					Cation sum	17.86

```
* = <2 Sigma

Fit Indices
--------------------
Na K    14.8
Mg K     1.6
Al K     0.8
Si K     0.4
K  K     0.2
Ca K     0.2
Ti K     0.5
Fe K     0.4
O  Ka    0.0
```
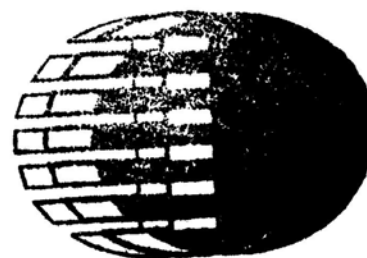
TISTR

Appendix Figure D2 Chemical composition analysis of mordenite calcined at
150ºC

```
SEMQuant results. Listed at 15:22:30 PM on 19/5/06
Operator: Chaweewan
Client: none
Job: Job 2006_1
Spectrum label: 3000 C

System resolution =  77 eV

Quantitative method: ZAF ( 3 iterations).
 Analysed elements combined with: O ( Valency: -2)
 Method : Stoichiometry Normalised results.
 Nos. of ions calculation based on  32 anions per formula.

 4 peaks possibly omitted: -0.02, 0.24, 8.02,
 8.62 keV

Standards :
 Na K     NaCl 8/27/02
 Mg K     mgo sem 3/13/98
 Al K     Al 5/22/02
 Si K     sic_c 3/19/98
 K  K     KBr 5/22/02
 Ca K     CaSiO 8/27/02
 Ti K     Ti 5/22/02
 Fe K     Fe 8/27/02
```

Elmt	Spect. Type	Element %	Atomic %		Compound %	Nos. of ions
Na K	ED	0.81	0.72	Na2O	1.09	0.36
Mg K	ED	0.40	0.34	MgO	0.66	0.17
Al K	ED	5.97	4.55	Al2O3	11.27	2.26
Si K	ED	37.23	27.30	SiO2	79.64	13.56
K K	ED	1.49	0.78	K2O	1.79	0.39
Ca K	ED	2.46	1.27	CaO	3.45	0.63
Ti K	ED	0.13	0.06	TiO2	0.22	0.03
Fe K	ED	1.46	0.54	FeO	1.88	0.27
O		50.06	64.44			32.00
Total		100.00	100.00		100.00	
					Cation sum 17.66	

```
* = <2 Sigma

Fit Indices
--------------------
Na K    24.8
Mg K     2.9
Al K     1.0
Si K     0.6
K  K     0.2
Ca K     0.2
Ti K     0.4
Fe K     0.6
O  Ka    0.0
```
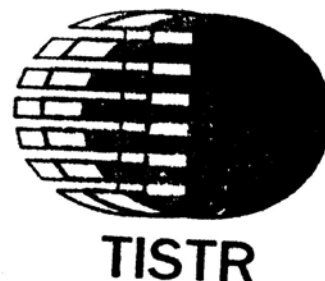

Appendix Figure D3 Chemical composition analysis of mordenite calcined at 300ºC

```
SEMQuant results. Listed at 11:22:18 PM on 28/2/06
Operator: Chaweewan
Client: none
Job: Job 2006_1
Spectrum label: 450 C ADSORB

System resolution =  77 eV

Quantitative method: ZAF ( 3 iterations).
 Analysed elements combined with: O ( Valency: -2)
 Method : Stoichiometry Normalised results.
 Nos. of ions calculation based on  32 anions per formula.

 4 peaks possibly omitted: -0.02, 0.24, 4.54,
 8.08 keV

Standards :
 Na K       NaCl 8/27/02
 Mg K       mgo sem 3/13/98
 Al K       Al 5/22/02
 Si K       sic_c 3/19/98
 K  K       KBr 5/22/02
 Ca K       CaSiO 8/27/02
 Fe K       Fe 8/27/02


Elmt    Spect. Element  Atomic           Compound   Nos. of
        Type     %        %                 %        ions
Na K     ED     0.65     0.63   Na2O       0.88      0.33
Mg K     ED     0.55     0.50   MgO        0.91      0.26
Al K     ED     4.78     3.90   Al2O3      9.03      2.03
Si K     ED    27.72    21.73   SiO2      59.31     11.30
K  K     ED     1.07     0.60   K2O        1.29      0.31
Ca K     ED    19.48    10.70   CaO       27.26
Fe K     ED     1.03     0.40   FeO        1.32
O              44.71    61.53
Total         100.00   100.00            100.00
                                         Cation

* = <2 Sigma

Fit Indices
--------------------
Na K    14.8
Mg K     1.0
Al K     1.4
Si K     2.7
K  K     0.2
Ca K     0.9
Fe K     0.4
O  Ka    0.0
```
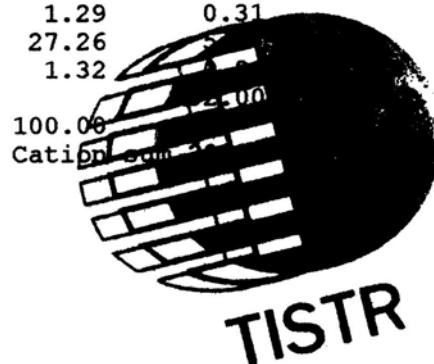
Appendix Figure D4 Chemical composition analysis of mordenite calcined at

450ºC

```
SEMQuant results. Listed at 15:27:47 PM on 19/5/06
Operator: Chaweewan
Client: none
Job: Job 2006_1
Spectrum label: 6000 C

System resolution =  77 eV

Quantitative method: ZAF ( 3 iterations).
 Analysed elements combined with: O ( Valency: -2)
 Method : Stoichiometry Normalised results.
 Nos. of ions calculation based on  32 anions per formula.

 2 peaks possibly omitted: -0.02, 0.24 keV

Standards :
 Na K       NaCl 8/27/02
 Mg K       mgo sem 3/13/98
 Al K       Al 5/22/02
 Si K       sic_c 3/19/98
 K  K       KBr 5/22/02
 Ca K       CaSiO 8/27/02
 Ti K       Ti 5/22/02
 Fe K       Fe 8/27/02
```

Elmt	Spect. Type	Element %	Atomic %		Compound %	Nos. of ions
Na K	ED	0.98	0.88	Na2O	1.32	0.44
Mg K	ED	0.46	0.39	MgO	0.76	0.19
Al K	ED	6.19	4.73	Al2O3	11.69	2.35
Si K	ED	36.70	26.94	SiO2	78.52	13.42
K K	ED	1.59	0.84	K2O	1.92	0.42
Ca K	ED	2.68	1.38	CaO	3.75	0.69
Ti K	ED	0.19	0.08	TiO2	0.32	0.04
Fe K	ED	1.34	0.49	FeO	1.72	0.25
O		49.87	64.27			32.00
Total		100.00	100.00		100.00	
					Cation sum	17.79

```
* = <2 Sigma

Fit Indices
--------------------
Na K    24.3
Mg K     1.8
Al K     0.8
Si K     2.5
K  K     0.1
Ca K     0.1
Ti K     0.1
Fe K     0.2
O  Ka    0.0
```

TISTR
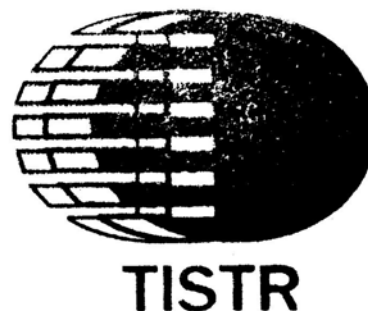
Appendix Figure D5 Chemical composition analysis of mordenite calcined at 600°C

```
*X 'SQ
SQ -3B/80

SQ: SETUP DEFINITIONS

SQ: QUANTIFY

CLINOPTILOLITE P3 4/10/47
Standardless Analysis
  25.0 kV   40.0 Degrees

Refit _MNK' _MNK"
Refit _TIK' _TIK" _MNK
Chi-sqd = 1.98

Element      Rel. K-ratio           Net Counts
  Na-K    0.00737 +/- 0.00218     270 +/-     80
  Mg-K    0.00734 +/- 0.00253     528 +/-    182
  Al-K    0.12283 +/- 0.00407   10996 +/-    364
  Si-K    0.63923 +/- 0.00487   68322 +/-    521
  K -K    0.06088 +/- 0.00225    5643 +/-    209
  Ca-K    0.10522 +/- 0.00329    8472 +/-    265
  Ti-K    0.00456 +/- 0.00104     325 +/-     74
  Mn-K    0.00000 +/- 0.00000       0 +/-      0
  Fe-K    0.05257 +/- 0.00351    2622 +/-    175

PRZ Correction 25.00 kV  40.00 deg
No.of Iterations = 18

Element  K-ratio    Z      A      F     Atom%    Wt%    Formula   Compound%
  Na-K    0.002   1.040  3.198  0.995   0.75    0.83    Na2O       1.11
  Mg-K    0.002   1.021  2.206  0.991   0.48    0.55    MgO        0.92
  Al-K    0.042   1.058  1.665  0.987   5.61    7.23    Al2O3     13.66
  Si-K    0.211   1.033  1.540  0.999  24.97   33.46    SiO2      71.59
  K -K    0.021   1.097  1.185  0.992   1.42    2.66    K 2O       3.20
  Ca-K    0.036   1.075  1.143  0.998   2.29    4.37    CaO        6.12
  Ti-K    0.002   1.181  1.085  0.997   0.09    0.20    TiO2       0.33
  Mn-K    0.000   1.212  1.023  1.000   0.00    0.00    MnO        0.00
  Fe-K    0.018   1.193  1.012  1.000   0.81    2.15    Fe2O3      3.07
  O -K    0.109   0.947  4.693  1.000  63.59   48.55 S  ---        ---
                                              Total= 100.00%   Total=  100.00%
```

Appendix Figure D6 Chemical composition analysis of mordenite calcined at

750ºC

```
SQ: QUANTIFY

CLINOPTILOLITE P1 4/10/47
Standardless Analysis
  25.0 kV   40.0 Degrees

Refit _MNK' _MNK"
Refit _NAK" _TIK" _MNK
Chi-sqd = 2.08

Element        Rel. K-ratio           Net Counts
  Na-K    0.00443 +/- 0.00114       174 +/-    45
  Mg-K    0.00680 +/- 0.00231       526 +/-   179
  Al-K    0.12289 +/- 0.00379     11817 +/-   364
  Si-K    0.63337 +/- 0.00474     72718 +/-   544
  K -K    0.05748 +/- 0.00219      5724 +/-   218
  Ca-K    0.12003 +/- 0.00326     10381 +/-   282
  Ti-K    0.00516 +/- 0.00100       396 +/-    77
  Mn-K    0.00000 +/- 0.00000         0 +/-     0
  Fe-K    0.04984 +/- 0.00332      2670 +/-   178

PRZ Correction 25.00 kV  40.00 deg
No.of Iterations = 2

Element  K-ratio    Z      A      F    Atom%    Wt%    Formula  Compound%
  Na-K    0.001   1.042  3.176  0.995   0.44    0.49    Na2O      0.66
  Mg-K    0.002   1.023  2.172  0.991   0.43    0.50    MgO       0.83
  Al-K    0.041   1.059  1.647  0.986   5.49    7.07    Al2O3    13.35
  Si-K    0.213   1.034  1.531  0.999  25.13   33.67    SiO2     72.02
  K -K    0.019   1.099  1.188  0.992   1.34    2.49    K 2O      3.00
  Ca-K    0.040   1.077  1.141  0.999   2.58    4.92    CaO       6.89
  Ti-K    0.002   1.184  1.084  0.997   0.10    0.22    TiO2      0.37
  Mn-K    0.000   1.215  1.021  1.000   0.00    0.00    MnO       0.00
  Fe-K    0.017   1.195  1.011  1.000   0.76    2.01    Fe2O3     2.88
  O -K    0.113   0.949  4.533  1.000  63.73   48.63 S  ---       ---
                                       Total= 100.00%   Total=  100.00%
```

Appendix Figure D7 Chemical composition analysis of mordenite calcined at
750ºC (cont'd)

```
SQ: QUANTIFY

CLINOPTILOLITE P2 4/10/47
Standardless Analysis
  25.0 kV   40.0 Degrees

Refit _MNK' _MNK"
Refit _TIK" _MNK  _FEK"
Chi-sqd = 1.88

Element       Rel. K-ratio          Net Counts
  Na-K    0.00886 +/- 0.00209      335 +/-    79
  Mg-K    0.00876 +/- 0.00249      652 +/-   185
  Al-K    0.13012 +/- 0.00403    12037 +/-   373
  Si-K    0.63486 +/- 0.00483    70121 +/-   534
  K -K    0.05629 +/- 0.00218     5392 +/-   209
  Ca-K    0.11341 +/- 0.00327     9486 +/-   272
  Ti-K    0.00417 +/- 0.00103      308 +/-    76
  Mn-K    0.00000 +/- 0.00000        0 +/-     0
  Fe-K    0.04352 +/- 0.00188     2243 +/-    97

PRZ Correction 25.00 kV  40.00 deg
No.of Iterations = 1

Element  K-ratio    Z      A      F     Atom%    Wt%    Formula  Compound%
  Na-K    0.003   1.043  3.138  0.995   0.87    0.96    Na2O      1.29
  Mg-K    0.003   1.023  2.172  0.991   0.55    0.64    MgO       1.06
  Al-K    0.043   1.060  1.652  0.986   5.78    7.46    Al2O3    14.10
  Si-K    0.209   1.034  1.543  0.999  24.83   33.35    SiO2     71.35
  K -K    0.019   1.100  1.189  0.993   1.30    2.43    K 2O      2.92
  Ca-K    0.038   1.077  1.141  0.999   2.41    4.63    CaO       6.48
  Ti-K    0.001   1.184  1.082  0.998   0.08    0.18    TiO2      0.30
  Mn-K    0.000   1.216  1.020  1.000   0.00    0.00    MnO       0.00
  Fe-K    0.014   1.196  1.010  1.000   0.65    1.75    Fe2O3     2.50   -
  O -K    0.115   0.949  4.471  1.000  63.52   48.60 S   ---       ---
                                      Total= 100.00%  Total=  100.00%
```



```
NORAN SERIES II    ***  TISTR  ***      MON 04-OCT-04  13:48
Cursor: 0.010keV = 0
```

```
0.000                                      VFS = 8192   10.240
```
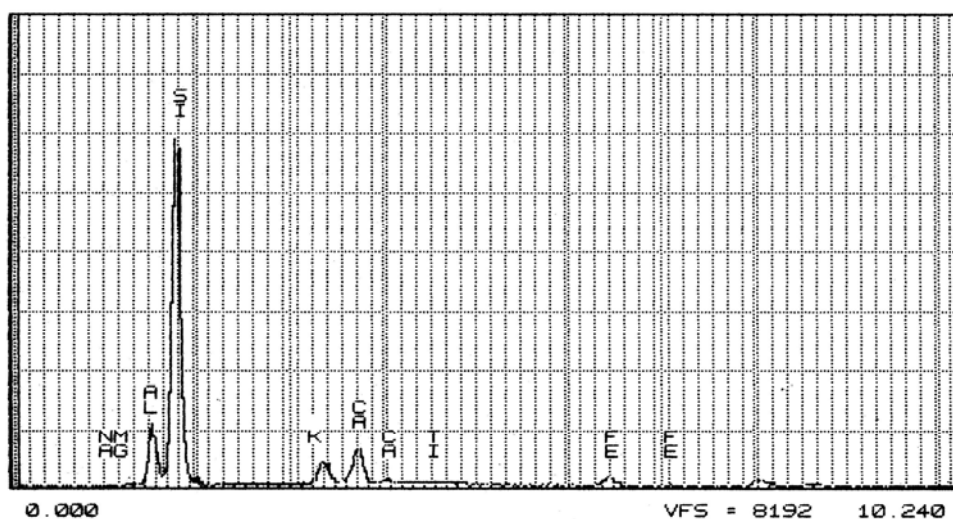
Appendix Figure D8 Chemical composition analysis of mordenite calcined at

750ºC (cont'd)

```
SEMQuant results. Listed at 15:32:40 PM on 19/5/06
Operator: Chaweewan
Client: none
Job: Job 2006_1
Spectrum label: 9000 C

System resolution =  77 eV

Quantitative method: ZAF ( 3 iterations).
 Analysed elements combined with: O ( Valency: -2)
 Method : Stoichiometry Normalised results.
 Nos. of ions calculation based on  32 anions per formula.

 4 peaks possibly omitted: -0.02, 0.24, 2.26,
 8.02 keV

Standards :
 Na K      NaCl 8/27/02
 Mg K      mgo sem 3/13/98
 Al K      Al 5/22/02
 Si K      sic_c 3/19/98
 K  K      KBr 5/22/02
 Ca K      CaSiO 8/27/02
 Ti K      Ti 5/22/02
 Fe K      Fe 8/27/02
```

Elmt	Spect. Type	Element %	Atomic %		Compound %	Nos. of ions
Na K	ED	1.09	0.98	Na2O	1.48	0.49
Mg K	ED	0.51	0.43	MgO	0.84	0.21
Al K	ED	5.97	4.57	Al2O3	11.29	2.28
Si K	ED	36.55	26.85	SiO2	78.19	13.38
K K	ED	1.31	0.69	K2O	1.58	0.35
Ca K	ED	3.60	1.86	CaO	5.04	0.92
Ti K	ED	0.16	0.07	TiO2	0.27	0.03
Fe K	ED	1.02	0.38	FeO	1.31	0.19
O		49.78	64.18			32.00
Total		100.00	100.00		100.00	

```
                                        Cation sum 17.86

* = <2 Sigma

Fit Indices
--------------------
Na K    34.5
Mg K     3.3
Al K     0.8
Si K     1.6
K  K     0.1
Ca K     0.1
Ti K     0.4
Fe K     0.6
O  Ka    0.0
```

TISTR
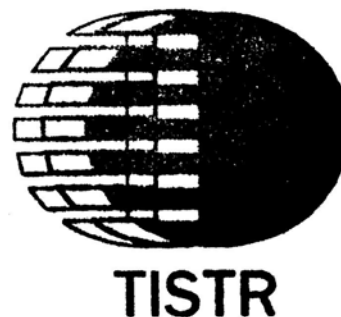
Appendix Figure D9 Chemical composition analysis of mordenite calcined at

900°C

Appendix E

```
***    Multi Plot  ***

File Name    : ying\cli25
Sample Name  : Clinoptilolite              Comment : 1/11/48
Date & Time  : 11-01-05 13:09:29
Condition
  X-ray Tube : Cu(1.54060 A)    Voltage : 40.0 kV    Current : 30.0 mA
  Scan Range : 2.0000 <-> 80.0000 deg    Step Size : 0.0200 deg
  Count Time : 0.60 sec    Slit  DS : 1.00 deg  SS : 1.00 deg  RS : 0.15 mm
```
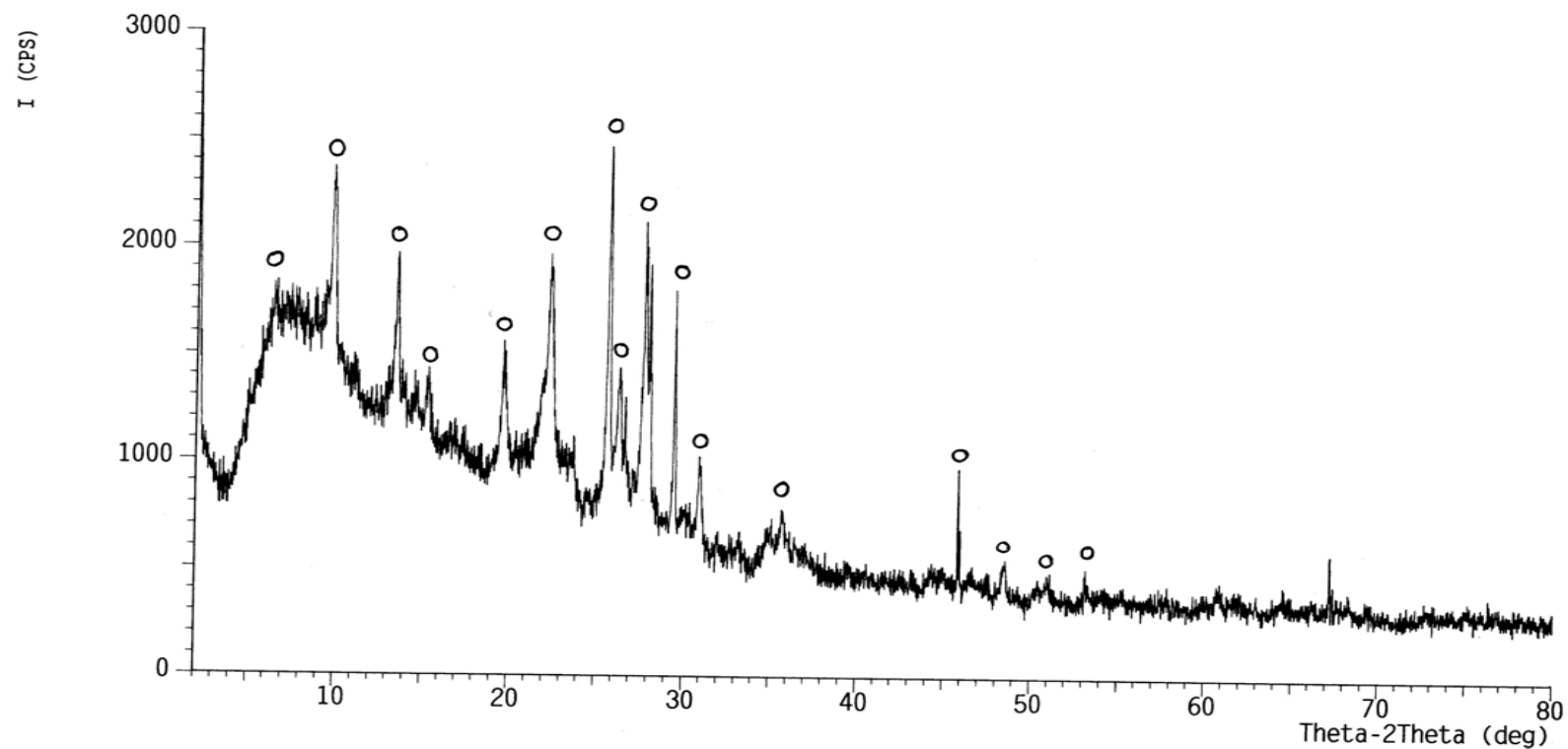
Appendix Figure E1 XRD pattern of mordenite un- calcined

***   Multi Plot   ***

File Name   : service\150C Mordenite
Sample Name   : 150C Mordenite   Comment : 6/6/49
Date & Time   : 06-06-06 09:10:10
Condition
  X-ray Tube : Cu(1.54060 A)   Voltage : 30.0 kV   Current : 30.0 mA
  Scan Range : 10.0000 <-> 80.0000 deg   Step Size : 0.0500 deg
  Count Time : 1.50 sec   Slit DS : 1.00 deg SS : 1.00 deg RS : 0.15 mm
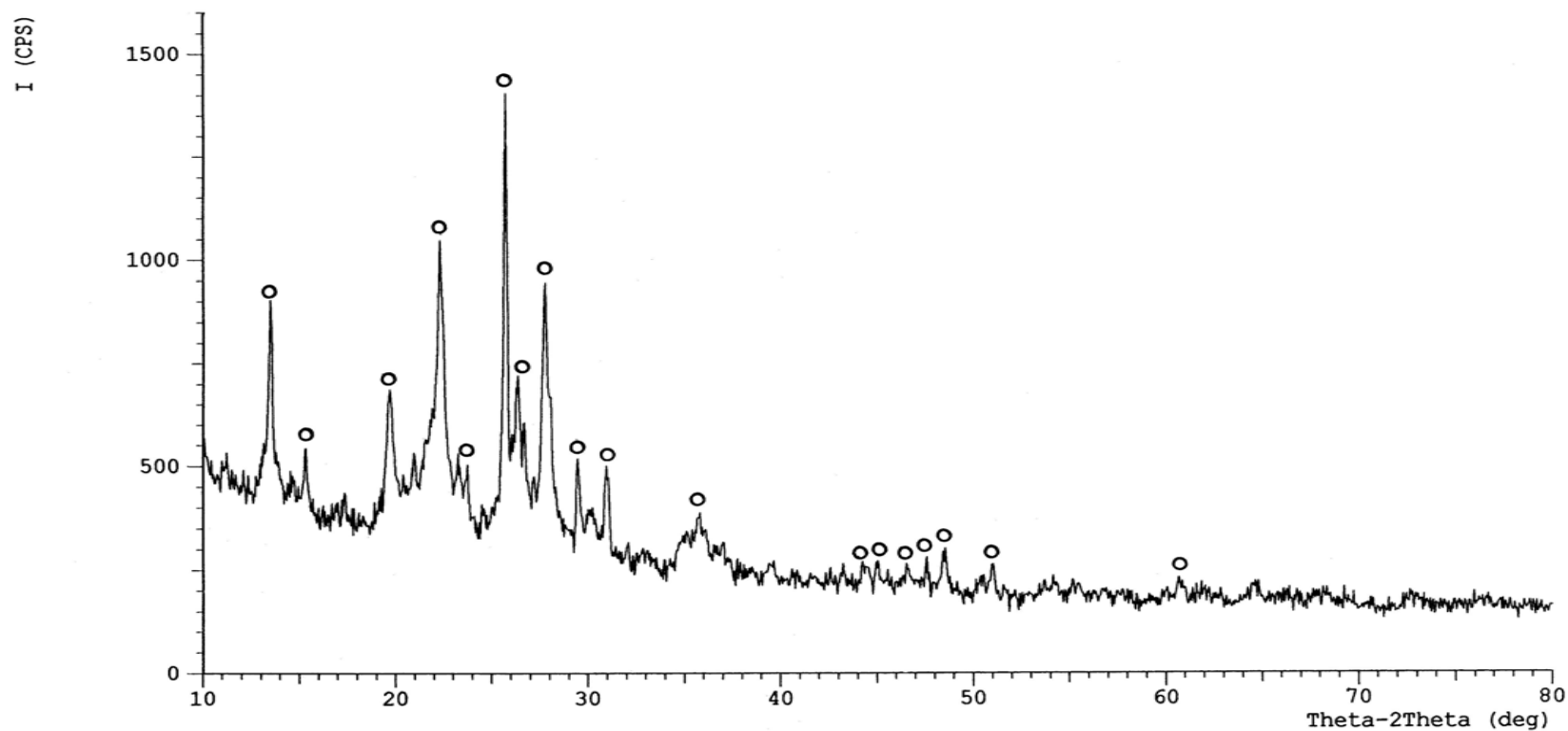
Appendix Figure E2 XRD pattern of mordenite calcined at 150ºC
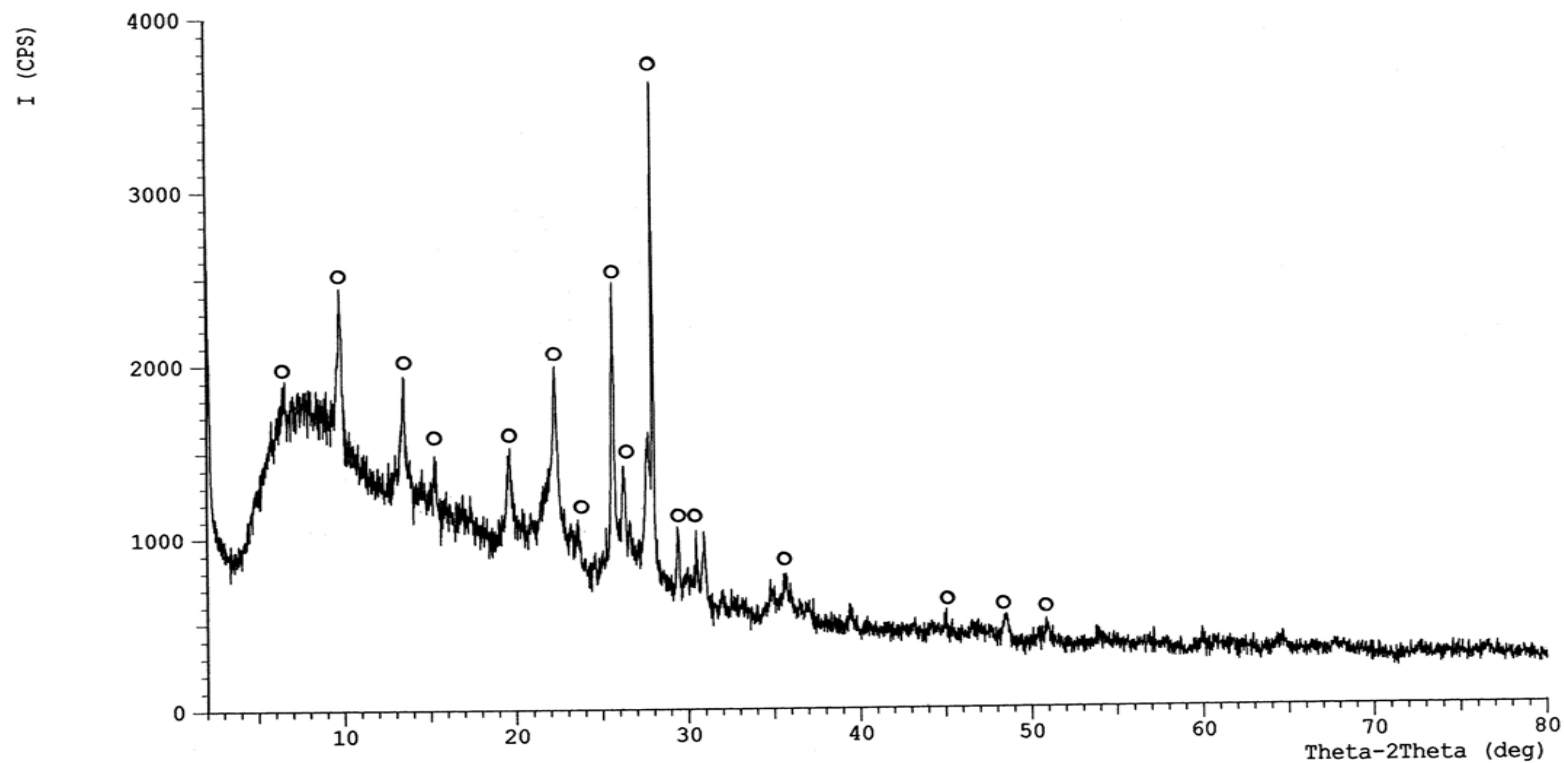
Appendix Figure E3 XRD pattern of mordenite calcined at 300ºC

```
                    ***    Multi Plot    ***

File Name    : ying\Cli450(2)
Sample Name  : Clinoptilolite              Comment : 9/11/48
Date & Time  : 11-09-05 09:48:30
Condition
  X-ray Tube : Cu(1.54060 A)    Voltage : 40.0 kV    Current : 30.0 mA
  Scan Range : 2.0000 <-> 80.0000 deg    Step Size : 0.0200 deg
  Count Time : 0.60 sec     Slit  DS : 1.00 deg  SS : 1.00 deg  RS : 0.15 mm
```
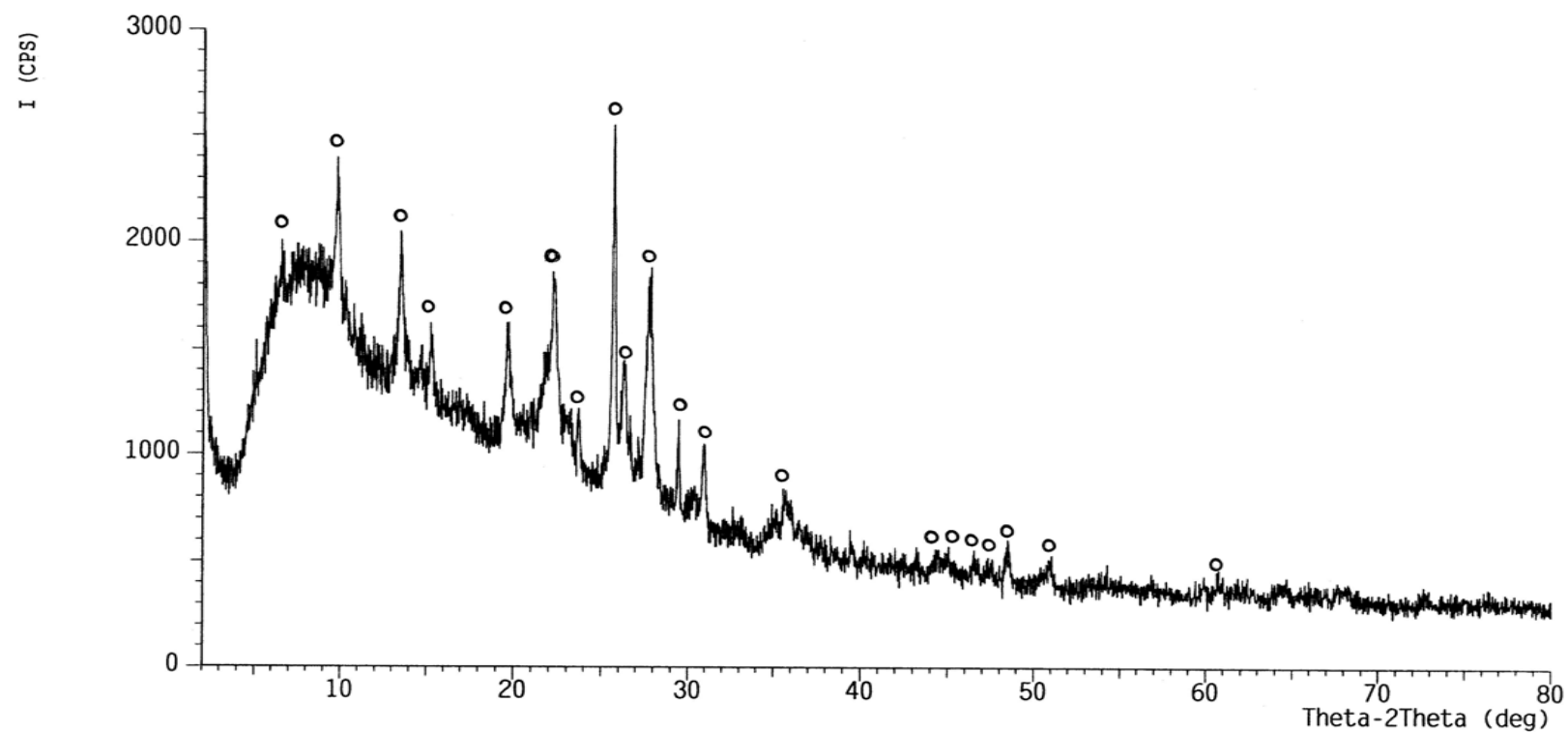
Appendix Figure E4 XRD pattern of mordenite calcined at 450ºC

File Name   : ying\Cli600
Sample Name   : Clinoptilolite   Comment : 9/11/48
Date & Time   : 11-09-05 10:29:47
Condition
  X-ray Tube : Cu(1.54060 A)   Voltage : 40.0 kV   Current : 30.0 mA
  Scan Range : 2.0000 <-> 80.0000 deg   Step Size : 0.0200 deg
  Count Time : 0.60 sec   Slit DS : 1.00 deg SS : 1.00 deg RS : 0.15 mm
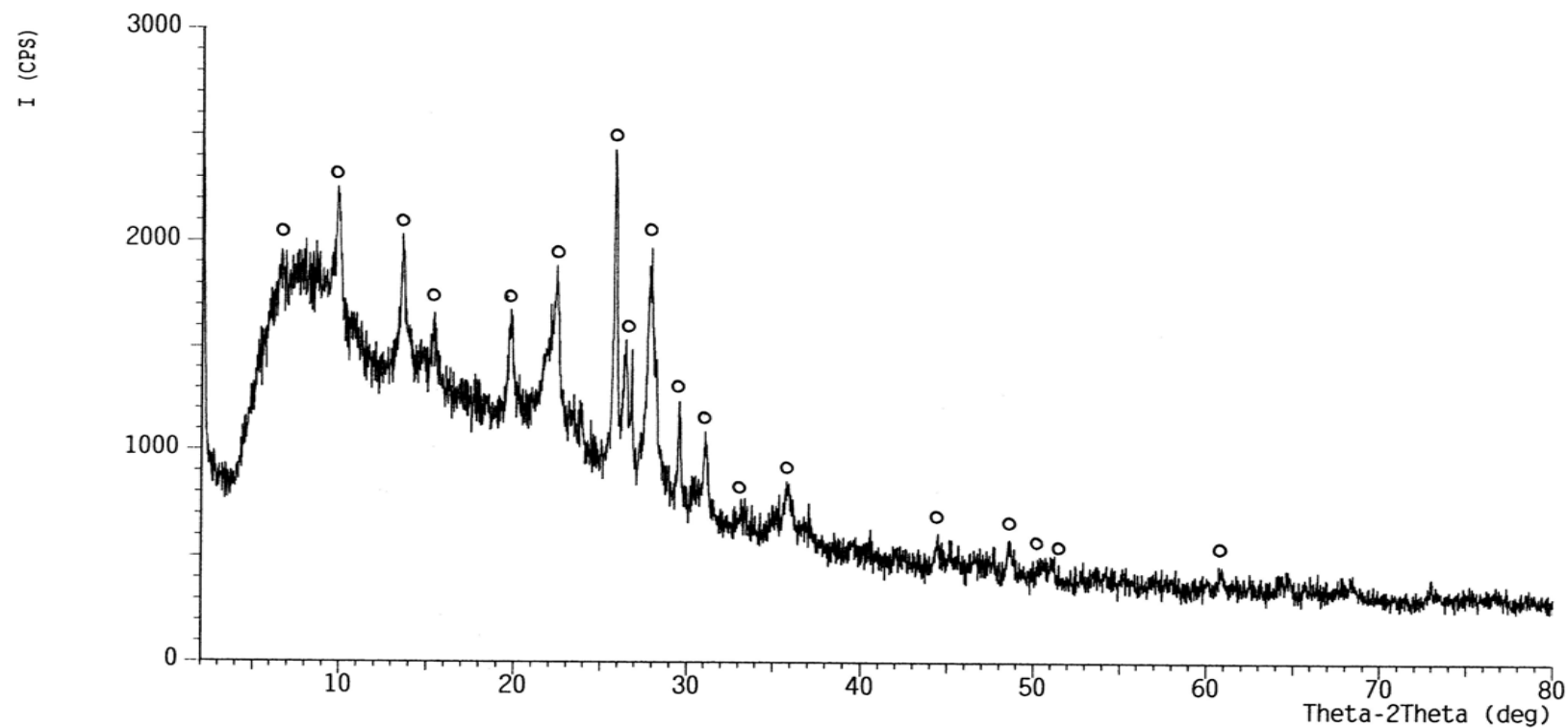
Appendix Figure E5 XRD pattern of mordenite calcined at 600ºC

```
***    Multi Plot   ***

File Name      : ying\cli750
Sample Name    : Clinoptilolite              Comment : 1/11/48
Date & Time    : 11-01-05 13:50:15
Condition
  X-ray Tube : Cu(1.54060 A)    Voltage : 40.0 kV    Current : 30.0 mA
  Scan Range : 2.0000 <-> 80.0000 deg    Step Size : 0.0200 deg
  Count Time : 0.60 sec    Slit  DS : 1.00 deg  SS : 1.00 deg  RS : 0.15 mm
```
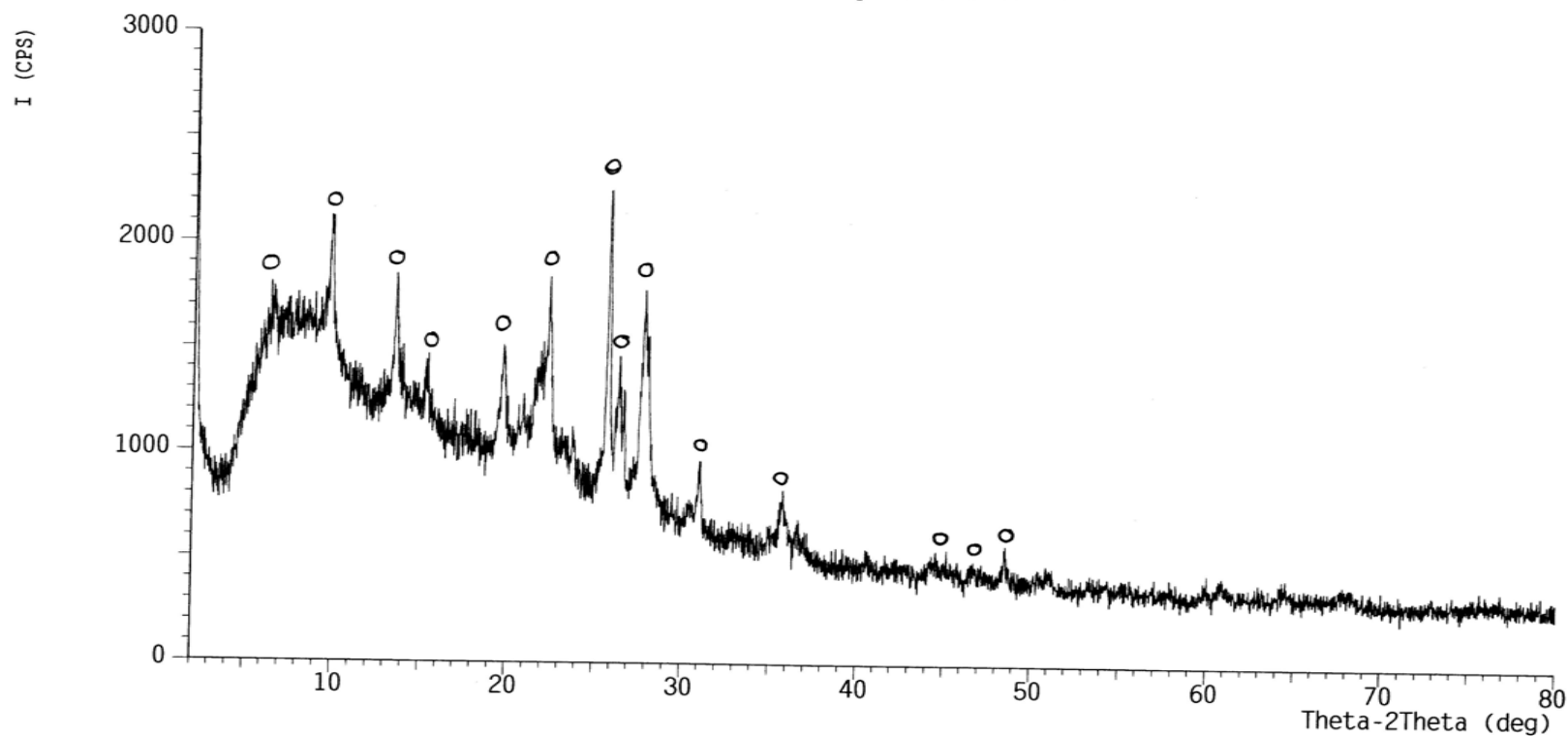
Appendix Figure E6 XRD pattern of mordenite calcined at 750ºC

```
                    ***    Multi Plot   ***

File Name     : service\Calcine at KU
Sample Name   : Calcine at KU              Comment : 26/4/49
Date & Time   : 04-26-06 08:38:26
Condition
  X-ray Tube  : Cu(1.54060 A)    Voltage : 40.0 kV    Current : 30.0 mA
  Scan Range  : 2.0000 <-> 80.0000 deg   Step Size : 0.0200 deg
  Count Time  : 0.60 sec    Slit  DS : 1.00 deg  SS : 1.00 deg  RS : 0.15 mm
```

o = Silicon Oxide (SiO_2): Cristobalite

□ = Aluminum Silicate (Al_2SiO_5): Kyanite
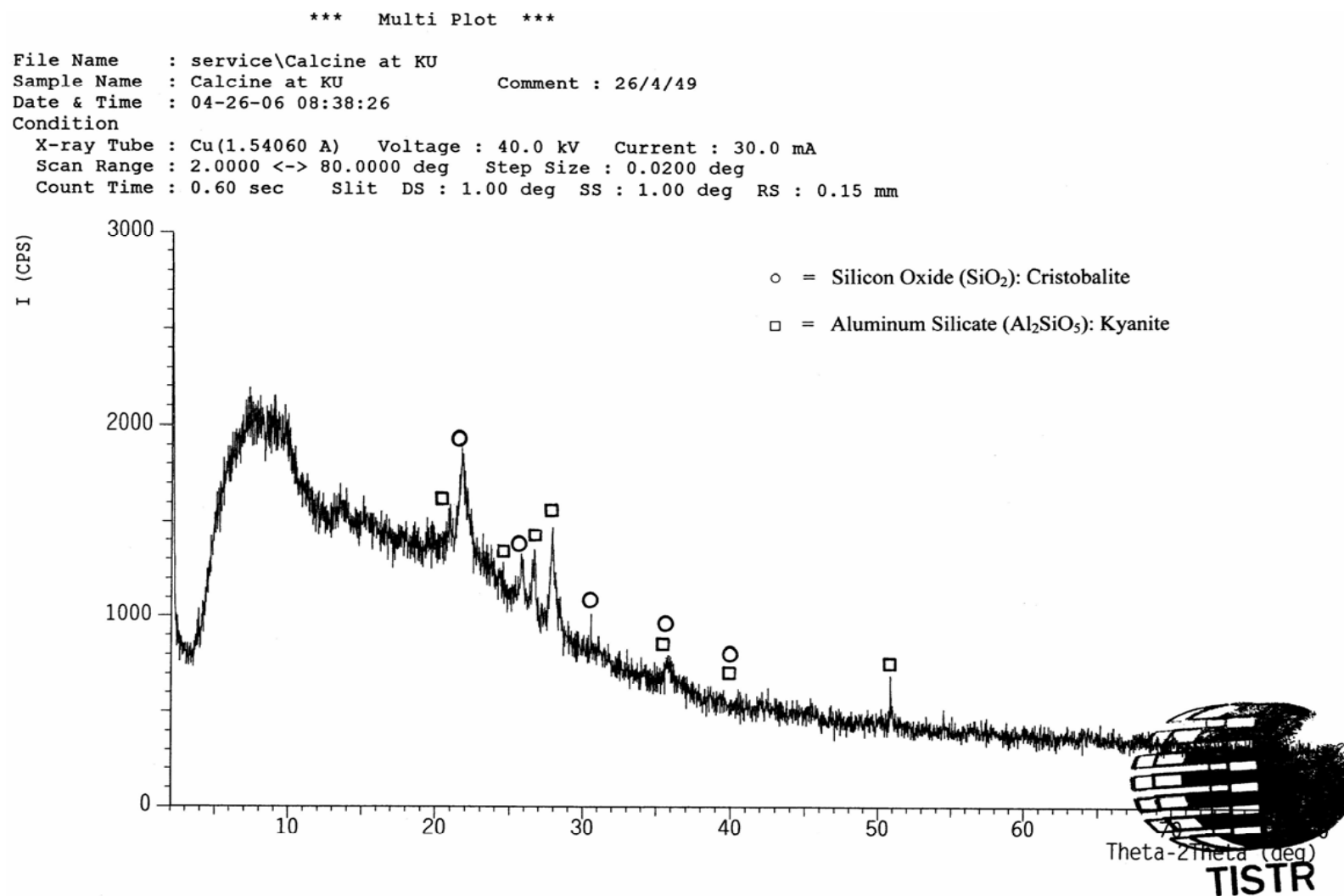
Appendix Figure E7 XRD pattern of mordenite calcined at 900°C

Appendix F
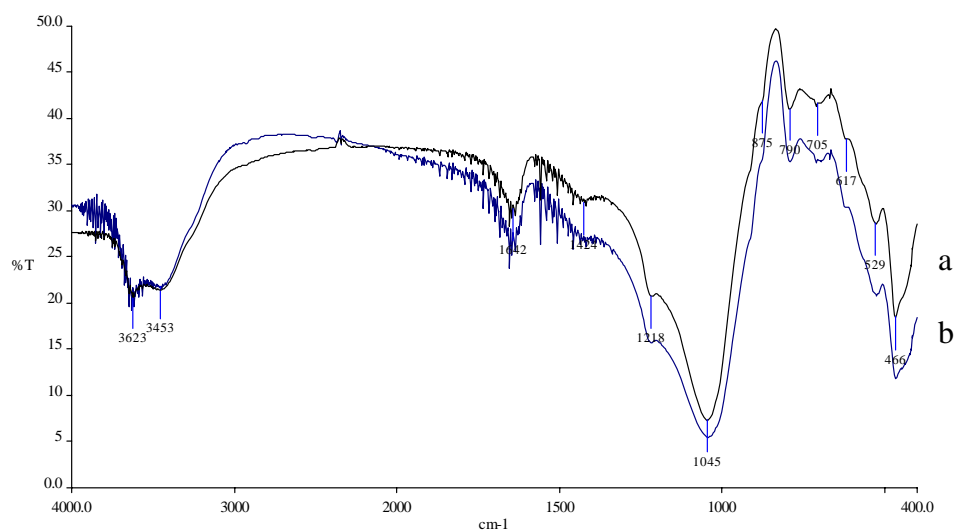
Appendix Figure F1 FTIR spectra of uncalcined mordenite: (a) before
adsorbed, (b) after adsorbed orthophosphate
30 mg-P/L
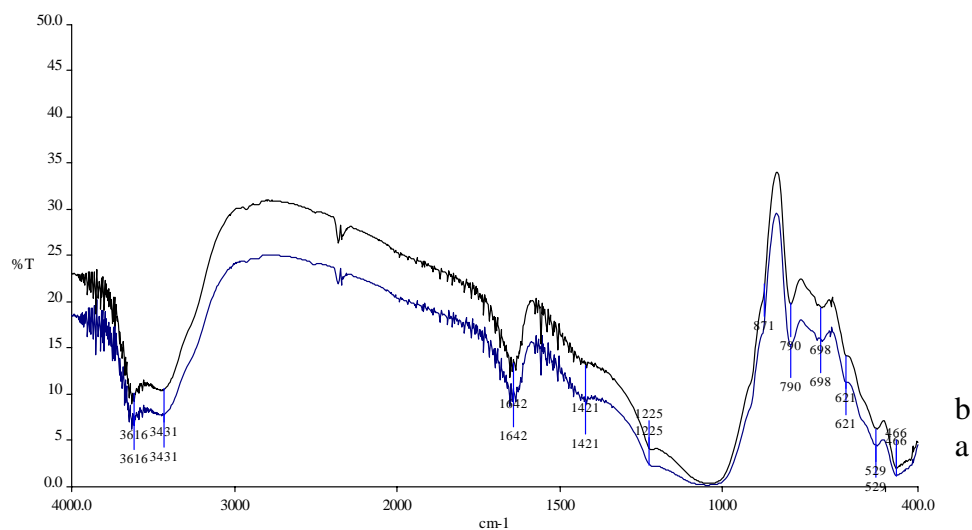
Appendix Figure F2 FTIR spectra of mordenite calcination at 150ºC:
(a)before adsorbed, (b) after adsorbed orthophosphate
30 mg-P/L
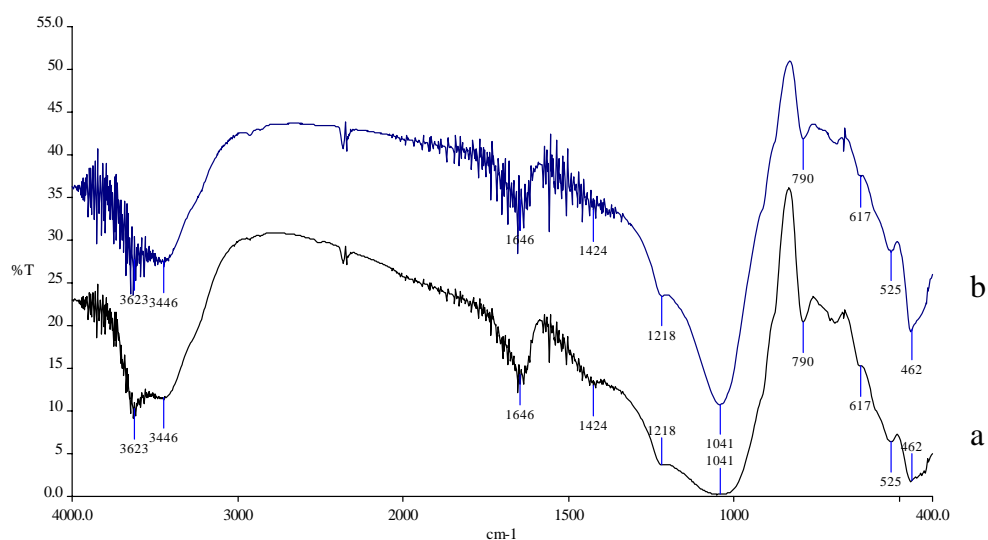
Appendix Figure F3 FTIR spectra of mordenite calcination at 300ºC:
(a)before adsorbed, (b) after adsorbed orthophosphate
30 mg-P/L
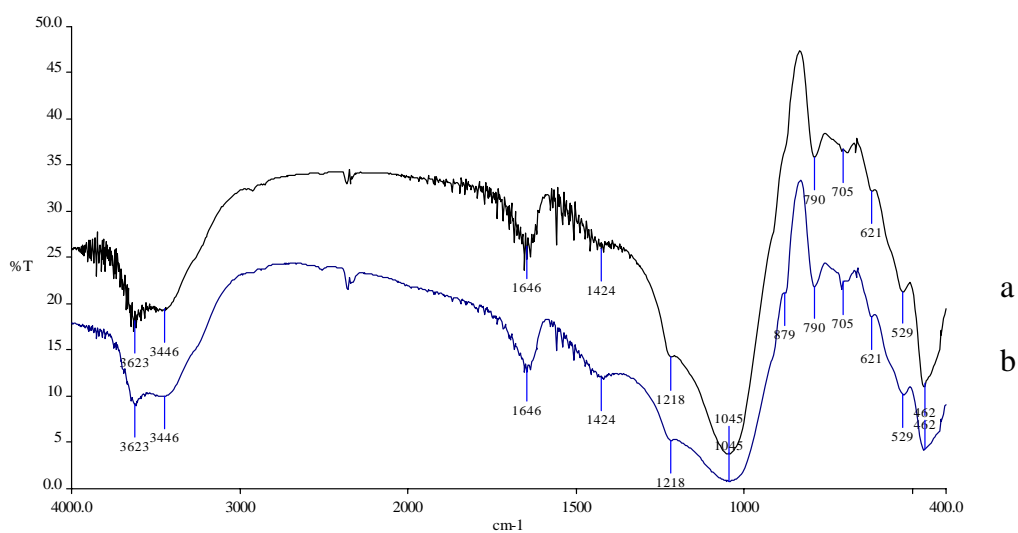
Appendix Figure F4 FTIR spectra of mordenite calcination at 450ºC:
(a)before adsorbed, (b) after adsorbed orthophosphate
30 mg-P/L
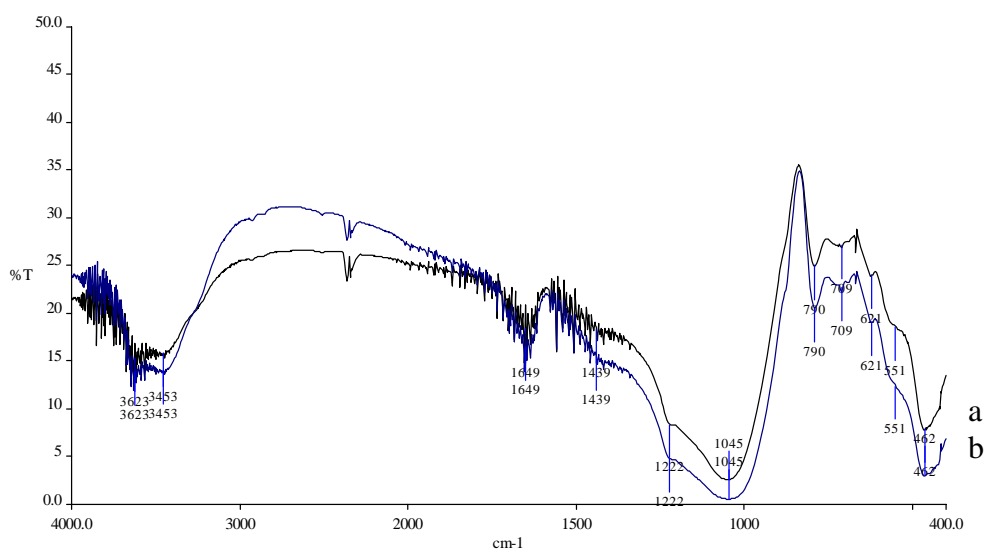
Appendix Figure F5 FTIR spectra of mordenite calcination at 600ºC:
(a)before adsorbed, (b) after adsorbed orthophosphate
30 mg-P/L
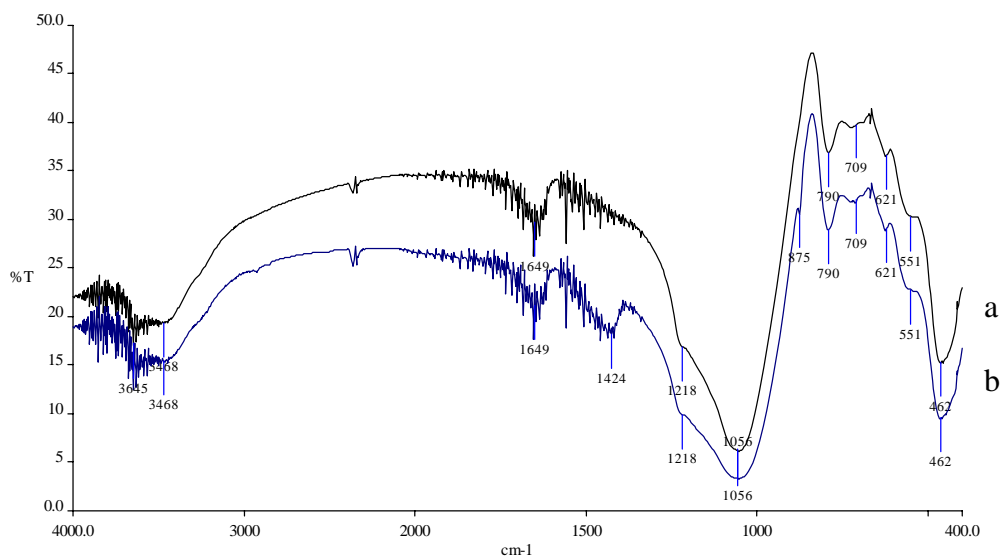
Appendix Figure F6 FTIR spectra of mordenite calcination at 750ºC:
(a)before adsorbed, (b) after adsorbed orthophosphate
30 mg-P/L
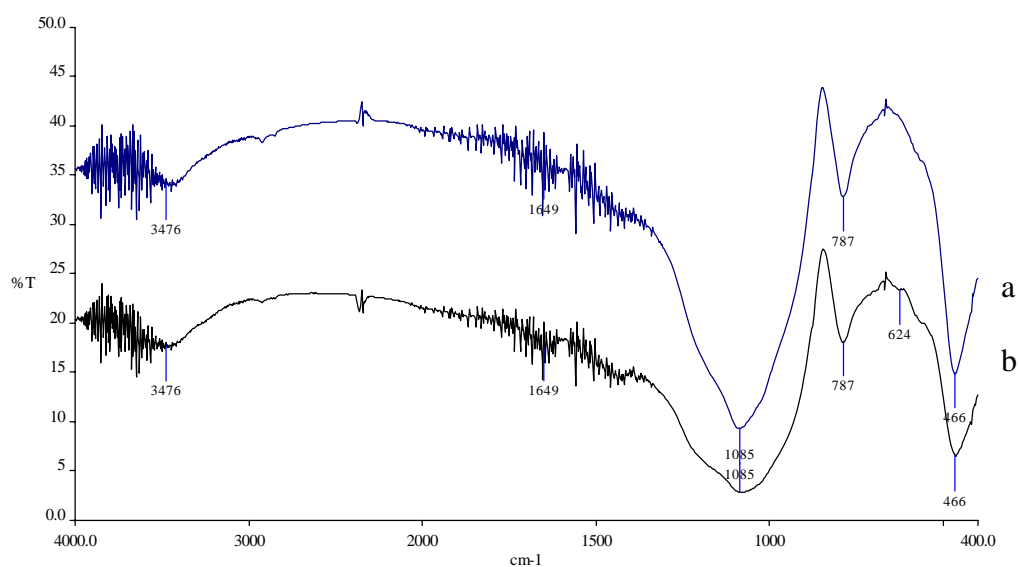
Appendix Figure F7 FTIR spectra of mordenite calcination at 900ºC:
(a)before adsorbed, (b) after adsorbed orthophosphate
30 mg-P/L
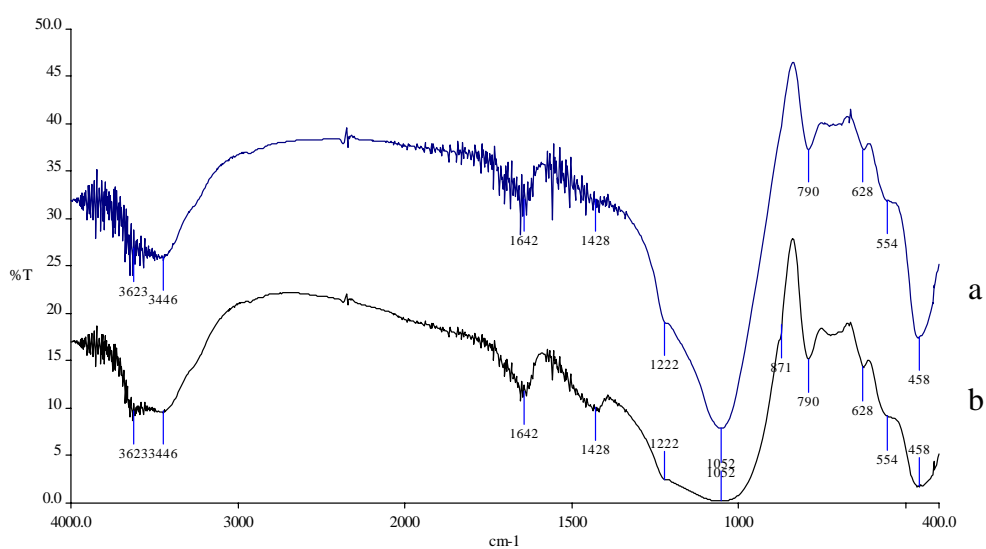
Appendix Figure F8 FTIR spectra of mordenite calcination at 750ºC and
treated with EDTA 0.05M: (a) before adsorbed, (b) after
adsorbed orthophosphate 30 ppm
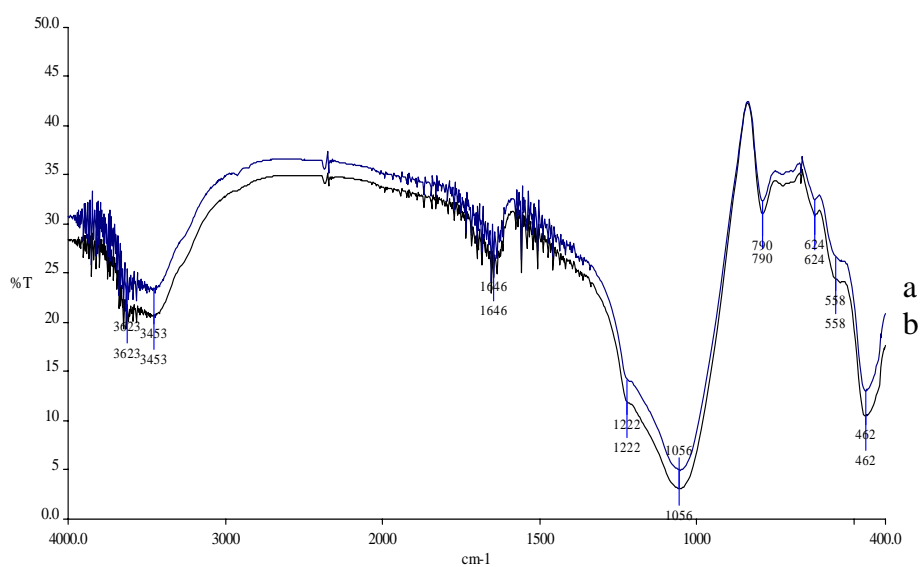
Appendix Figure F9 FTIR spectra of mordenite calcination at 750ºC and
treated with HCl 0.5M: (a) before adsorbed, (b) after
adsorbed orthophosphate 30 ppm

Appendix G

Appendix Table G1 The calibration curve data of orthophosphate

Phosphorus concentration (mg-P/L)	Absorbance			
	trial 1	trial 2	trial 3	Average
0.0995	0.060	0.061	0.061	0.0607
0.2985	0.206	0.205	0.206	0.2057
0.4975	0.326	0.326	0.326	0.3260
0.7960	0.514	0.514	0.514	0.5140
0.9951	0.629	0.630	0.631	0.6300
1.1941	0.741	0.741	0.743	0.7417
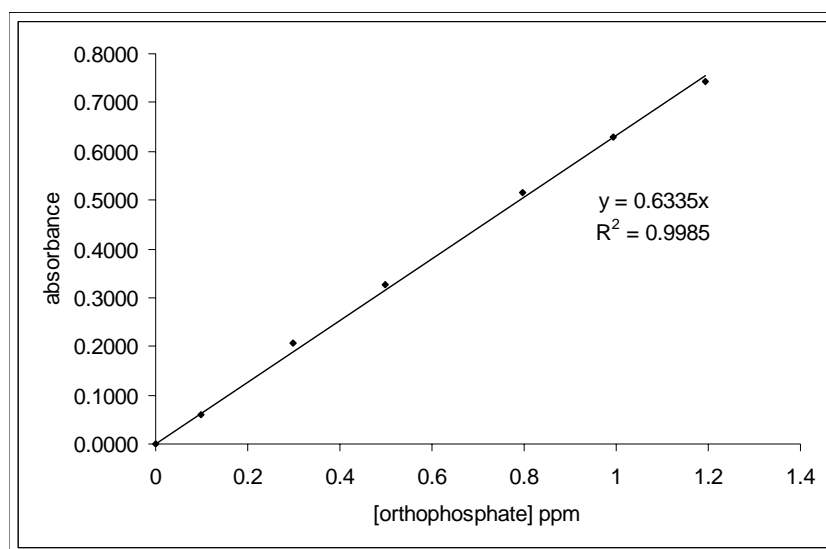
Appendix Figure G1 Orthophosphate calibration curve

Appendix Table G2 Data from experiment of uncalcined mordenite after orthophosphate adsorption

| Phosphate concentration (mg-P/L) | Shaking time (minute) | pH | Mordenite weight (g) | Phosphate concentration (mg-P/L) | | | %adsorbed per 1g MOR | absorbance (average) |
				Before adsorption	After adsorption	Amount adsorption		
5	20	7.49	1.0142	5.0322	4.7272	0.3051	5.9807	0.3009
	40	7.70	1.0149	5.0322	4.8254	0.2068	4.0496	0.3071
	60	7.76	1.0125	5.0322	4.7991	0.2331	4.5779	0.3054
	120	7.75	1.0047	5.0322	4.6009	0.4313	8.5310	0.2929
	180	8.08	1.0077	5.0322	4.6518	0.3805	7.5035	0.2961
	240	8.00	1.0143	5.0322	4.6062	0.4261	8.3467	0.2932
10	20	7.24	1.0087	10.0645	9.6987	0.3658	3.6034	0.2463
	40	7.52	1.0204	10.0645	9.4444	0.6201	6.0392	0.2399
	60	7.60	1.0070	10.0645	9.4882	0.5763	5.6891	0.2410
	120	7.62	1.0147	10.0645	9.2076	0.8569	8.3939	0.2339
	180	7.82	1.0042	10.0645	9.2427	0.8218	8.1319	0.2348
	240	7.96	1.0068	10.0645	9.1857	0.8788	8.6722	0.2333
20	20	6.96	1.0074	20.1289	19.3146	0.8144	4.0143	0.2450
	40	7.21	1.0101	20.1289	19.6390	0.4899	2.4105	0.2491
	60	7.27	1.0095	20.1289	19.0690	1.0599	5.2163	0.2419
	120	7.36	1.0138	20.1289	19.1304	0.9985	4.8946	0.2427
	180	7.49	1.0123	20.1289	19.2795	0.8495	4.1688	0.2446
	240	7.56	1.0079	20.1289	19.4110	0.7179	3.5385	0.2462
30	20	6.92	1.0086	30.1934	29.2944	0.8990	2.9520	0.3714
	40	7.14	1.0082	30.1934	29.5750	0.6184	2.0312	0.3750
	60	7.17	1.0097	30.1934	29.4873	0.7061	2.3173	0.3739
	120	7.23	1.0054	30.1934	28.8998	1.2937	4.2607	0.3664
	180	7.23	1.0054	30.1934	28.8998	1.2937	4.2607	0.3664
	240	7.49	1.0152	30.1934	29.6890	0.5044	1.6486	0.3764
blank	240	8.62	1.0067	0.0000	0.0225	-0.0225		0.0142

Appendix Table G3 Data from experiment of calcination mordenite at 150ºC
after orthophosphate adsorption

Phosphate concentration (mg-P/L)	Shaking time (minute)	pH	Mordenite weight (g)	Phosphate concentration (mg-P/L)			%adsorbed per 1g MOR	absorbance (average)
				Before adsorption	After adsorption	Amount adsorption		
5	20	8.03	1.0049	5.0163	4.5521	0.4642	9.2084	0.2891
	40	7.94	1.0135	5.0163	4.7363	0.2800	5.5088	0.3008
	60	8.03	1.0049	5.0163	4.4960	0.5203	10.3214	0.2856
	120	8.15	1.0059	5.0163	4.4188	0.5975	11.8384	0.2807
	180	8.35	1.0044	5.0163	4.3259	0.6904	13.7031	0.2748
	240	8.29	1.0059	5.0163	4.2592	0.7571	15.0008	0.2706
10	20	7.65	1.0140	10.0326	9.2535	0.7791	7.6586	0.2348
	40	7.80	1.0093	10.0326	9.2535	0.7791	7.6991	0.2348
	60	7.75	1.0061	10.0326	8.9027	1.1299	11.1933	0.2259
	120	7.87	1.0099	10.0326	8.7537	1.2789	12.6234	0.2221
	180	8.09	1.0093	10.0326	8.4818	1.5508	15.3133	0.2152
	240	8.06	1.0116	10.0326	8.5651	1.4675	14.4597	0.2173
20	20	7.29	1.0123	20.0652	19.6236	0.4416	2.1742	0.2488
	40	7.48	1.0053	20.0652	19.5535	0.5117	2.5365	0.2479
	60	7.28	1.0175	20.0652	18.8870	1.1782	5.7691	0.2394
	120	7.47	1.0055	20.0652	18.6502	1.4150	7.0115	0.2364
	180	7.56	1.0108	20.0652	18.0012	2.0640	10.1796	0.2282
	240	7.76	1.0103	20.0652	18.0100	2.0552	10.1379	0.2283
30	20	7.19	1.0066	30.0978	29.0597	1.0381	3.4299	0.3683
	40	7.40	1.0147	30.0978	28.9720	1.1258	3.6852	0.3672
	60	7.16	1.0147	30.0978	28.0424	2.0554	6.7296	0.3554
	120	7.26	1.0120	30.0978	27.8671	2.2307	7.3207	0.3532
	180	7.48	1.0119	30.0978	27.7004	2.3974	7.8714	0.3511
	240	7.52	1.0153	30.0978	27.0866	3.0112	9.8526	0.3433
blank	240	9.10	1.0134	0.0000	0.0116	-0.0116		0.0073

Appendix Table G4 Data from experiment of calcination mordenite at 300ºC after orthophosphate adsorption

Phosphate concentration (mg-P/L)	Shaking time (minute)	pH	Mordenite weight (g)	Phosphate concentration (mg-P/L)			%adsorbed per 1g MOR	absorbance (average)
				Before adsorption	After adsorption	Amount adsorption		
5	20	7.87	1.0049	5.0254	4.6775	0.3479	6.8882	0.2972
	40	8.30	1.0054	5.0254	4.4706	0.5548	10.9819	0.2841
	60	8.17	1.0063	5.0254	4.2934	0.7320	14.4768	0.2729
	120	8.26	1.0016	5.0254	4.1479	0.8775	17.4342	0.2637
	180	8.27	1.0055	5.0254	4.0321	0.9933	19.6566	0.2563
	240	8.31	1.0061	5.0254	3.9654	1.0600	20.9624	0.2521
10	20	7.73	1.0071	10.0508	9.0843	0.9665	9.5483	0.2306
	40	8.01	1.0059	10.0508	8.9659	1.0849	10.7315	0.2276
	60	7.91	1.0063	10.0508	8.6765	1.3743	13.5885	0.2202
	120	8.02	1.0090	10.0508	8.4441	1.6067	15.8425	0.2143
	180	7.62	1.0014	20.1016	17.4987	2.6029	12.9301	0.2219
	240	8.22	1.0096	10.0508	8.2336	1.8172	17.9097	0.2090
20	20	7.66	1.0093	20.1016	18.6475	1.4541	7.1682	0.2364
	40	7.66	1.0100	20.1016	18.6563	1.4453	7.1178	0.2366
	60	7.51	1.0141	20.1016	18.7002	1.4014	6.8736	0.2371
	120	7.57	1.0039	20.1016	17.7092	2.3924	11.8574	0.2246
	180	7.62	1.0014	20.1016	17.4987	2.6029	12.9301	0.2219
	240	7.81	1.0026	20.1016	17.5075	2.5941	12.8697	0.2220
30	20	7.41	1.0077	30.1525	28.2064	1.9461	6.4045	0.3576
	40	7.47	1.0060	30.1525	28.0223	2.1302	7.0231	0.3552
	60	7.40	1.0071	30.1525	27.5136	2.6389	8.6875	0.3488
	120	7.41	1.0041	30.1525	28.1450	2.0075	6.6299	0.3568
	180	7.47	1.0054	30.1525	27.5312	2.6213	8.6442	0.3490
	240	7.48	1.0115	30.1525	27.4522	2.7003	8.8529	0.3480
blank	240	8.68	1.0066	0.0000	0.0142	-0.0142		0.0090

Appendix Table G5 Data from experiment of calcination mordenite at 450ºC after orthophosphate adsorption

| Phosphate concentration (mg-P/L) | Shaking time (minute) | pH | Mordenite weight (g) | Phosphate concentration (mg-P/L) | | | %adsorbed per 1g MOR | absorbance (average) |
				Before adsorption	After adsorption	Amount adsorption		
5	20	7.52	1.0237	4.9947	5.0546	-0.0599	-1.1699	0.3214
	40	7.58	1.0493	4.9947	5.0178	-0.0231	-0.4461	0.3191
	60	7.77	1.0791	4.9947	4.6986	0.2961	5.5094	0.2989
	120	7.61	1.0967	4.9947	4.6635	0.3312	6.0552	0.2967
	180	7.81	3.0528	12.5547	5.6676	5.4259	13.1950	0.2795
	240	7.89	1.0998	4.9947	4.5057	0.4890	8.9079	0.2867
10	20	7.30	1.0671	9.9894	10.0621	-0.0727	-0.7025	0.6387
	40	7.48	1.0811	9.9894	9.9428	0.0466	0.4316	0.6311
	60	7.63	1.0532	9.9894	9.6131	0.3763	3.5694	0.6102
	120	7.52	1.0449	9.9894	9.6026	0.3868	3.6919	0.6096
	180	7.55	1.0995	9.9894	9.4798	0.5096	4.5593	0.6018
	240	7.68	1.0729	9.9894	9.1746	0.8148	7.6030	0.5824
20	20	7.12	1.0210	19.9787	22.0011	-2.0224	-9.9203	0.5580
	40	7.33	1.0495	19.9787	21.9528	-1.9741	-9.4140	0.5568
	60	7.28	1.0405	19.9787	19.6946	0.2841	1.3389	0.2498
	120	7.40	1.0730	19.9787	20.3699	-0.3912	-1.8183	0.2583
	180	7.41	1.0656	19.9787	19.3175	0.6612	3.0709	0.2450
	240	7.43	1.0558	19.9787	19.2299	0.7488	3.5020	0.2439
30	20	7.01	1.0555	29.9681	28.8629	1.1052	3.5258	0.7312
	40	7.14	1.0713	29.9681	31.1297	-1.1616	-3.6102	0.7883
	60	7.10	1.0246	29.9681	29.4728	0.4953	1.6192	0.3737
	120	7.16	1.0278	29.9681	29.0694	0.8987	2.9136	0.3686
	180	7.29	1.0402	29.9681	28.7274	1.2407	3.9822	0.3642
	240	7.36	1.0526	29.9681	28.4116	1.5565	4.9563	0.3602
blank	240	8.43	1.0489	0.0000	0.0195	-0.0195		0.0123

Appendix Table G6 Data from experiment of calcination mordenite at 600ºC after orthophosphate adsorption

Phosphate concentration (mg-P/L)	Shaking time (minute)	pH	Mordenite weight (g)	Phosphate concentration (mg-P/L)			%adsorbed per 1g MOR	absorbance (average)
				Before adsorption	After adsorption	Amount adsorption		
5	20	7.09	1.0329	5.0447	4.9869	0.0578	1.1179	0.3178
	40	7.26	1.0038	5.0447	5.0132	0.0315	0.6203	0.3194
	60	7.51	1.0175	5.0447	4.8238	0.2209	4.2921	0.3074
	120	7.51	1.0175	5.0447	4.8238	0.2209	4.2921	0.3074
	180	7.74	1.0125	5.0447	5.0887	-0.0440	-0.8628	0.3242
	240	7.86	1.0317	5.0447	5.2044	-0.1597	-3.0698	0.3316
10	20	6.91	1.0438	10.0895	10.1873	-0.0978	-0.9259	0.2589
	40	7.12	1.0046	10.0895	10.0689	0.0206	0.2021	0.2559
	60	7.24	1.0056	10.0895	9.9242	0.1653	1.6349	0.2522
	120	7.44	1.0048	10.0895	9.6787	0.4108	4.0532	0.2460
	180	7.54	1.0114	10.0895	9.6743	0.4152	4.0686	0.2459
	240	7.63	1.0027	10.0895	9.8672	0.2223	2.1976	0.2508
20	20	6.75	1.0458	20.1790	19.9304	0.2486	1.2049	0.2529
	40	6.88	1.0025	20.1790	19.6234	0.5556	2.7453	0.2490
	60	7.01	1.0074	20.1790	20.1321	0.0469	0.2285	0.2554
	120	7.12	1.0081	20.1790	19.8953	0.2837	1.3962	0.2524
	180	7.31	1.0269	20.1790	20.0268	0.1522	0.7357	0.2541
	240	7.32	1.0162	23.1790	28.4030	0.6544	3.2251	5.5038
30	20	6.56	1.0183	30.2685	28.7965	1.4720	4.7790	0.3652
	40	6.74	1.0040	30.2685	29.3753	0.8932	2.9364	0.3726
	60	6.91	1.0238	30.2685	29.5331	0.7354	2.3733	0.3746
	120	7.03	1.0131	30.2685	31.1029	-0.8344	-2.7200	0.3944
	180	7.15	1.0176	30.2685	29.2700	0.9985	3.2466	0.3712
	240	7.16	1.0268	30.2685	30.1645	0.1040	0.3291	0.3826
blank	240	8.39	1.0209	0.0000	0.0293	-0.0293		0.0186

Appendix Table G7 Data from experiment of calcination mordenite at 750ºC after orthophosphate adsorption

Phosphate concentration (mg-P/L)	Shaking time (minute)	pH	Mordenite weight (g)	Phosphate concentration (mg-P/L)			%adsorbed per 1g MOR	absorbance (average)
				Before adsorption	After adsorption	Amount adsorption		
5	20	10.70	1.0426	4.9753	0.7447	4.2306	81.6365	0.0476
	40	11.01	1.0536	4.9753	0.4027	4.5726	87.2858	0.0259
	60	11.25	1.0270	4.9753	0.3045	4.6708	91.4108	0.0197
	120	11.58	1.0199	4.9753	0.5798	4.3955	86.5929	0.0371
	180	11.68	1.0143	4.9753	0.6360	4.3393	85.9825	0.0407
	240	11.69	1.0536	4.9753	0.5974	4.3779	83.5395	0.0382
10	20	10.06	1.0481	9.9506	3.9334	6.0172	57.6150	0.2496
	40	10.62	1.0570	9.9506	1.5463	8.4043	79.9157	0.0983
	60	11.28	1.0453	9.9506	0.4413	9.5093	91.4216	0.0283
	120	10.96	1.0135	9.9506	0.5588	9.3918	93.1219	0.0358
	180	11.72	1.0351	9.9506	0.4237	9.5269	92.5843	0.0272
	240	11.46	1.0556	9.9506	0.6640	9.2866	88.5303	0.0424
20	20	8.80	1.0090	19.9013	13.0871	6.8142	33.9255	0.8294
	40	10.15	1.0216	19.9013	8.7444	11.1569	54.8579	0.5543
	60	10.19	1.0498	19.9013	1.7409	18.1604	86.9140	0.1107
	120	10.40	1.0229	19.9013	1.4779	18.4234	90.5514	0.0940
	180	10.98	1.0280	19.9013	1.3621	18.5392	90.6330	0.0867
	240	11.22	1.0201	19.9013	1.2393	18.6620	91.9391	0.0789
30	20	7.80	1.0560	29.9681	27.0308	2.9373	9.3701	0.6851
	40	8.72	1.0702	29.9681	23.1415	6.8266	21.3252	0.5866
	60	10.20	1.0246	29.8520	11.8137	18.0383	58.9839	0.7488
	120	10.75	1.0278	29.8520	9.2320	20.6200	67.1904	0.5852
	180	11.11	1.0402	29.8520	6.5432	23.3088	74.8841	0.4149
	240	11.29	1.0526	29.8520	2.6863	27.1657	86.4578	0.1706
blank	240	11.73	1.0358	0.0000	0.0060	-0.0060		0.0038

Appendix Table G8 Data from experiment of calcination mordenite at 900ºC
after orthophosphate adsorption

| Phosphate concentration (mg-P/L) | Shaking time (minute) | pH | Mordenite weight (g) | Phosphate concentration (mg-P/L) | | | %adsorbed per 1g MOR | absorbance (average) |
				Before adsorption	After adsorption	Amount adsorption		
5	20	11.12	1.0070	4.9981	0.8768	4.1213	81.8888	0.0568
	40	10.98	1.0015	4.9981	0.7365	4.2616	85.1380	0.0479
	60	11.24	1.0046	4.9981	0.4401	4.5580	90.7764	0.0291
	120	11.40	1.0049	4.9981	0.6698	4.3283	86.1870	0.0437
	180	11.72	1.0096	4.9981	0.2331	4.7650	94.4239	0.0160
	240	11.59	1.0343	4.9981	0.5137	4.4844	86.7743	0.0338
10	20	10.62	1.0096	9.9962	4.7302	5.2660	52.1865	0.3009
	40	10.92	1.0062	9.9962	1.5713	8.4249	83.7653	0.1008
	60	11.15	1.0044	9.9962	1.5784	8.4178	83.8417	0.1012
	120	11.24	1.0077	9.9962	1.2960	8.7002	86.3721	0.0833
	180	11.70	1.0246	9.9962	0.2822	9.7140	94.8414	0.0191
	240	11.53	1.0089	9.9962	1.2855	8.7107	86.3676	0.0827
20	20	8.62	1.0099	19.9924	16.6691	3.3233	16.4483	0.2114
	40	9.45	1.0078	19.9924	11.0215	8.9709	44.5300	0.1399
	60	10.12	1.0044	19.9924	9.0308	10.9616	54.5893	0.1147
	120	10.72	1.0046	19.9924	3.7427	16.2497	80.9048	0.0477
	180	11.05	1.0088	19.9924	2.3834	17.6090	87.3140	0.0304
	240	11.36	1.0098	19.9924	1.4801	18.5123	91.6914	0.0190
30	20	7.58	1.0064	29.9886	28.2012	1.7874	5.9269	0.3576
	40	7.98	1.0065	29.9886	26.2017	3.7869	12.5338	0.3322
	60	8.87	1.0043	29.9886	22.5535	7.4351	24.6912	0.2860
	120	10.40	1.0016	29.9886	13.8102	16.1784	53.8637	0.1752
	180	10.58	1.0253	29.9886	11.4512	18.5374	60.2547	0.1453
	240	11.01	1.0395	29.9886	8.1100	21.8786	70.2121	0.1030
blank	240	11.69	1.0303	0.0000	0.0195	-0.0195		0.0123

Appendix H

Appendix Table H1 The data from thermal treatment at 750ºC

Phosphate concentration (mg-P/L)	Time(m)	Ce*	Ce/(X/M)*	X/M*	logCe*	log(X/M)*
5	20	0.7447	0.0062	121.8498	-0.1280	2.0858
10		3.9334	0.0233	171.9911	0.5948	2.2355
20		13.0871	0.0649	202.5484	1.1168	2.3065
30		27.0308	0.3370	84.2408	1.4319	1.9255
5	40	0.4027	0.0031	130.2819	-0.3950	2.1149
10		1.5463	0.0065	238.5628	0.1893	2.3776
20		8.7444	0.0271	327.5230	0.9417	2.5152
30		23.1415	0.1216	191.7229	1.3644	2.2827
5	60	0.3045	0.0022	136.4388	-0.5164	2.1349
10		0.4413	0.0016	272.9100	-0.3553	2.4360
20		1.7409	0.0034	518.9106	0.2408	2.7151
30		11.8137	0.0223	531.6357	1.0724	2.7256
5	120	0.5798	0.0045	129.2477	-0.2367	2.1114
10		0.5588	0.0020	277.9857	-0.2527	2.4440
20		1.4779	0.0027	540.6269	0.1696	2.7329
30		9.2320	0.0153	605.1196	0.9653	2.7818
5	180	0.6360	0.0050	128.3366	-0.1966	2.1084
10		0.4237	0.0015	276.3809	-0.3729	2.4415
20		1.3621	0.0025	541.1143	0.1342	2.7333
30		6.5432	0.0105	673.9819	0.8158	2.8286
5	240	0.5974	0.0048	124.6902	-0.2237	2.0958
10		0.6640	0.0025	264.2789	-0.1778	2.4221
20		1.2393	0.0023	548.9123	0.0932	2.7395
30		2.6863	0.0035	777.5918	0.4292	2.8908

* average 3 trials from experiment

Appendix I

Appendix Table I1 The orthophosphate desorption from mordenite at
temperature of calcination 750ºC

| Phosphate concentration (mg-P/L) | Shaking time (minute) | pH | Mordenite weight (g) | Phosphate concentration (mg-P/L) | | | %desorbed per 1g MOR | absorbance (average) |
				Before adsorption	Amount adsorption	Amount desorption		
5	60	10.15	1.0083	5.0254	4.7385	0.0735	1.4497	0.0503
	120	10.55	1.0051	5.0254	4.7578	0.0640	1.2666	0.0443
	180	10.67	1.0052	5.0254	4.8065	0.0233	0.4608	0.0186
	240	10.64	1.0007	5.0254	4.8703	0.0640	1.2722	0.0443
	300	10.90	1.0045	5.0254	4.8065	0.0247	0.4892	0.0194
	360	10.89	1.0049	5.0254	4.8703	0.0150	0.2980	0.0133
10	60	10.08	1.0074	10.0508	9.0118	0.1328	1.3113	0.0617
	120	9.88	1.0043	10.0508	8.7193	0.1151	1.1403	0.0819
	180	9.94	1.0047	10.0508	8.0123	0.1159	1.1471	0.1268
	240	9.94	1.0044	10.0508	8.7891	0.0726	0.7194	0.0776
	300	10.00	1.0046	10.0508	8.5793	0.1145	1.1341	0.0908
20	60	9.73	1.0040	20.1016	18.1359	0.3096	1.5335	0.1993
	120	9.69	1.0077	20.1016	17.2789	0.1331	0.6571	0.0876
	180	9.91	1.0037	20.1016	17.0348	0.0987	0.4894	0.0658
30	60	10.35	1.0041	30.1525	27.2715	0.1192	0.3938	0.0793
	120	10.44	1.0059	30.1525	27.2926	0.0882	0.2908	0.0597
blank	360	11.73	1.0358	0.0000	0.0060	-0.0060		0.0038

Appendix J

Appendix Table J1 The amount of Fe^{2+} were extracted from calcination
mordenite at 750° extraction with 0.05M EDTA

sample	Trial	$[Fe^{2+}]$ (mg/L)	
		/1g MOR	Average
750C	1	2.0759	2.0956 ± 0.1294
	2	2.0374	
	3	1.9554	
	4	2.1195	
	5	2.1591	
	6	2.2688	
	7	2.2433	
	8	2.1291	
	9	1.9082	
	10	2.0480	
	11	1.9196	
	12	2.2824	

Appendix Table J2 The amount of Fe^{2+} were extracted from calcination mordenite at 750º extraction with 0.5M HCl

Sample	Trial	[Fe^{2+}] (mg/L)	
		/1g MOR	Average
750C	1	1.4149	2.2170 ± 0.3807
	2	1.4735	
	3	1.6437	
	4	1.8652	
	5	1.6767	
	6	1.8396	
	7	1.9390	
	8	2.2313	
	9	2.3794	
	10	2.3768	
	11	2.5177	
	12	2.4873	
	13	2.7427	
	14	2.6045	
	15	2.6339	
	16	2.6347	
	17	2.4281	
	18	2.3341	
	19	2.4893	
	20	2.3059	
	21	2.3881	
	22	2.3036	
	23	2.2004	
	24	2.2965	

Appendix Table J3 Orthophosphate adsorption of mordenite after metal oxide extraction with 0.05M EDTA

Phosphate concentration (mg-P/L)	Shaking time (minute)	Trial	pH	Mordenite weight (g)	Phosphate concentration (mg-P/L)			%adsorbed per 1g MOR	absorbance (average)
					Before adsorption	After adsorption	Amount adsorption		
5	60	1	7.08	1.0036	5.0254	5.2772	-0.2518	-4.9926	0.3343
		2	6.96	1.0068	5.0254	5.2404	-0.2150	-4.2487	0.3320
		3	7.01	1.0053	5.0254	5.2772	-0.2518	-4.9841	0.3343
blank	60	1	7.69	1.0031	0.0000	0.0000	0.0000		0.0000
		2	8.45	1.0045	0.0000	0.0000	0.0000		0.0000
		3	8.04	1.0030	0.0000	0.0011	-0.0011		0.0007
		average				0.0004	-0.0004		
30	300	1	6.90	1.0049	30.1525	30.5655	-0.4130	-1.3629	0.3873
		2	6.87	1.0086	30.1525	30.4602	-0.3077	-1.0119	0.3860
		3	6.88	1.0078	30.1525	30.1445	0.0080	0.0262	0.3820
blank	300	1	8.87	8.8700	1.0016	0.0000	0.0058		0.0037
		2	9.27	9.2700	1.0074	0.0000	0.0026		0.0017
		3	9.22	9.2200	1.0064	0.0000	0.0079		0.0050
		average					0.0054		

Appendix Table J4 Orthophosphate adsorption of mordenite after metal oxide extraction with 0.5M HCl

Phosphate concentration (mg-P/L)	Shaking time (minute)	Trial	pH	Mordenite weight (g)	Phosphate concentration (mg-P/L)			%adsorbed per 1g MOR	absorbance (average)
					Before adsorption	After adsorption	Amount adsorption		
5	60	1	5.21	1.0043	5.0254	5.8537	-0.8283	-16.4120	0.3710
		2	5.38	1.0006	5.0254	5.8853	-0.8599	-17.1005	0.3730
		3	4.76	1.001	5.0254	5.7169	-0.6915	-13.7465	0.3623
blank	60	1	4.79	1.0024	0.0000	0.0042	-0.0042		0.0027
		2	5.69	1.0004	0.0000	0.0021	-0.0021		0.0013
		3	5.48	1.0047	0.0000	0.0016	-0.0016		0.0010
		average				0.0026	-0.0026		
10	120	1	4.38	1.0028	10.0508	9.5729	0.4779	4.7414	0.2427
		2	4.35	1.0007	10.0508	9.4808	0.5700	5.6668	0.2403
		3	4.24	1.0013	10.0508	9.2835	0.7673	7.6241	0.2353
blank	120	1	4.84	1.0024	0.0000	0.0037	-0.0037		0.0023
		2	4.95	1.0057	0.0000	0.0032	-0.0032		0.0020
		3	4.93	1.0094	0.0000	0.0037	-0.0037		0.0023
		average				0.0035	-0.0035		
20	240	1	4.08	1.0050	20.1016	17.9372	2.1644	10.7137	0.2273
		2	4.11	1.0050	20.1016	18.1214	1.9802	9.8021	0.2297
		3	4.10	1.0019	20.1016	17.8057	2.2959	11.4000	0.2257
blank	240	1	4.78	1.0016	0.0000	0.0047	-0.0047		0.0030
		2	4.78	1.0076	0.0000	0.0016	-0.0016		0.0010
		3	4.73	1.0024	0.0000	0.0100	-0.0100		0.0063
		average				0.0054	-0.0054		
30	300	1	4.00	1.0043	30.1525	31.8567	-1.7042	-5.6278	0.4037
		2	4.02	1.0054	30.1525	32.4618	-2.3093	-7.6176	0.4113
		3	4.00	1.0021	30.1525	32.4618	-2.3093	-7.6427	0.4113
blank	300	1	4.78	1.0064	0.0000	0.0074	-0.0074		0.0047
		2	4.70	1.0002	0.0000	0.0011	-0.0011		0.0007
		3	4.78	1.0002	0.0000	0.0016	-0.0016		0.0010
		average				0.0033	-0.0033		

Appendix K

Appendix Table K1 The zeta potential of mordenite which varies pH

samples	Zeta potential (mV)										
	pH 12	pH11	pH 10	pH 9	pH 8	pH 7	pH 6	pH 5	pH 4	pH 3	pH 2
room temperature	-29.10	-31.00	-33.70	-33.50	-32.60	-31.40	-19.80	-15.50	-15.60	-8.70	-7.90
room temperature adsorbed	-36.50	-34.00	-38.60	-37.90	-38.00	-39.90	-33.10	-27.60	-25.00	-21.50	-12.90
calcined at 150ºC	-35.40	-35.30	-35.60	-35.80	-34.20	-36.80	-35.40	-33.60	-28.70	-22.90	-16.80
calcined at 150ºC adsorbed	-36.40	-37.00	-36.30	-34.40	-37.10	-34.80	-36.40	-34.80	-29.90	-22.20	-18.10
calcined at 300ºC	-35.40	-34.90	-33.70	-38.40	-36.90	-36.00	-31.80	-27.00	-22.50	20.60	-12.30
calcined at 300ºC adsorbed	-33.80	-32.20	-32.30	-34.30	-36.10	-36.10	-30.30	-25.30	-21.70	-20.10	-9.60
calcined at 450ºC	-32.20	-34.60	-37.10	-38.40	-37.40	-37.40	-29.40	-26.20	-23.50	-20.10	-16.30
calcined at 450ºC adsorbed	-35.70	-35.70	-37.70	-38.40	-39.60	-36.50	-28.10	-24.40	-23.00	-17.70	-12.60
calcined at 600ºC	-29.50	-30.10	-24.40	-19.90	-25.50	-23.20	-4.60	-1.50	0.20	1.00	-2.20
calcined at 600ºC adsorbed	-26.70	-27.90	-25.00	-21.00	-24.00	-26.00	-0.70	2.00	2.30	2.60	2.90
calcined at 750ºC	0.00	-24.70	-22.20	-6.70	-7.50	-0.50	-5.20	-1.00	-2.80	0.20	-0.90
calcined at 750ºC adsorbed	-25.90	-26.30	-26.30	-26.10	-29.10	-24.30	-9.80	-6.10	-6.50	13.70	4.80
calcined at 900ºC	-28.90	-26.10	-29.90	-27.00	-28.90	-24.00	-13.50	-6.90	-10.40	-4.10	5.00
calcined at 900ºC adsorbed	-23.80	-19.90	-26.20	-20.40	-15.60	-14.10	-6.60	-14.70	-8.40	-2.00	2.70

Appendix Table K2 The zeta potential of mordenite at pH of adsorption

conditions		pH	zeta potential (mV)
uncalcined	before	6.87	-15.14
	after	5.49	-13.5
150ºC	before	6.86	-14.8
	after	6.31	-15.4
300ºC	before	6.38	-15.3
	after	5.82	-15.4
450ºC	before	5.67	-15.8
	after	6.13	-13.6
600ºC	before	5.97	-15.1
	after	6.10	-16.2
750ºC	before	6.17	-12.8
	after	6.07	-14.7
900ºC	before	6.02	-17.8
	after	6.34	-14.7

Appendix L

Appendix Table L1 Equilibrium reactions of element at 25ºC

Reaction No.	Equilibrium reaction	$\log K^0$
1	$Al(OH)_3 \text{ (amorp)} + 3H^+ \rightleftharpoons Al^{3+} + 3H_2O$	9.66
2	$Al^{3+} + H_2O \rightleftharpoons AlOH^{2+} + H^+$	-5.02
3	$SiO_2 \text{ (amorp)} + 3H_2O \rightleftharpoons H_4SiO_4^0$	-2.74
4	$SiO_2 \text{ (soil)} + 2H_2O \rightleftharpoons H_4SiO_4^0$	-3.10
5	$Ca^{2+} + H_2PO_4^- \rightleftharpoons CaH_2PO_4^+$	1.40
6	$Ca^{2+} + H_2PO_4^- \rightleftharpoons CaHPO_4^0 + H^+$	-4.46
7	$Ca^{2+} + H_2PO_4^- \rightleftharpoons CaPO_4^- + 2H^+$	-13.09
8	$H_2PO_4^- \rightleftharpoons HPO_4^{2-} + H^+$	-7.20
9	$HPO_4^{2-} \rightleftharpoons PO_4^{3-} + 2H^+$	-12.35
10	$H_2PO_4^- \rightleftharpoons PO_4^{3-} + 2H^+$	-19.55
11	$H_3PO_4^0 \rightleftharpoons H_2PO_4^- + H^+$	-2.15
12	$Fe^{2+} + H_2PO_4^- \rightleftharpoons FeH_2PO_4^+$	2.70
13	$Fe^{2+} + H_2PO_4^- \rightleftharpoons FeHPO_4^0 + H^+$	-3.60
14	$Fe^{3+} + e^- \rightleftharpoons Fe^{2+}$	13.04
15	$AlPO_4. 2H_2O \text{ (variscite)} + 2H^+ \rightleftharpoons Al^{3+} + H_2PO_4^- + 2H_2O$	-2.50
16	$FePO_4. 2H_2O \text{ (strengite)} + 2H^+ \rightleftharpoons Fe^{3+} + H_2PO_4^- + 2H_2O$	-6.85
17	$CaHPO_4. 2H_2O \text{ (brushite)} + H^+ \rightleftharpoons Ca^{2+} + H_2PO_4^- + 2H_2O$	0.63

CURRICULUM VITEA

NAME   : Miss Noppakao Ex-un

BIRTH DATE   : November 7, 1979

BIRTH PLACE   : Sakon Nakhon, Thailand

EDUCATION   : <u>YEAR</u>   <u>INSTITUTION</u>   <u>DEGREE/DIPLOMA</u>

                            2002   Khon Kaen Univ.   B.Sc. (Chemistry)

                            2006   Kasetsart Univ.   M.S. (Chemistry)

WORK PLACE   : Faculty of Science, Kasetsart University

SCHOLARSHIP/AWARDS   : Teaching Assistant of Laboratory in

                                      General Chemistry